INVESTIGATION INTO PHYSICAL AND MECHANICAL PROPERTIES AND FAILURE MODE OF RESISTANCE SPOT WELDED DISSIMILAR METAL JOINTS.

By

Md. Rysul Alam Shawon

A thesis submitted in partial fulfillment of the requirements for the degree of Master of Science in Materials and Metallurgical Engineering.

DEPARTMENT OF MATERIALS AND METALLURGICAL ENGINEERING
BANGLADESH UNIVERSITY OF ENGINEERING AND TECHNOLODGY
DHAKA-1000, BANGLADESH.
March, 2014.

DECLARATION

This is to certify that this work has been carried out by the auther under the supervision of Professor A.S.W. Kurny, Department of Materials and Metallurgical Engineering, BUET, Dhaka and it has not been submitted elsewhere for the award of any degree or diploma.

Countersigned

Professor A.S.W. Kurny

Md. Rysul Alam Shawon

ACKNOWLEDGEMENT

I would like to thank and express my sincere gratefulness to my supervisor Professor A.S.W Kurny, Department of Materials and Metallurgical Engineering, Bangladesh University of Engineering and Technology, Dhaka, for his complete guidance and support in this thesis work. His inspiring guidance, cordial encouragement, comments, suggestions and tolerance are so helpful and without him, I would face many difficulties to complete my thesis work.

I am also grateful to Head, Materials and Metallurgical Engineering, for providing me with the laboratory facilities and wish to thanks all staff of the department for their co-operation.

I am grateful to Dr. Abdul Gafur, and Md. Rakibul Qadir of BCSIR and M.A. Mamun in Atomic Energy Commission for their continuous support during my thesis work.

Finally, I am grateful to my parents and wife for understanding and constant encouragement throughout the period of my study.

ABSTRACT

Resistance spot welding is a widely used technique for fabricating sheet metal assemblies because of its high speed, efficiency, reduced cost and suitability for automation. The objective of this thesis was to study the effect of process parameters particularly on the structure and properties of resistance spot welded dissimilar sheet metal joint. Process parameters were optimized and a discussion was made on failure mode of this welding technique.

Two different materials, austenitic stainless steel and low carbon steel were used to be welded. Thickness of these two sheets were around 1.5 mm. Welding current in the range of 3 kA to 9 kA and welding cycle of 30 to 90 was used as process variables. The welded coupons were examined by different characterization techniques such as macroscopic, optical microscopic and scanning electron microscopy, EDX analysis, tensile testing and micro hardness measurements. Failure mode was also identified by analysis of the fractured samples.

In this study, asymmetrical shape weld nugget was formed to join two different materials. Weld nugget size increased with an increase in welding current and welding cycle and this affected the mechanical properties. Optical microscopy and SEM analysis clearly showed different zones like base metal, heat affected zone and fusion zone. The heat affected zone consist martensite, grain boundary ferrite and widmanstatten ferrite in low carbon steel side but in case of austenitic stainless steel no phase change occurs in the heat affected zone. The fusion zone had a cast structure with coarse columnar grain and dendrite with excess delta ferrite in austenitic matrix. Micro hardness of the weld nugget was maximum because of the formation of martensite. An increase in both welding current and cycle, increases tensile strength of the weld coupon. Three types of failure mode were found and these are base metal tearing, pullout failure mode and interfacial failure mode.

CONTENT

.

List of Figure

List **Page No**

Chapter 1

Chapter 2

— Interfacial; B — pull-out.

Chapter 3

Chapter 4

List of Table

Chapter 1

Introduction

1.1 Background:

In resistance Spot welding sheet metals are joined by electrical resistance heating and application of force without using any filler metal. It is widely used for fabricating sheet metal assemblies such as automobiles, truck cabins, rail vehicles, motor cycles and home appliances like refrigerators of high suitability. For examples, a modern auto body assembly needs 7000 to 12000 spots of welding according to its size. Spot welding is an economical method because of its speed, precision, and ease of automation.

1.2 Resistance spot welding

During the resistance spot welding process two continuously cooled electrodes clamp down on two worksheets as shown in Figure 1.1. AC or DC current is then passed through the electrodes at low voltage which results in fusion at the faying surface of the worksheet.

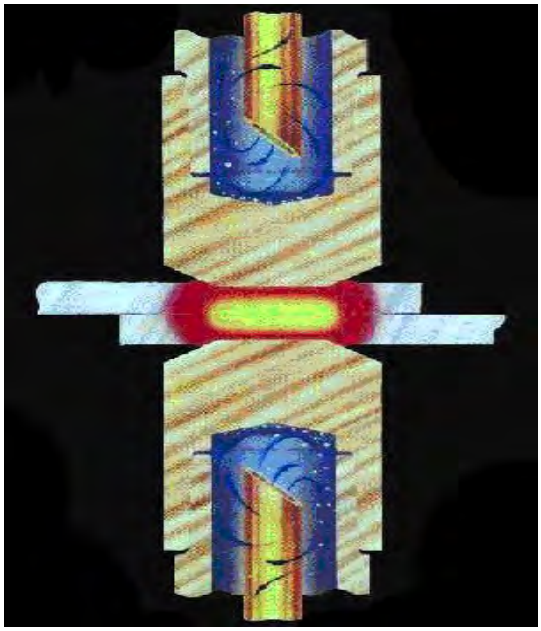

Figure1.1: Schematic of resistance spot welding process

Each welding schedule typically involves five sequential steps which shown in Figure 1.2. These are

1. The initial squeeze where the electrode clamps the materials.

2. Application of force at which welding occurs.
3. The application of current which results in fusion.
4. A hold time to allow for solidification of molten metal and finally
5. Electrode release.

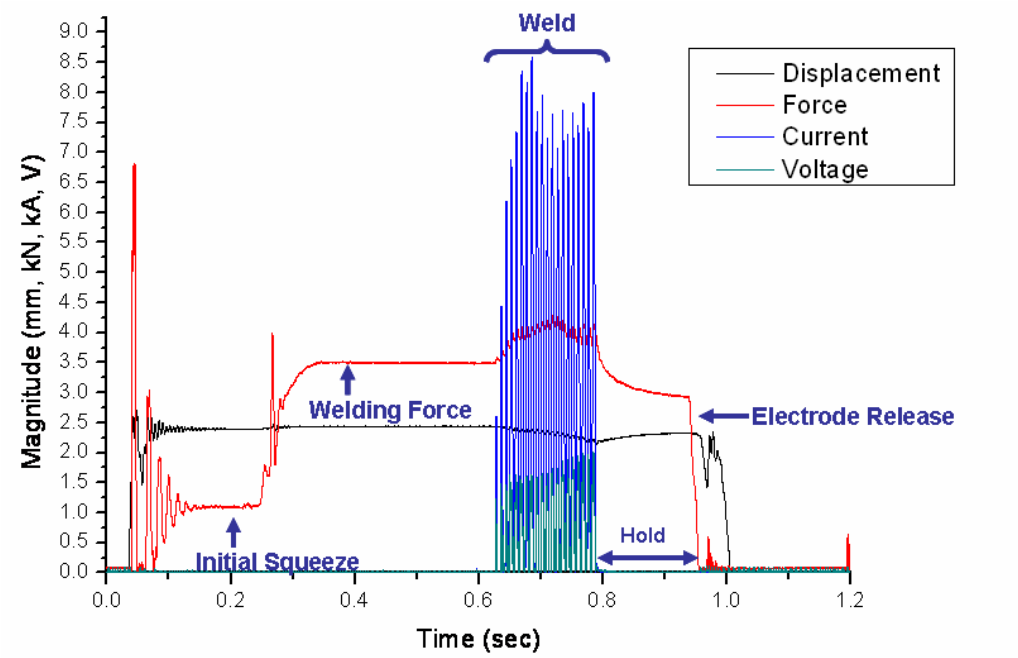

Figure 1.2: Full welding schedule

The heat generated during the resistance spot welding process due to inter face contact resistance and bulk resistance is given by the following equation:

$$Q = kI^2Rt \qquad 1.1$$

Where Q is the total heat, k is a calibration constant, I the weld current, R the total circuit resistance, and t the weld time. From this equation it can be shown that the current, resistance and time are the key parameters for heat generation and hence the quality of the weld. Furthermore the contact resistance is dependent on the magnitude of the force applied, which can decrease with increased force.

Spot welding parameters that affect the strength and quality of the joint include:

1) Electrode force
2) Diameter of the electrode contact surface
3) Squeeze time
4) Weld time

5) Hold time

6) Weld current

The strength of the spot welded joint depends on the number, the size of spot, and the structure of the welds. The diameters of the spots are range from 3 mm to 12.5 mm. To investigate the strength of spot welds in terms of the specimen geometry, welding parameter, welding schedule, base metal strength, testing speed and testing configuration the tensile test method also can use to investigate the strength of the spot weld.

1.3 Scope of Work

The majority of the research investigations in spot welding have been carried out on the joining of similar metals, particularly non-stainless steels. Few documented data, guideline values and resistance weld ability diagrams exist for resistance spot welding of dissimilar steels. Most of these are however, for non-stainless steels. There are limited information about resistance spot welding of dissimilar metals like stainless steel and carbon steel. In Bangladesh, no work has so far been reported on resistance spot welding of dissimilar metals but It is has a lot of application in Bangladesh in home appliance.

1.4 Objective with specific aims:

The primary aim of this work is to optimize the parameters for resistance spot welding of dissimilar metals with particular reference of stainless steel and low carbon steel. The physical and mechanical properties of welded joints will be determined. The properties will be correlated with the microstructure of the welded joint. The mode of failure will be investigated and attempts will be made to relate the mode of failure to the welding parameters used. The importance of this research works are given below.

- To study the effects of different parameter on resistance welded dissimilar sheet metal and optimize process parameters.
- To study the failure mode of the welded samples.
- To estimate the amount of load that could be apply to each different nugget diameter size before the welded joints is fails or rupture.

1.5 Possible outcome:

The results obtained will help optimize the welding parameters and be useful in producing sound resistance spot welded joints in dissimilar metals. It may also lead to a cost effective joining method that will be adopted by the automobile industry.

Chapter 2

Literature Review

2.1 Principle of Operation for Resistance Spot Welding.

Resistance Spot welding is one of the important welding processes of sheet metal industries. It is included in the group of resistance welding processes, in which the heat is generated by conducting of electric current through the metal bodies to be joined. Spot welding process is different from another welding process such as arc welding because filler metal or fluxes are not required during the welding process. This spot welding process is unique because the weld nugget is formed at between the surfaces of specimen. Figure 2.1 below show the comparison between nugget form for resistance spot weld and gas tungsten-arc weld.

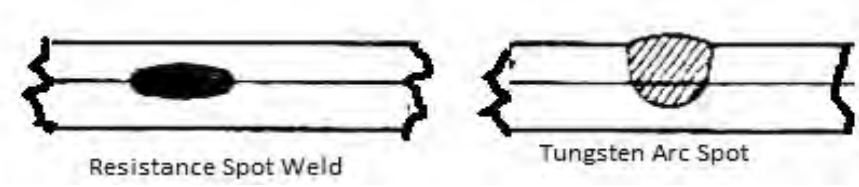

Figure 2.1: Resistances and Tig Spot Weld Comparison

In resistance spot welding, two overlapping sheets of metal are joined by resistance heating by applying electric current and pressure in the zone to be welded (Figure 2.2). There is no extra external heat source. Heat is produced only on the parts to be welded and pressure is applied by the rocker arms or electrode arms. The high current density is provided by the transformers and the pressure is provided by the hydraulic and pneumatic equipment. Spot welding operates based on four factors.

1. Amount of current that passes trough the work piece.
2. The pressure applied to the work piece by the electrode
3. The time of current flow trough the work piece.
4. The area of the electrode tip contact with the work piece.

Alignment of the sheets and electrodes as well as the surface condition of the sheets affects the quality of the weld. Therefore, a spot welding process needs the optimum process

conditions that can afford allowance in parametric values for good quality of welding. The optimum condition has to consider the amount and duration of electric current, welding cycle, weld force, the shape and material properties of electrode, the surface condition and alignment of sheets. Thus, the behavior of resistance spot welding process is extremely important to the quality of the entire welding structure.

The displacement of the electrodes is also considered as an important feature during the resistance spot welding process due to its performance in the control of the quality of welding.

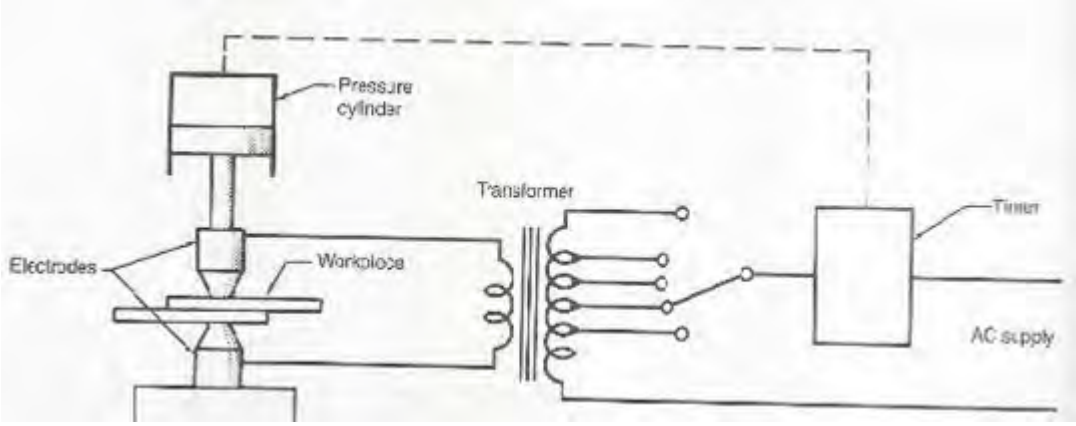

FIGURE 2.2: Fundamental resistance welding machine circuits.

During the welding process, Electric current is flows from the electrodes to the work pieces. The shape and size of the weld are controlled by the size and contour of the electrode. This process also depends on the welding time where a timer controls by four different steps (Figure 2.3 and Figure 2.4).

1. Squeeze time, or the time between the first application of electrode force and the first application of welding current
2. Weld time or the actual time when the current flows through the work piece. The application of right or suitable amount of pressure on the work piece is very important in order to obtain a good quality weld.
3. Hold time, the period during which the electrode force is applied and the welding current is shut off.
4. Off period, or the time during which the electrodes are not contacting the work piece.

When electric current flows through electrode tips to the separate work pieces of metal to be joined, the resistance of the base metal to electrical current flow causes heat and the heat is

limited to the area which the tip of the electrode and weld area contacts. While the welding force is maintained, the heat is generating. In the holding stage (where the pressure is still maintained), the current is switched off and the nugget is cooled under the pressure.

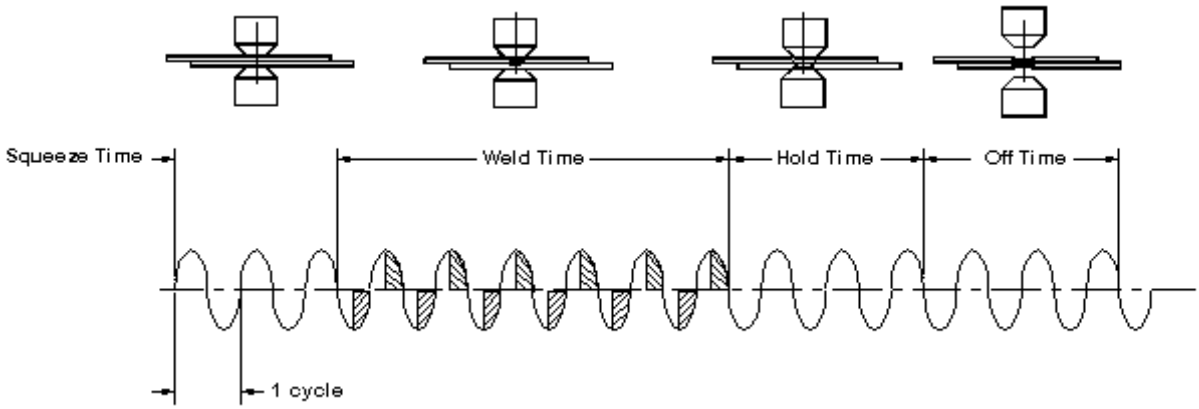

FIGURE 2.3: Basic period of Spot welding

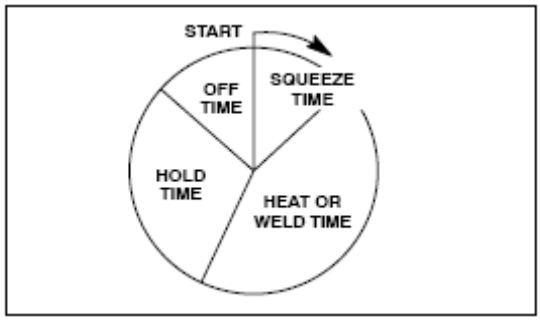

Figure 2.4: spot welding time cycle

The heat required for these resistance welding processes is produced by the resistance of the work pieces to an electric current passing through the material. Because of the short electric current path in the work and limited weld time, relatively high welding currents are required to develop the necessary welding heat. The amount of heat generated depends upon three factors: (1) the amount of current, (2) the resistance of the conductor and (3) the duration of current. These three factors affect the heat generated as expressed in the formula below

$$\mathbf{Q = I^2 R t} \qquad 2.0$$

But for the practical purpose a factor *K* (heat losses) should be include. Then the actual resistance welding is expressed by the Equation 2.1

$$Q = I^2 R t K \qquad 2.1$$

Where

Q = Heat is generated in joules (watt- second)

I = Current (in amperes)

R = Resistance (in ohms)

t = Time to current flow (in seconds)

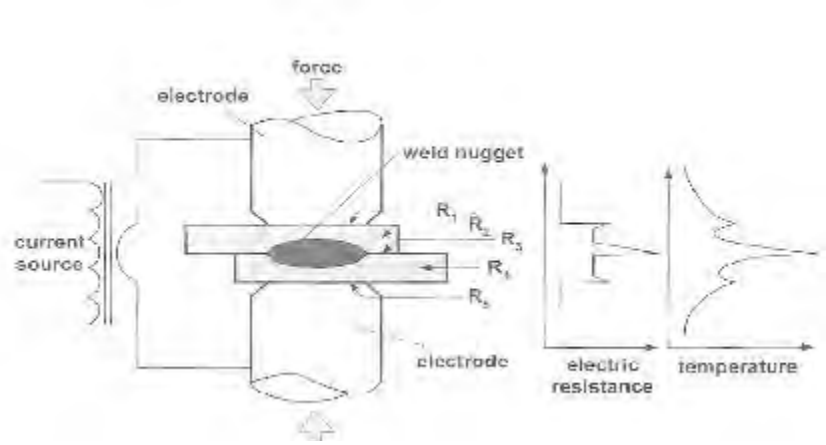

FIGURE 2.5: Electrode – work – piece interface resistance – R1 and R5; resistance of the work- pieces – R2 and R4; resistance in the interface between works – pieces- R3.

The secondary circuit of a resistance welding machine and the work being welded constitute a series of resistances. The total resistance of the current path affects the current magnitude. There are, in effect, at least five resistances connected in series in a weld that account for the temperature distribution and the sum of them is expressed as R as shown in Figure 2.5 above,

$$R=R_1+R_2+R_3+R_4+R_5 \qquad 2.2$$

In the spot welding process there are six major point of resistance in the area. They are following:

1. The contact point between the electrode and the top work piece.
2. The top work piece
3. The interface of the top and bottom work piece.
4. The bottom work piece.
5. The contact between the bottom work piece and the electrode.
6. Resistance of electrode tips.

The resistances of material are in series, and each point of resistance will retard current flow. The amount of resistance at point 3, the interface of the work pieces will depend to the heat transfer capabilities of the material, its electrical resistance, and the combined thickness of the materials at the weld joint. It is at this part of the circuit that the nugget of the weld is formed. The heat generated depends basically on the electrical current and time being setup and on the electrical resistance of materials between electrodes. These inter electrodes resistance is composed by five separated resistance, as indicated in Figure 2.5. Resistance at R1 and R5 are undesirable because they produce heating and consequently degradation of the electrodes. Resistance at R2 and R4 are the resistance of the work-pieces and they assume particular importance in the final period of the welds. To weld low resistive material is difficult because of reduced heat generated in the pieces. Resistance at R3 is important to determine the nugget formation, assuring the establishment of the weld.

Resistance welding is used commonly for mass-production industries, where production run and consistent conditions are maintained. The resistance welding machine works automatically and less skilled workers are needed. Resistance welding has the advantage of producing a high volume of work at a high speed, the product can be produced at high quality. It is the most common form of electric resistance welding as its method is very easy, practical and easeful. Although it seems to be very basic, its process is very complex and requires the continuous control of specified parameters. The method may be used for joining sheet to sheet, sheets to rolled sections or extrusions, wire to wire, for sundry special applications using combinations of the above. By far the widest application in industry is the spot welding together of sheet-metal parts, as in the hollow-ware industry (handles to kettles and saucepans) or the automotive industry. For example, the typical car body contains about 5000 spot welds joining a mixture of sheet metal material types and thicknesses. This welding method is very advantageous corresponding to its high speed of operation, hence its adaptability to mass production, its cleanliness, no need for welding rods, and its high degree of control possible by electrical means (i.e., reducing the necessity for a degree of operational skill). Resistance spot welding also has been used in the repair industry, for example in Europe and Japan the resistance spot welding has been used in unibody collision repair industry for more than 25 years. This method is acceptable because resistance spot welding is ideal for welding many parts of unibody’s thin-gauge area that need good strength and no distortion.

2.2 RESISTANCE SPOT WELDING EQUIPMENT

The equipment needed for resistance spot welding can be simple and inexpensive or complex and expensive, depending on the degree of automation. Spot welding machines are generally composed of three principal elements:

- **Electrical Circuit:** It is composed of a welding transformer, tap switch and a secondary circuit.
- **Control Circuit:** It initiates and times the duration of current flow and regulates the welding current.
- **Mechanical System:** This system consists of the frame, fixtures and devices that hold and clamp work piece and apply welding pressure.

Welding operations in highly automated production lines are based primarily on multiple spot welders and robotic cells. In addition, manual welding operations can be used to manufacture either subassemblies, which are fed into the main production/assembly lines, or in many instances, finished products. These differing end uses require machines of varying designs and characteristics. RSW machines can be divided into three basic types:

- Pedestal-type welding machines
- Portable welding guns
- Multiple welding machines incorporating lightweight gun welding units.

Specifications for resistance welding equipment have been standardized by the Resistance Welder Manufacturers Association (RWMA), and specifications for controls are issued by the National Electrical Manufacturers Association (NEMA).

The welding force can influence the contact resistance of a material. Higher welding forces typically results in better interfacial contact and reduced resistance. This can result in lower heat generated during welding, which needs to be compensated with increase weld time or higher current inputs. In addition, excessive welding force can cause excessive indentation in the work piece.

2.3 Electrodes and Electrode Degradation

The function of alloyed copper RSW electrodes include applying force to the work piece, providing necessary current densities and facilitating post-weld cooling. Typical electrode geometries are shown in Figure 2.6. Truncated electrodes are commonly used in industrial applications due their limited contact tip growth. However care must be taken during alignment of truncated electrodes since the weld quality can be severely affected with misalignment. Dome type electrodes are less susceptible to misalignment issues and are commonly employed for industrial applications.

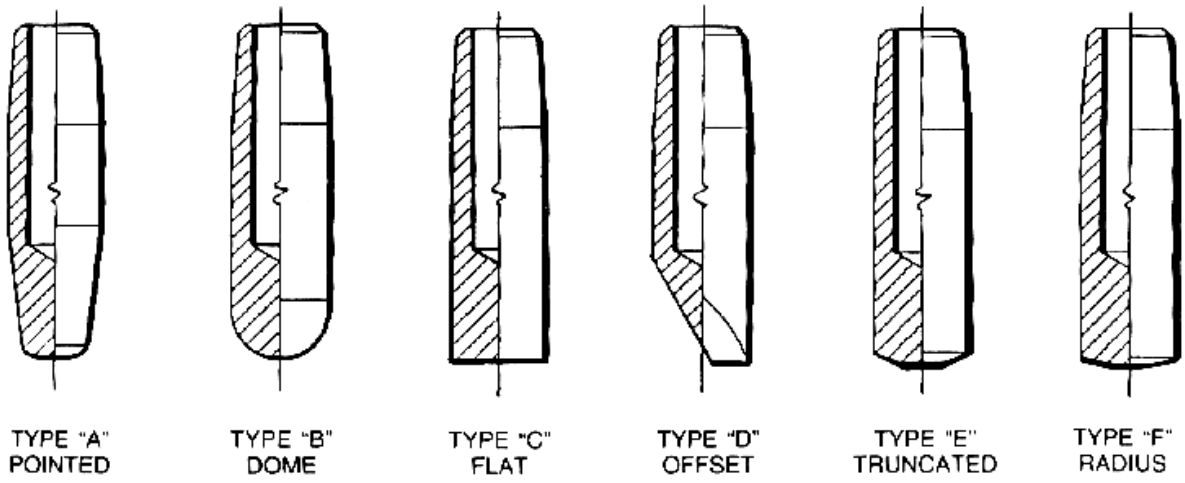

Figure 2.6: Common electrode geometries

Electrode degradation can result in welds with insufficient fusion or irregular nugget formation. During degradation the electrode contact area increases and reaches a size where adequate current densities can not be attained. Ultimately this results in poor quality welds. Hence it is important to maximize electrode life to consistently achieve acceptable welds. In order to enhance corrosion resistance, automotive steels are typically zinc coated. The addition of coatings can alter the resistance profile at the interface of an RSW stack-up. Increased temperatures aid in melting and vaporization of the Zn-coatings. This in turn can aid inter-diffusion of copper and zinc which results in the formation of alloys. Furthermore, increased peak temperatures at the electrode-sheet interface have shown to accelerate electrode degradation during welding.

2.4 Welding Parameters

Key welding parameters for RSW are welding current, weld force, welding time and post weld hold time. Other factors that can also influence welds include conduction angles and electrode shape and size. Welding parameters for sheet steel RSW has been studied in great detail and has resulted in the standardization for particular material thicknesses. These standards were derived for conventional high strength steels and are constituted by the “Recommended Practices for Evaluating the Resistance Spot Welding Behavior of Automotive Sheet Steel Materials” [01] and the “Resistance Welding Manual” [02].The three main parameters which require detailed experimental testing include weld current, weld time, and weld force and these are detailed in the following sections.

2.4.1 Weld current

Welding current is essential for heat generation. Both AC and DC welding processes can be used to provide high current densities which subsequently generate the heat required for fusion. Hofman [03] showed that both types of current provide similar weld qualities; however, the DC system can reduce electrical demands when welding Advanced High-Strength Steels (AHSS), Making DC RSW more efficient. Current profiles for RSW can be altered with the addition of up slopes, down slopes and pulsing. Tawade [04] showed that the addition of up sloping can aid in increasing the window in the welding lobe for AHSS. Khan [05] showed use of pulsing for in-situ tempering of the weldments. It was shown that the mechanical performance of weldments could be altered with the addition of weld pulses, which resulted in hardening or softening of the final weld microstructure.

If the current passed during the weld time is too high for the combination of electrode caps in use, their condition and contact area, the weld time, the weld force, and the materials being welded, it will generate more heat and results in excessive indentation, cracks and holes, expulsion/burn through, sticking electrodes, rapid electrode cap wear and “brassy” appearance to weld surface on galvanized steels.

2.4.2 Weld Time

Welding time is directly proportional to the amount of heat being generated. Increased welding time results in increased heat generation. For AC welding supplies the unit time measurements is in cycles (1 Second= 50 cycles). Weld time for DC power supplies is measured in milliseconds. Weld time is normally set depending on the material thickness and coating conditions. The interaction of zinc coating at the interface can require increased welding time. Dickenson [06] showed a 50%-100% increase in time was required to weld zinc coated steel. Increased time allows for the molten zinc to be displaced from the weld area; furthermore, it facilitates nugget growth which enhances the mechanical performance of weldments. However, excessive welding time results in expulsion due to nugget overgrowth. This can introduce weld defects into the weldment, such as voids and excessive indentation, which adversely affect weld performance.

2.4.3 Weld Force

Most RSW processes utilize two distinct welding forces, an initial squeeze followed by an increase to the full welding force. The initial squeeze is required to avoid impacting of the electrodes and aid in material alignment. This is followed by the application of a full force which can be experimentally determined or selected from recommended handbook values. The welding force can influence the contact resistance of a material. Higher welding forces typically results in better interfacial contact and reduced resistance. This can result in lower heat generation during welding, which needs to be compensated with increase weld time or higher current inputs. In addition, excessive welding force can cause excessive indentation in the work piece.

2.5.1 Nugget Formation

The nugget is a volume of melted material that forms in the interface of work pieces with a diameter related to sizes of those electrodes, as shown in the Figure 2.6. The penetration for nugget should be at least 20 % of the thinnest sheet member but not more than 80% of the same thickness. Flowing of current initiates after the application of the electrode force will increases the temperature in the interface and develops a molten nugget. In the final part of

the welding cycles plastic deformation occurs in the work-pieces. If current or pressure is too high, melted material can be expulsed (splashed) to the atmosphere.

During the RSW process, resistance at the faying surface generates heat which can cause peak temperatures to exceed liquidus. Studies have shown that the zinc coating on coated steels melts at the faying surface and is pushed to the periphery of the contact area. This in turn causes annular shunting and localized heating. With increased time the annulus grows to form a spheroid shaped fusion zone. Figure 2.7 shows the un-coated steel which does not exhibit the annular melting and instead shows localized heating that facilitates nugget formation at the centre of the faying surface.

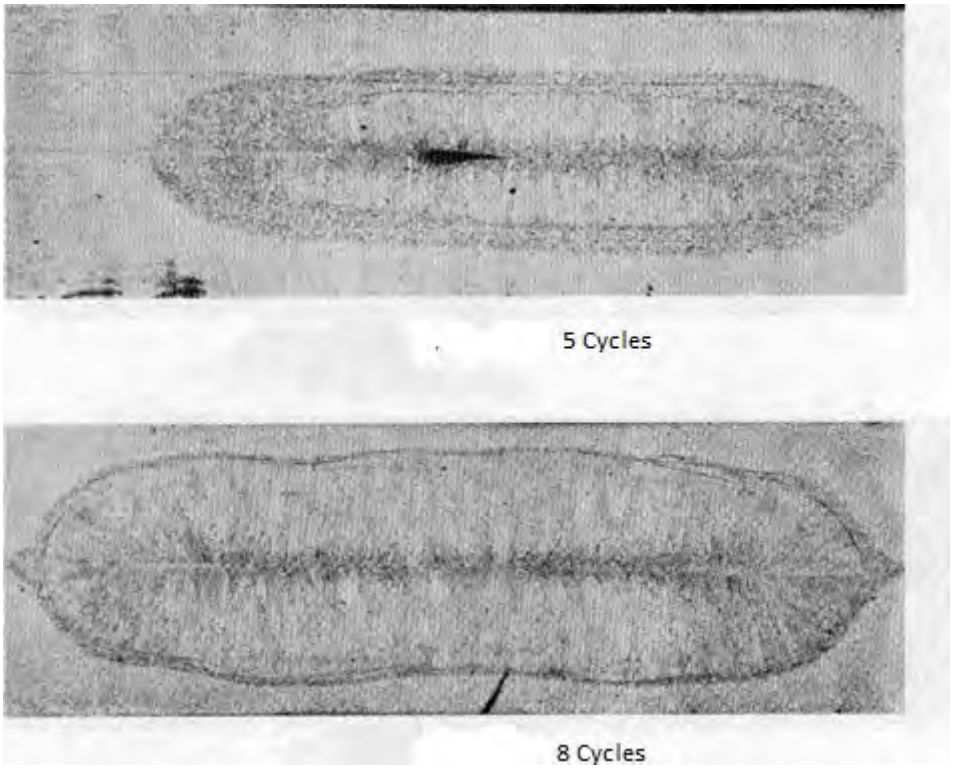

Figure 2.7: Cross-section of welded uncoated sheet steel

As the weld current flows through the clamped work pieces, the highest resistance will be at their contacting surface. The heat develops at this side, causing a rapid rise in the temperature. The temperature rise culminates in melting of the metal starting at the center of the current path. Thus, a pool of molten metal from the workpieces begins to grow outward for the duration of the current flow. When the weld current is turned off, this volume of molten metal cools down and solidifies.

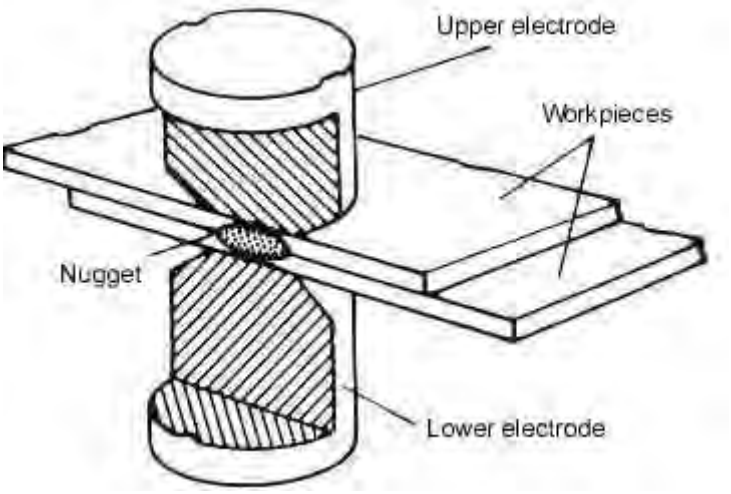

Figure 2.8: The cutaway view of the location and shape of a weld nugget.

The volume of metal from the work pieces undergoes heating, melting, fusion and re solidification, which is the weld nugget. The cutaway view of a typical spot weld nugget is given in Figure 2.8. The weld nugget forms at the faying surfaces, but does not extend completely to the other surfaces. In a cross section, the nugget in a properly formed spot weld is round or oval in shape; in plain view it has the same shape as electrode face and approximately the same size. The ratio of the temperature gradient to the growth rate governs the mode of solidification. The product of the temperature gradient and the growth rate, on the other hand, governs the scale of the solidification structure. It has been observed that the greater the product, the finer the solidified cellular or dendritic structure. It is also to be noted that the product is equivalent to the cooling rate, since both have the same units of degrees centigrade per second.

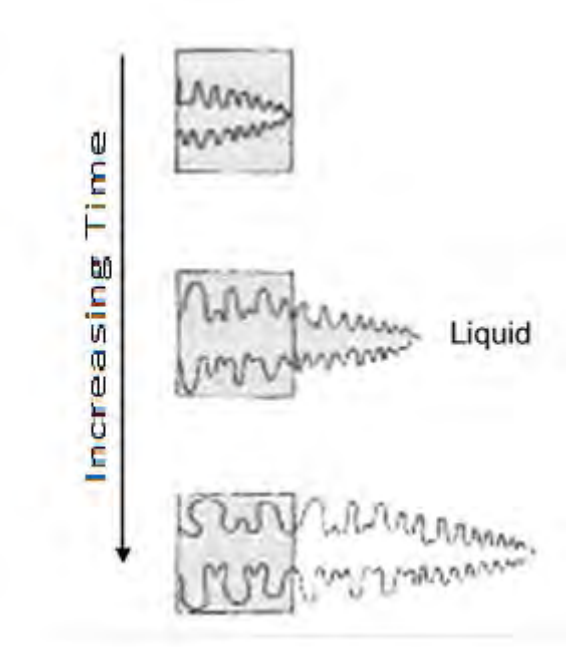

Figure 2.9: Schematic diagram of the growth of dendrite in an alloy at a fixed position at various stages of solidification.

The Figure 2.9 shows a schematic sketch of the growth of a dendrite during solidification. As can be seen, large dendrite arms grow at the expense of smaller ones as solidification proceeds. Slower the cooling rate during solidification, longer the time available for this mechanism to operate, is resulting in larger dendrite arm. This phenomenon is called the coarsening effect. The effect of the temperature gradient G and the solidification rate R on the solidification microstructure of alloys is summarized in Figure 2.10

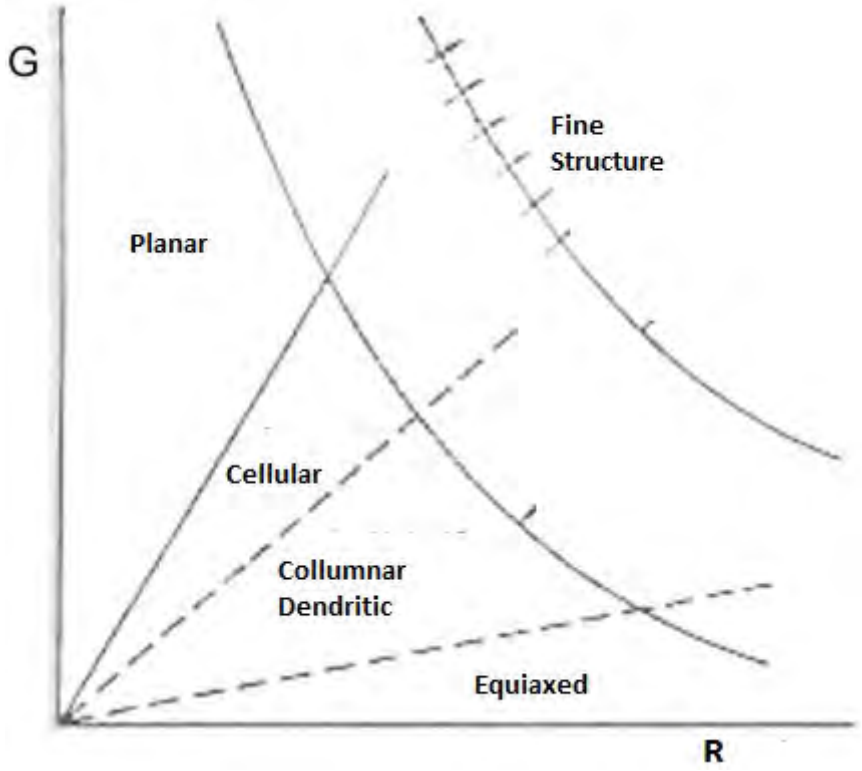

Figure 2.10: Schematic rate-gradient map showing transitions in microstructure as well as the refining effect of high cooling rates.

The product Growth rate is lower for spot weld nuggets than the parent metal since temperature gradient and growth rate is expected to be lower and higher than that of the parent metal, respectively. So, the grain structure in the nugget volume takes on a cast-like columnar and dendritic structure, which is considerably coarser than the grain structure in the parent metal (Figure 2.11).

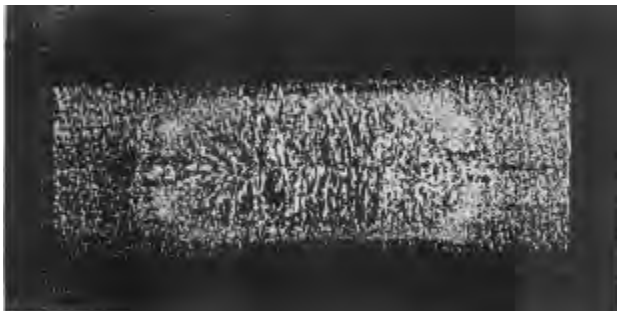

Figure 2.11: Photomicrograph of a grain structure in a good spot weld.

Like other welds, spot welds are subject to shrinkage on cooling. To minimize distortion, welds should be positioned to balance shrinkage forces. Distortion can also result from

electrode skidding. This is related to stress introduced at the time of electrode impact and machine deflection under high electrode force. The components must be designed to provide methods of accommodating variations. Spot-welded assemblies should be designed so that joint areas are readily accessible to the electrode and simple, inexpensive electrodes can be used. Deep, narrow joint areas should be avoided.

The strength of a single spot weld in shear depends on the cross-sectional area of the nugget in the plane of the faying surfaces. A minimum nugget diameter that is unique to the type of the base material, surface condition and metal gage used is required in order to obtain failure by base metal tearing. Increasing the nugget diameter above this minimum value can produce an increase in the weld strength. Figure 2.12 shows the slight increase in strength values obtained for low carbon steel as a result of increases in nugget size.

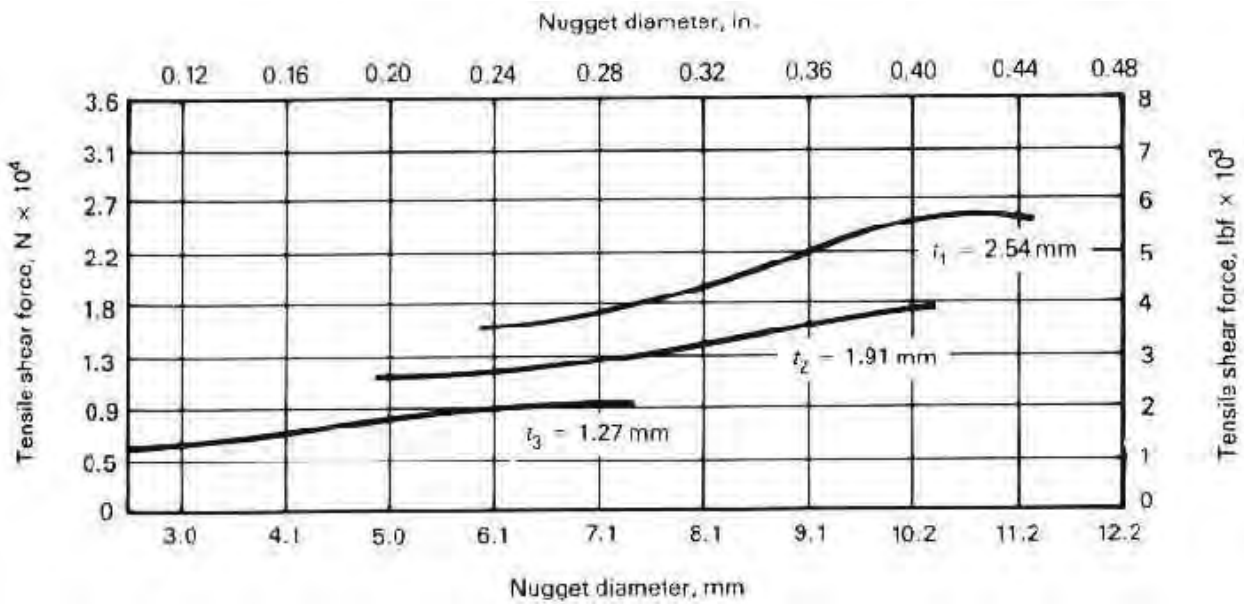

Figure 2.12: Plot of tensile shear strength vs. spot weld nugget diameter as a function of sheet metal thickness, t, for 1008 low-carbon steel.

The strength of multiple spot- welded joints depends on material thickness, spot weld spacing and weld pattern. As the spacing between adjacent spot weld decreases the joint shear strength may decrease.

The size of the spot weld nugget depends on the service conditions and various other attributes. Usually the surface of the spot welded sheet metal has the impression of

indentation (caused by the electrodes) which may cause surface irregularities if electrode pressure is not controlled properly. As seen from Equation 1.1, current flow has a higher effect on heat generation in the welding process because of second order parameter in the equation. Therefore it should also be very carefully controlled. When the current flows through the work pieces and the electrodes, the resistance against the current flow heats up the work piece locally. Due to this thermal load the work piece metal tries to expand in all possible directions except in the transverse direction of the sheet. The applied pressure through the electrodes restricts the metal flow in the transverse direction. So the heated metal usually expands radially in the plane of the sheets.

In general along the radial direction of one spot weld there are three distinct regions.

a) The Base Metal (BM)
b) The Heat Affected Zone (HAZ)
c) The weld pool which becomes the Spot Weld Nugget (SWN) after the completion of the welding process.

The schematic representation of the various zones is shown in Figure 2.13.

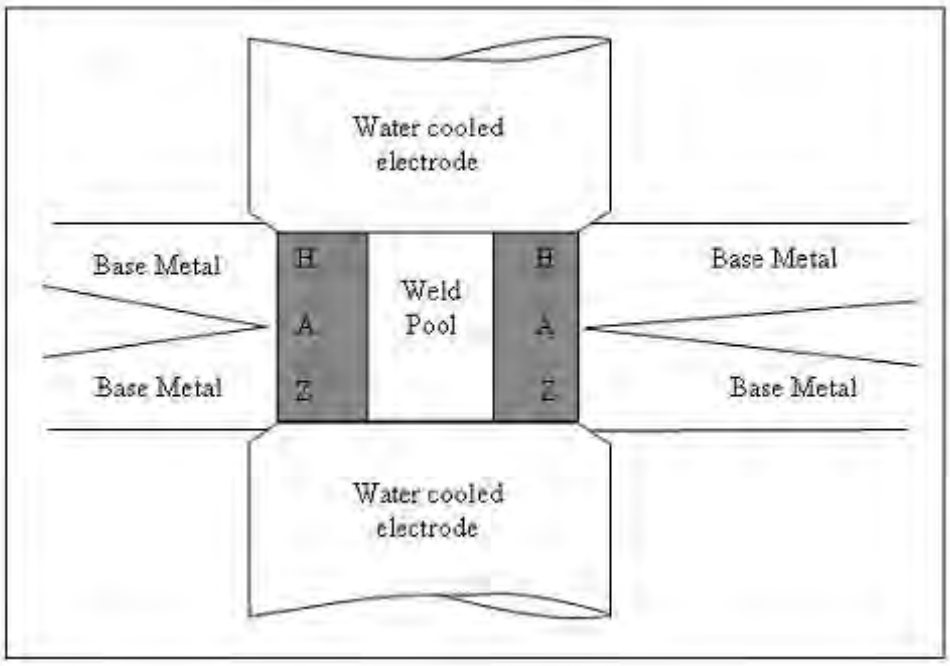

Figure 2.13: Schematic cross section of spot welded sheet metal

Darwish [07] critically examined the microstructure of spot welded low carbon steel. According to the study the key features of the spot welded joints from the metallurgical point of view are:

1) Fusion zone with a columnar dendritic structure.
2) Heat affected zone which shows a gradual transition from a coarse overheated structure through a normalized region to an original structure of unaffected base metal.
3) A narrow ferritic zone in the interface between the overheated and unaffected zones which is not always well defined.

These features are more concisely summarized in the following Figure 2.14.

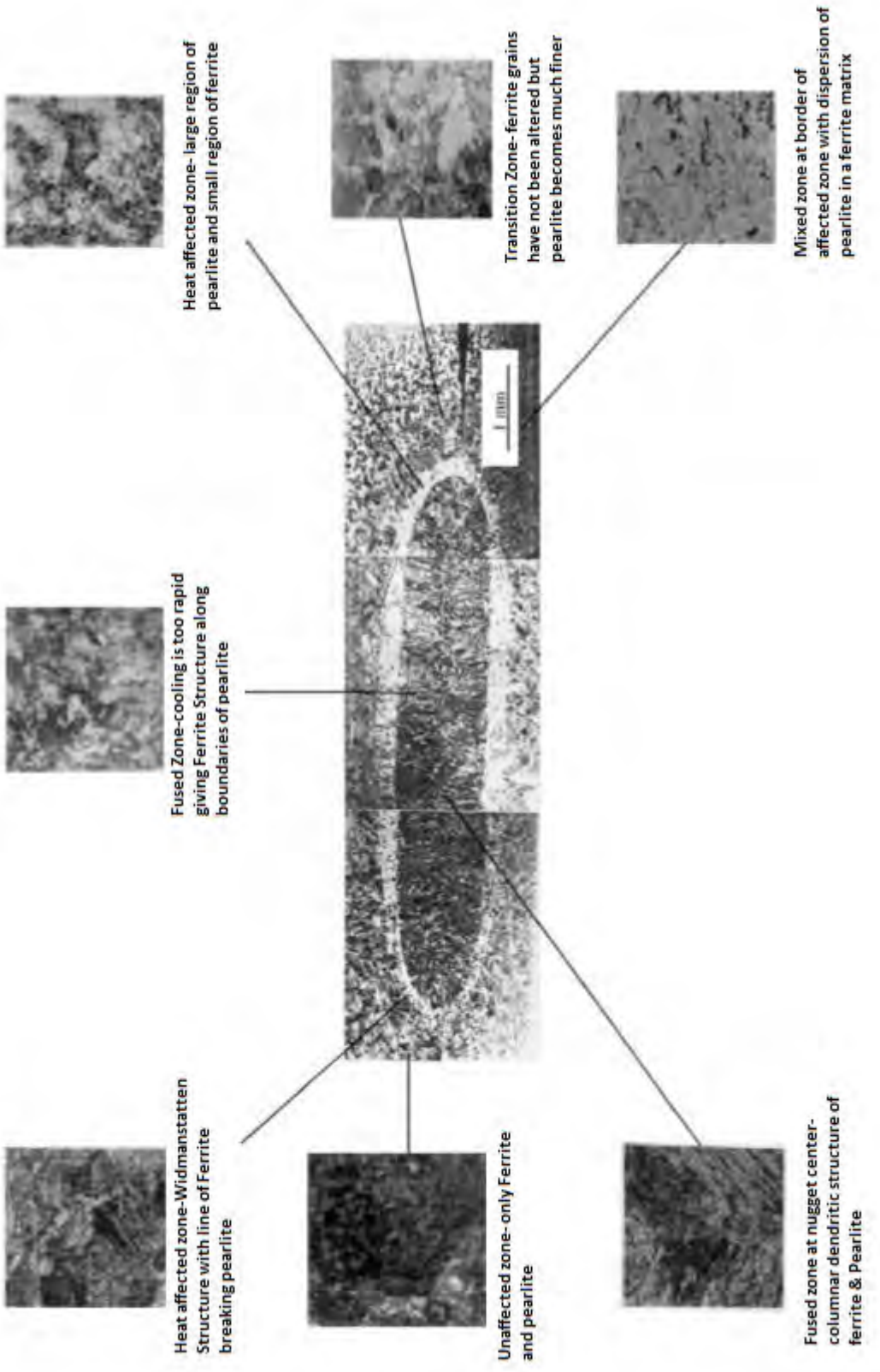

Figure 2.14: Micro structural feature of spot welded low carbon steel

2.5.2 Phase Transformations

2.5.2.1 Fe-C Phase Diagram

The Fe-C phase diagram in Figure 2.15 shows a range below the eutectoid composition of steel (0.8 wt% C) which is typically found in automotive steel alloys. When peak temperatures surpass A_3 a fully austenitized structure is created and subsequently cooled. With slow cooling the austenite volume fraction decreases as regions of soft BCC ferrite nucleate and grow containing small amounts of dissolved carbon within the structure. At the eutectoid temperature (723°C) remaining austenite transforms into pearlite producing a eutectoid structure consisting of ferrite and cementite. Higher cooling rates can bring the transformation temperature below those marked on the phase diagram

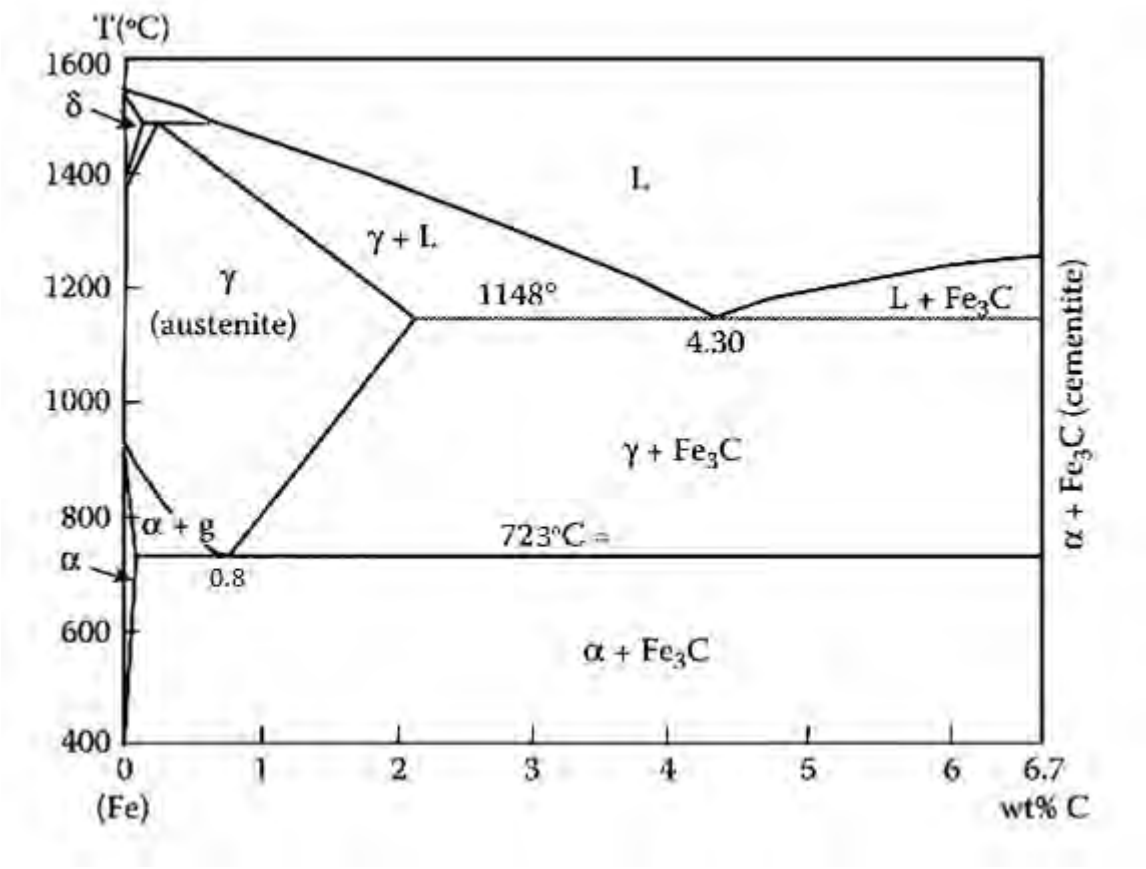

Figure 2.15: Iron carbon binary phase diagram

Significantly higher cooling rates typically experienced during RSW can alter transformation temperatures from those predicted from the equilibrium phase diagram. Depending on the

cooling rate and alloy composition, morphology of phases can alter and form bainite, pearlite or martensite. Rapid cooling during RSW depresses transformation temperatures found on phase diagrams. At lower temperatures this can result in high nucleation combined with reduced growth forming a finer structure. At elevated peak temperatures fully austenitized regions typically transform into martensite. However the binary phase diagram can aid in understanding phase transformations occurring in typical automotive steels.

2.5.2.2 Time-Temperature Transformation Diagrams

Transformation diagrams are important tools which aid in understand the types of microstructures produced during cooling. Since the majority of industrial heat treatments undergo controlled cooling methods rather than isothermal transformations, continuous cooling transformation (CCT) diagrams are more applicable than time-temperature transformation (TTT) diagrams. CCT and TTT diagrams are similar except CCT diagrams encompass a wide range of transformation temperatures while TTT diagrams detail isothermal transformations. A typical CCT diagram for mild steel is shown in Figure 2.16.

Slow cooling rates results in a mixture of ferrite and pearlite. Intermediate cooling has a tendency to produce a ferrite, bainite and martensite mixture. Finally, rapid cooling results in the instantaneous and diffusionless transformation to martensite.

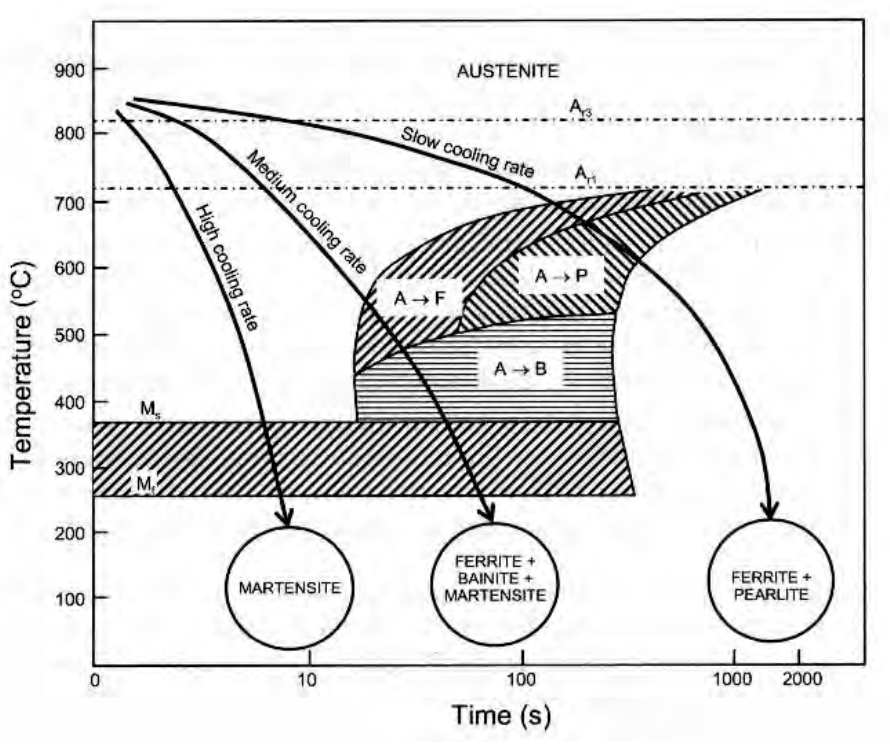

Figure 2.16: CCT diagram for mild steel

Various alloying elements in steel can alter the pearlite nose position in the CCT diagram. Elements such as titanium, tungsten and molybdenum are known ferrite stabilizers and aid in lowering the eutectoid carbon content and raise transformation temperatures. In CCT diagrams these elements raise the pearlite nose and move it to the left, which results in increased time and temperature for pearlite transformations to occur. Other elements, such as nickel and manganese, lower eutectoid carbon content and transformation temperature. These elements, also known as austenite stabilizers, affect the CCT diagram by lowering the pearlite nose and pushing it to the right. Most elements increase the hardenability of steels by moving the CCT curve to the right, allowing martensite to form at lower cooling rates.

2.5.2.3 Carbon Equivalence

The carbon equivalence (CE) value of transformable steels is an index which predicts a materials susceptibility to post-weld cold cracking in the HAZ. The susceptibility of cold cracking is directly related to the amount of martensite within the HAZ. Alloying elements can aid in the formation of martensite by increasing required transformation times and hence the CE provides an index measure of the effects that alloying elements have on the formation of martensite. Multiple CE equations are available in literature each taking into account

numerous alloying elements, which include ferrite and austenite stabilizers. Available equations include the CE developed by Ito which is expressed in Equation 2.1.

$$\mathbf{CE = C + Mn/6 + (Cu+Ni)/15 + (Cr+Mo+V)/5} \qquad \mathbf{2.1}$$

Studies have shown the CE to better suit higher carbon steels with greater then 0.16% carbon. However, the wide range of carbon contents found in AHSS can not be accommodated using one simple equation.

2.6 RSW Characterization

Figure 2.17 shows the relationship between peak temperature during gas metal arc welding (GMAW) and the Fe-C binary phase diagram. Similar peak temperatures and weld regions are attained during the RSW process. A typical fusion weld is composed of the fusion zone (FZ) and heat affected zone (HAZ). Temperatures in the FZ exceed liquidus temperatures, which results in molten material. The HAZ undergoes transformations caused by peak temperatures surpassing eutectoid temperatures. As a result the base metal (BM) microstructure is altered. The HAZ can be subdivided in to three main regions which include the coarse grain (CG), fine grain (FG) and intercritical (IC) HAZ. Peak temperatures in CG HAZ are well above Ac3, transforming BM microstructure into austenite. The FG of HAZ experiences temperatures slightly surpassing AC_3 which results in fine recrystallized grains. Finally, the IC HAZ consists of a partially transformed microstructure caused by peak temperatures ranging between AC_1 and AC_3.

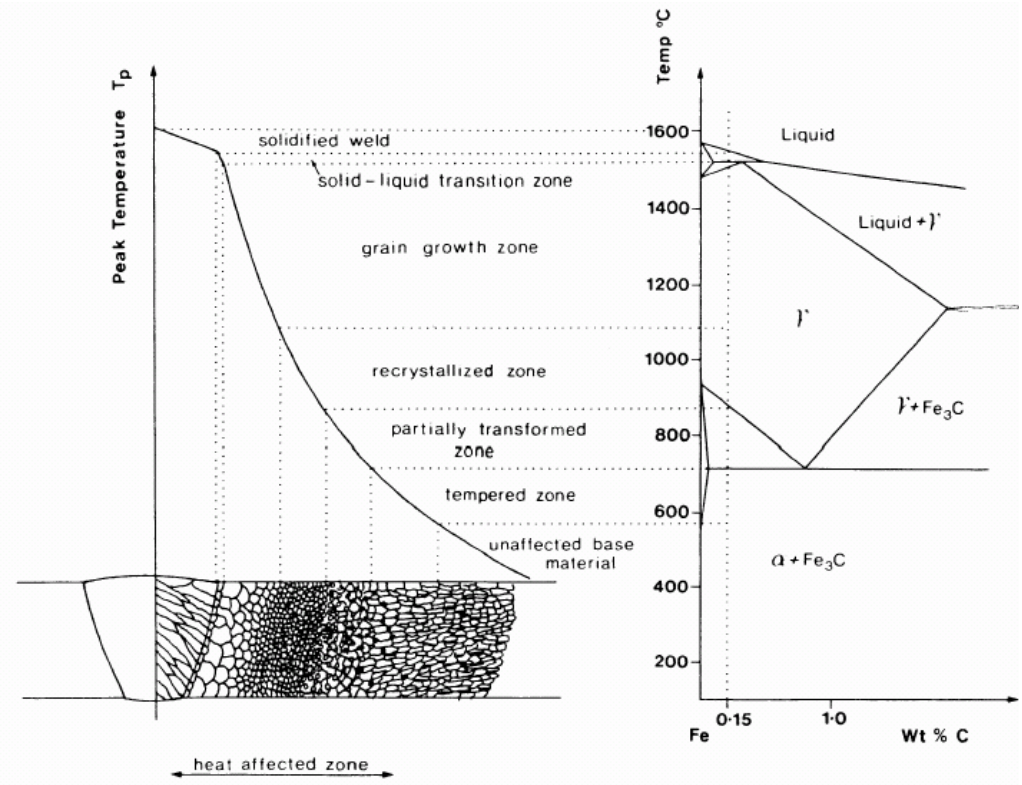

Figure 2.17: Peak temperatures of weld regions

2.7 RANGE OF MATERIALS FOR SPOT WELDING

Spot welding facilitates if:

- There is sufficient contact resistance sheet-to-sheet for heat to be generated by the heavy current flow.
- The heat is not conducted away too rapidly from the point at which welding is desired.

Therefore, that good conductor of heat and electricity such as copper, aliminium or silver present greater difficulties than do iron and steel, which are moderate conductors in comparison.

2.7.1 Spot weld of FERROUS METALS

2.7.1.1 MILD STEEL AND IRON

If the material whether sheet or rolled sections, is clean, little difficulty should be experienced. Low-carbon steel can be satisfactorily resistance welded using a wide range of time, current, and electrode force parameters. Carbon content has the greatest effect on weldability of steels; weld hardness increases rapidly with a small rise in carbon content. To

obtain acceptable weld performance, carbon content should be kept below 0.10% + 0.3t, where ‘t’ is the sheet thickness in inches. For materials above this range, post weld tempering may be necessary.

2.7.1.2 HARDENABLE STEELS (EXCLUDING HIGH-SPEED STEELS)

Only in thin material, the cooling rate from the welding temperature is exceedingly rapid, since the water-cooled electrodes conduct away much heat during the after-weld pressure period. The result of such a high cooling rate is an intense hardening effect on the weld nugget and its immediate surroundings, and such an effect might cause the welds to be brittle and unserviceable. To overcome this trouble with small parts, they are charged into an annealing furnace after welding, so that they are ‘’let down’’ gradually.

2.7.1.3 HIGH-SPEED STEELS

The welding of small pieces of high-speed steels to tool shanks for use in lathes, planers, etc., has received some attention, but it should be pointed out that in this respect spot welding is in nature of a makeshift, since modern electrically butt-welded tools are available with the advantages of cheapness and efficiency.

2.7.1.4 STAINLESS STEELS

These steels are divided into four groups:

1. Ferritic (stainless irons, etc.)
2. Martensitic (cuttery and similar quantities)
3. Austenitic (non-stabilized)
4. Austenitic (stabilized)

These groups behave differently with respect to spot welding, but it is doubtful whether very much spot welding is carried out in Groups 1 and 2.

- Group 1 behaves as mild steel: pressure should be kept on a little longer after welding, however.
- Group 2 has pronounced air hardening qualities and should therefore be treated as hardenable steels.
- Group 3 includes the well known 18/8 variety of stainless steel. Since this particular quality is subject to the phenomenon known as *weld decay*, a

machine of high capacity is to be preferred so that the heating and eventual cooling can take place in the shortest possible time.

- Group 4 has additional elements such as titanium and niobium, the presence of which tends to inhibit weld decay. Such steels, therefore, may be spot welded in the polished condition, and require no further treatment other than a little buffing to remove handling marks.

The short welding period is necessary in stainless steels to prevent carbide precipitation when the carbon content is high enough to permit it.

2.7.1.5 ZINC-COATED STEELS

The present trend in the automotive industry toward the use of larger amounts of zinc-coated steels in assemblies demands that certain strict guidelines regarding the selection of equipment and the choice of welding schedules are rigidly followed. The available welding ranges for zinc-iron and zinc-nickel coated steels are similar to those for uncoated mild steel although displaced toward slightly higher currents. When these steels are coated, it is necessary that the film thickness not exceed 1 to 1.5 μm in order to facilitate breakthrough of the film to enable current flow between the welding electrodes at the low secondary voltages.

2.7.2 NON-FERROUS MATERIALS

2.7.2.1 ALUMINIUM, AL-MAGNESIUM AND AL-MANGANESE ALLOYS

All of these may be spot welded satisfactorily if the insulating skin of oxide is removed and the machine has a sufficiently high capacity since aliminium is a good conductor of heat and electricity and therefore a ‘’difficult’’ metal. In addition, the narrow plastic range between softening and melting means that welding pressures, time and current need to be closely controlled. Moreover, careful control of the electrode force is necessary to minimize the probability of cracking or porosity in the weld.

2.7.3 DISSIMILAR MATERIALS

The dissimilar materials are harder to weld because of their different melting temperatures, thermal and electrical properties, plastic ranges and the alloys formed in the weld region.

However, the majority of the combinations of ductile metals and alloys can be spot welded. Some, like copper to aluminium, and aluminum to magnesium, form alloys having little strength. Others, such as zinc and some of the high-chromium alloys, experience grain growth even during a short welding period. The combination like low carbon steel to stainless steel is also studied by some researchers. Relative spot weldability ratings of selected metals and alloys are given below.

Table 2.1: Relative spot weldability ratings of selected metal and alloys

A: Excellent; B: Good; C: Fair; D: Poor; E: Very Poor; F: Impractical

METAL/ ALLOY	Aluminium	Stainless Steel	Steel	Galvanized Iron	Copper	Brass	Zinc	Nickel
Aluminium	B	F	D	C	E	D	C	D
Stainless Steel	F	A	A	B	A	E	F	C
Steel	D	A	A	B	E	D	F	C
Galvanized Iron	C	B	B	B	E	D	C	C
Copper	E	E	E	E	F	D	E	D
Brass	D	E	D	D	D	C	E	C
Zinc	C	E	F	C	E	E	C	F
Nickel	D	C	C	C	D	C	F	A

2.8 Quality of Spot Welds

The quality of the spot weld depends on many factors. It is a *"loosely defined term"* in literature because of the requirements at the service conditions. In a broad sense the quality of the spot weld can be estimated in

(a) Qualitative manner: The qualitative manner of spot weld quality identification can be described as flawless spot welds which do not have any manufacturing defects.
(b) Quantitative manner: The quantitative manner of spot weld quality identification can be described as the load bearing characteristics of the manufactured spot welds.

The quantitative identification of spot weld quality depends on the qualitative nature to some extent. Hence the spot welding process parameters play an important role for the quality assessment of the spot weld since they influence the nugget formation procedure during the manufacturing stage. According to Equation 2.0, for heat generation in the welding process, the current flow and the time for welding are the two most important parameters. A nominal amount of current is required to flow through the work piece for nominal period of time for the fusion to produce the weld nugget. Generally the shear strength of the weld may vary with the variation of the current flow and weld time during the welding process. The nature of the strength variations are given in Figure 2.18.

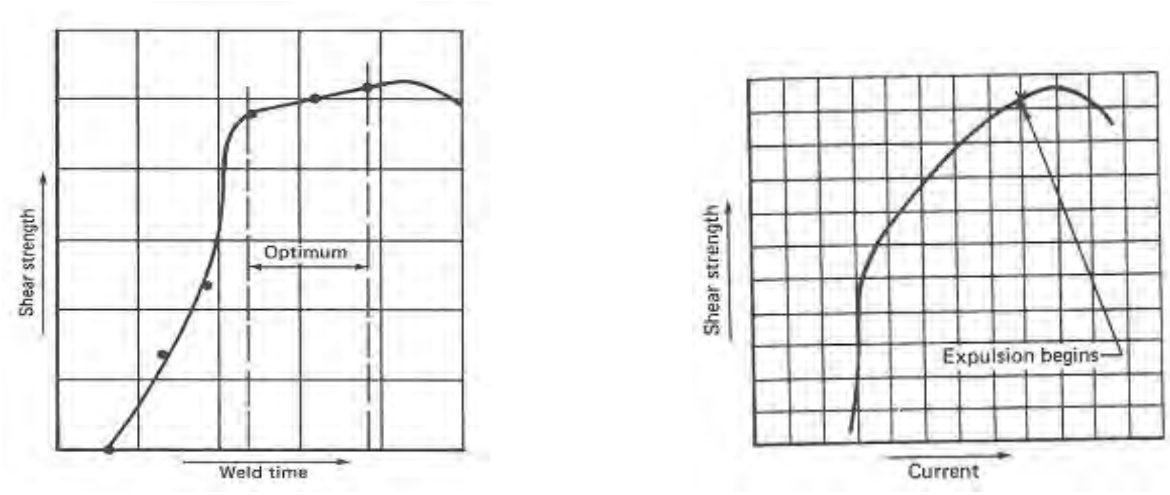

Fig 2.18: Spot weld shear strength variation with weld time and applied current after AWS Welding Handbook (1980)

The most recent study of the effect of process parameters on spot welded joint characteristics was conducted by B. Bouyousfi [08]. A statistical method based on a neural network was employed for this purpose for 304 L type austenitic stainless steel. The statistical model was verified by experiments with a cross tension coupon configuration. Due to utilization of the neural network approach the effect of the process parameters could be determined both individually and in a coupled manner. From the individual study it was shown that the welding force is the most influential factor on the yield strength of the spot welded cross tension sample, rather than the welding current intensity and welding duration (cycle) parameter. In case of the combined study for the welding force, welding current intensity and welding duration (cycle), the later two parameters seem to be insignificant for the strength prediction.

2.9 Mechanical Performance and Microstructure

Tumuluru [09] examined the RSW behaviour of hot-dipped galvanized Dual phase (DP) steel with tensile strengths of 590 MPa, 780 MPa and 980 MPa. As shown in Figure 2.19 the hardness for the 590 MPa steel was 380 Hv, which was slightly higher than the 780 MPa and 980MPa. From this data it was deduced that rapid cooling, which results from the RSW process, causes the formation of untempered martensite in the weld metal shown in Figure 2.20. Furthermore he stated that carbon content of this steel was the main factor which determined the hardness of martensite. Tumuluru concluded that since all three steels contained similar carbon contents they produced similar weld hardness; however, a slight difference can still be noted in the hardness data.

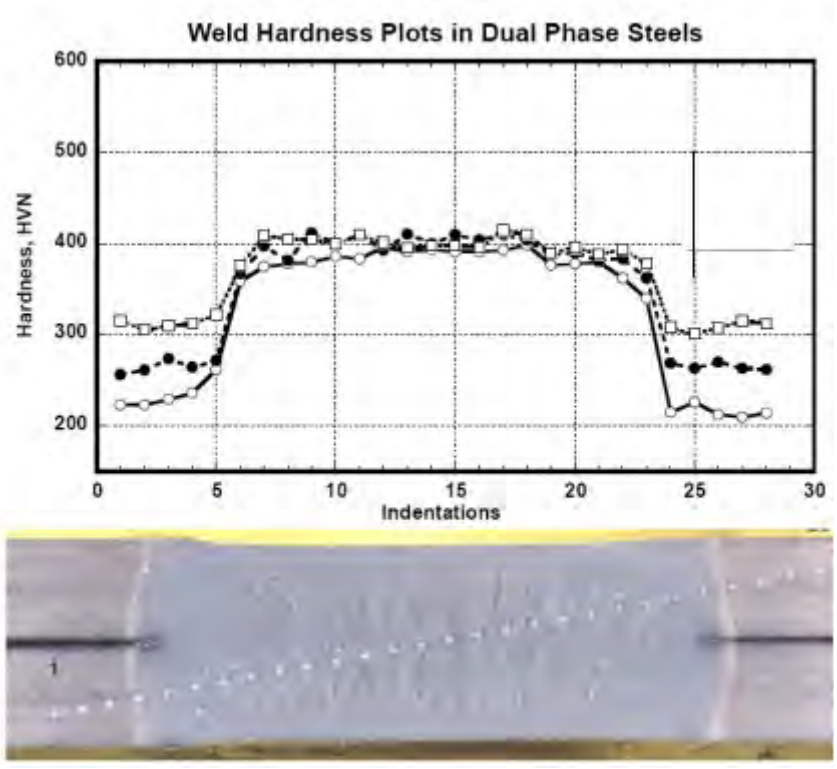

Figure 2.19: Hardness distribution across DP spot welds

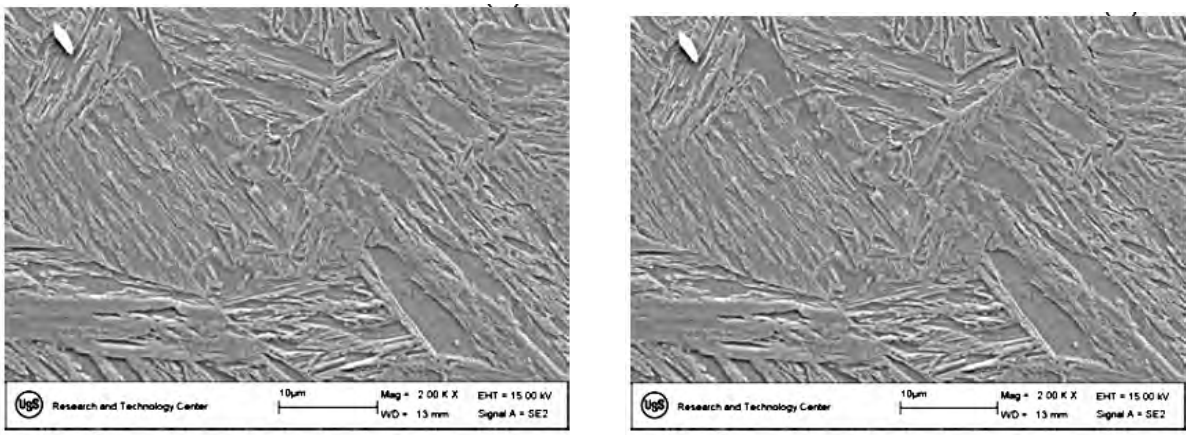

a) 780 MPa b) 980 MPa

Figure 2.20: Weld metal microstructure of RSW DP780 and DP980

Marya [10] investigated the weld fracture in relation to welding parameters for DP600. They used two grades of DP600 which contained different base metal chemistries including a richer 1.8 mm (DP18) and a lean 2.0 mm (DP20). Figure 2.20 shows the general trend where both materials exhibit an increase in weld diameter and failure load with increasing currents. Interfacial fracture was observed for the lower current levels while at higher currents produced button pull-outs. Causes for changes in failure modes were not detailed.

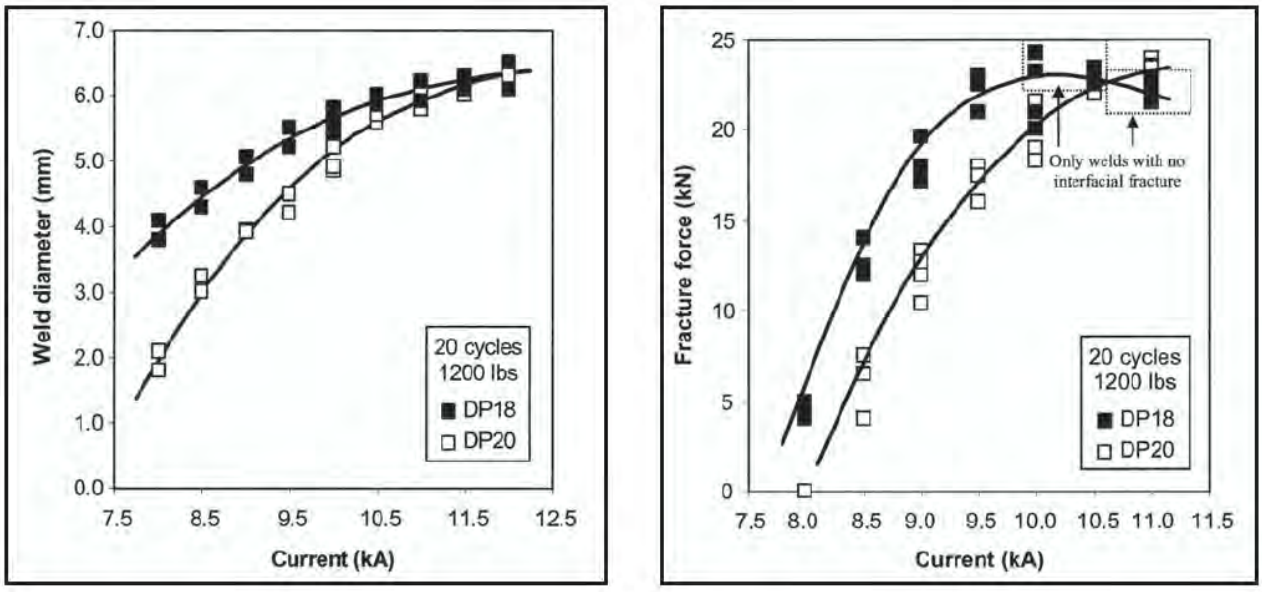

Figure 2.21: Weld diameter and failure load relative to current

Microstructures observed for the DP20 are shown in Figure 2.21. In the outer- HAZ micro-constituents were observed to be considerably finer than in the base metal (Figure 2.21b).

Further into the HAZ large aggregates of blocky phases were presumed to be ferrite (Figure 2.21c). In the fusion zone, (Figure 2.21c) small cracks were present within the predominately martensitic matrix. Dendrites shown in Figure 2.22 were located in large voids at the weld centerline. These voids were said to be caused by solidification shrinkage.

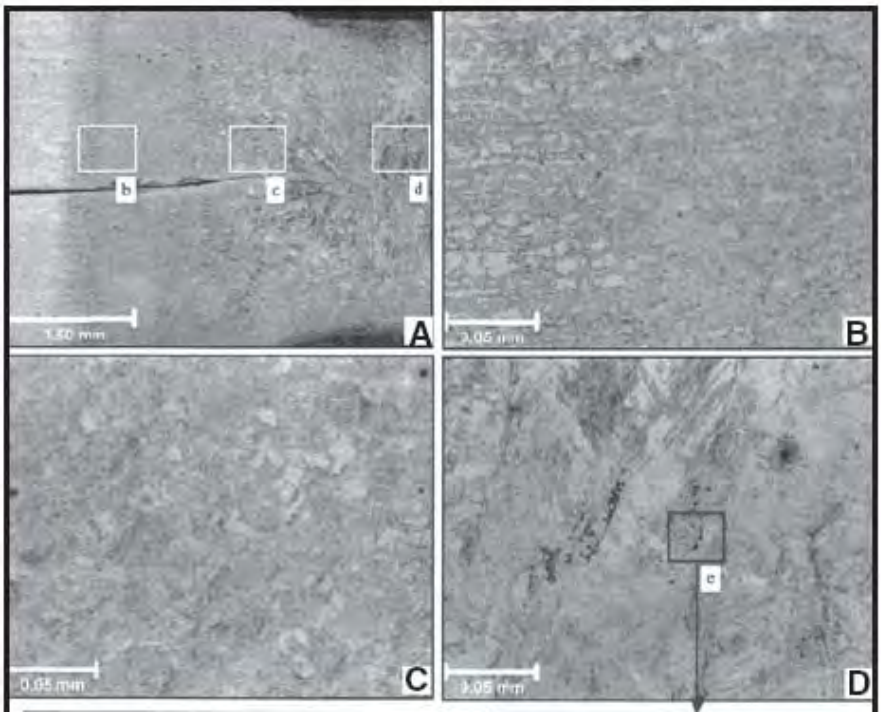

Figure 2.22: Microstructure of DP20 weld metal

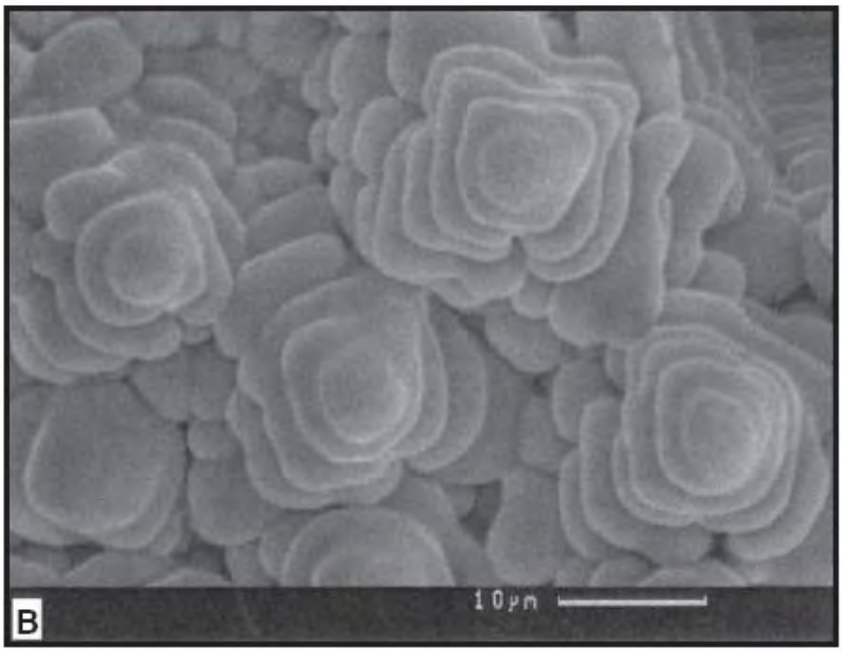

Figure 2.23: Dendrites in solidification voids

2.10 Spot weld failure modes

Failure of spot welds may affect the vehicle's stiffness and noise, vibration, and harshness (NVH) performance on a global level [11]. Therefore, the failure characteristics of spot welds are very important parameters for the automotive industry. Failure mode of resistance spot welds (RSWs) is a qualitative measure of mechanical properties. Figure 2.24 shows the schematic representation of the main fracture mode during mechanical testing of the spot welds. Basically, spot welds can fail in two distinct modes described as follows [12, 13]: Interfacial failure (IF) mode in which the fracture propagates through the fusion zone (FZ) — Figure 2.24A. It is believed that this failure mode has a detrimental effect on the crashworthiness of the vehicles. Pullout failure (PF) mode in which the failure occurs via withdrawal of the weld nugget from one sheet. In this mode, fracture may initiate in the base metal (BM), heat-affected zone (HAZ), or HAZ/FZ (Figure 2.24B) depending on the metallurgical and geometrical characteristics of the weld zone and the loading conditions. Generally, the PF mode exhibits the most satisfactory mechanical properties. Failure mode under which RSWs fail is an indicator of their load-bearing capacity and energy absorption capability. Spot welds that fail in the nugget pullout mode provide higher peak loads and energy absorption levels than spot welds that fail in the interfacial fracture one. To ensure reliability of spot welds during vehicle lifetime, process parameters should be adjusted so that the pullout failure mode is guaranteed. The transition from IF mode to PF mode is generally related to the increase in the size of the FZ above a minimum value. The minimum FZ size is a function of sheet thickness, BM/HAZ/FZ material properties, and loading conditions. Due to its significant impact on joint reliability, the failure mode has been an interesting issue for some recent studies.

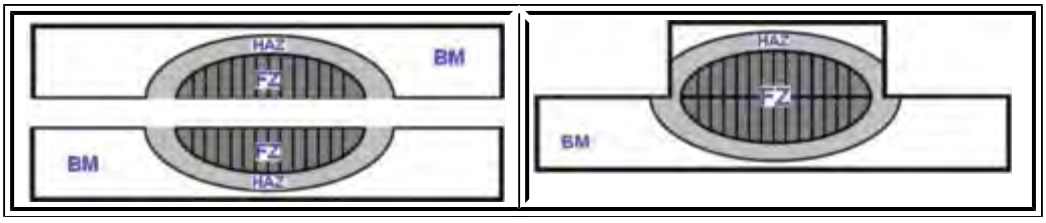

A **B**

Figure 2.24 Schematic representation of typical failure modes during mechanical testing: A — Interfacial; B — pull-out.

VandenBossche [14] had attempted to analyze the state of stress around the spot weld nugget to establish weldability criteria. A lap shear sample joint was used for the investigation. Two different failure modes for the spot welded joint were considered for this study, namely the interfacial mode and the nugget pull out mode. The interfacial mode was designated to be the failure in the spot weld nugget. The nugget pull out mode was assumed for the failure occurrences near the heat affected zone on the sheet metal coupon. For the nugget pull out mode the analysis procedure involved the equilibrium study of the assumed state of stresses caused by the normal and shear loads acting around the nugget on the sheet metal coupon. For the interfacial failure the analysis was done from the point of view of the formation of a plastic hinge at the weld nugget. For both stress states, the equivalent stress was calculated using the distortion energy theory. To determine the transition among the failure modes, the critical nugget diameter - to - thickness ratio was determined utilising the inequality condition.

Later Nakano [15] extended this study to investigate the strain rate effect on the failure of the spot welded joint. In this study the finite element simulation was undertaken along with the analytical approach. It was reported that the failure mode of the spot weld joint was not affected for the account of the strain rate effect. The experimental study of the failure mechanism of a single spot welded joint was undertaken extensively by Zuniga [16]. They studied the weld failure in tensile shear and coach peel coupons made from zinc coated HSLA grade 50 steel with yield stress of 368Mpa and ultimate strength of 425Mpa. Experiments were carried out for overload conditions in quasi static state at stroke rate of 0.0508 mm / sec. Failure of the welds were detected through the force displacement curves obtained from these experimental results together with the optical and Scanning Electron Microscopic (SEM) images of the weld nugget. Most of the specimens for the tensile shear coupon and the coach peel coupon failed in the nugget pull out mode of failure (which can be referred to as the material failure). But the causes of the initiations of failure in these two cases were different. The reason of failure for the tensile shear specimens was due to localized necking near the boundary of the base metal and heat affected zone. However the nugget pull out failure in the coach peel specimen was initiated by micro void coalescence. The fractography study by SEM and optical microscope of the cross sectioned coach peel specimen presented in the paper reveals that the development of excessive blunting of the notch front in the heat affected region caused the micro void.

2.11 TYPICAL DEFECTS DUE TO SPOT WELDING

A defect inversely affects the quality of a spot weld. Hence their reasons and their appearances should be understood carefully to adjust the spot welding process parameters in order to avoid them. The weld issues and their possible causes are given briefly in Table 2.2.

Table 2.2 Spot weld issues and their possible causes [17].
S: Strong Relationship; W: Weak Relationship

	Weld Issues							
No.	**Possible Causes**	**Missing Weld**	**Undersize Weldd**	**Stuck Weld**	**Excessive Indentation**	**Expulsion/ BurnThrogh**	**Cracks& Holes**	**Nonround Weld**
1	Weld current low	S	S	S				S
2	Weld current high				S	S	S	
3	Weld time short	S	S	W				S
4	Weld time long				S	W		

2.12 Summary

Many researchers investigated resistance spot welding of similar metal. There are many established data set up for similar metal like low carbon steel, stainless steel or non ferrous steel. But it is very important and interesting to study resistance spot welding of dissimilar metals. Above all discussion is shown different properties and characteristics of similar metal. Here we try to find different parametric effect on dissimilar spot welded low carbon steel to austenitic stainless steel and compare this with another material.

Mechanical properties of sheet metal promises improved crash performance and reductions in weight for automotive applications. The RSW process provides a quick and effective method for spot welding sheet steel and has been largely adapted in the automotive industry. The

various parameters involved in RSW can influence the weldability and mechanical performance of weldments. Some key parameters include:

1) Welding Force
2) Welding Time
3) Welding Current

Much of the literature can explain the effects of zinc coatings, electrode degradation and the weldability of traditional AHSS and other material. In depth examination and comparison of RSW low carbon steel to austenitic stainless steel as dissimilar metal is yet to be conducted. The majority of studies conducted on dissimilar metals are limited to process optimization. In turn, minimal work has been done to understand the metallurgical aspect of RSW dissimilar metals resistance welding. M. Mansouri [18] said that compared to similar welds, weld nugget of dissimilar Stainless steel (SS) / carbon steel (CS) RSWs has two distinct features: Asymmetrical shape (FZ size of SS side is greater than that of for CS side due to its higher resistivity) and shifting of final solidification line from sheet/sheet interface into the SS side. As a direct result, the mechanical performance of dissimilar SS/CS is determined by FZ size of CS side. In joint dissimilar RSWs of low carbon and austenitic stainless steel, microstructure and hardness of the fusion zone which are controlled by dilution and fusion zone size of low carbon steel side mainly govern the failure mode. By increase in welding current, increasing fusion zone size coupled with the formation a martensitic fusion zone will lead to transition from interfacial to pullout failure mode. It was shown that generally there is a direct relation between mechanical performance (peak load and failure energy) and FZ size of low carbon steel side. The peak load of CS/CS and SS/LCS was nearly same due to the fact that the pullout failure mode of SS/CS welds is initiated from CS base metal. However, the failure energy of the later was greater than the former weld which is a function of higher ductility of SS that helps increasing plastic deformation during process of pullout failure. M. Pouranvari [19] has noted that dssimilar RSW between low carbon galvanized steel and austenitic stainless steel asymmetric fusion zone was obtained due to their different electrical resistivity and thermal conductivity. Fusion zone size and failure mode are the most critical factors in the weld quality in terms of peak load and energy absorption which is governed by the welding parameters such as welding current, welding time and electrode force. Spot weld strength in the pullout failure mode is controlled by the strength and fusion zone size of the galvanized steel side. The hardness of the fusion zone which is governed by the dilution between two base metals, and fusion zone size of galvanized carbon steel side govern failure

mode. For spot welds made at low welding currents, low fusion zone hardness and small fusion zone size led to experiencing interfacial mode during shear-tensile test. While for spot welds made at high welding currents, higher hardness of fusion zone due to martensite formation and larger fusion zone led to experiencing pullout failure mode during tensile-shear test. This thesis examines the metallurgical and mechanical properties of RSW dissimilar metals.

From above discussion, it was clear that the spot weld nugget diameter is the most critical parameter to determine the mode of failure for the spot welded joint. Detailed analysis of microstructure and mechanical performance of welded dissimilar metals is conducted to attain an in depth understanding of phase transformation caused by weld thermal cycles. Finally, this is a comparative study was done on spot welded low carbon steel to austenitic stainless steel RSW process.

Chapter 3

Experimental Procedure

3.1 Introduction:

Resistance Spot welding is frequently used for a variety of work commonly in automotive and other manufacturing processes. Dissimilar metal welds are also important and their performance is often crucial to the function of the whole structure. If the quality of the products is considered, it is clear that the quality of a product is directly related to the quality of spot weld. However, Spot welding process contains several parameters that are not easily controlled. Since these variables directly affect the quality and integrity of the weld joint monitoring is necessary to achieve weld quality.

This chapter presents the methodology of the experimental study undertaken to analysis the spot welding behavior of dissimilar metal welding such as low carbon steel and austenitic stainless steel under different current and welding cycle. The majority of the researcher investigates the joining of similar sheet metal of with spot welding. However in many applications spot welds are made between dissimilar metals to tailor the mechanical properties as per local requirements. The aim of this study is to determine the criteria for selecting optimum condition of spot welding with dissimilar combination and to characterize the properties accordingly. Metallographic investigation, micro hardness measurement, tensile shear tests were performed here. Failure mode of this dissimilar metal weld was also analyzed.

3.2 Material Selection:

In this study the properties of resistance spot welds between low carbon steel and austenitic stainless steel sheet were determined. Materials were collected from the local market. The chemical compositions of the sheet metals are evaluated using an optical emission spectrometer (Model: FOUNDRY MASTER PRO) in Pilot Plant and Process Developed Centre (PP & PDC), BCSIR, Dhaka, Bangladesh. Surface preparation is critical, and particular care is required in sample preparation to ensure a clean flat surface for OES measurement. The surface finish should be smooth, with only fine tool marks, and should be

the same as the reference sample. Chemical composition of these two materials is given below.

Table3.1: Chemical composition of the selected Sheet metals

	%C	% Mn	%Si	P	S	Cu	Cr	NI	Mo
LCS	**0.03**	**0.20**	**--**	**0.01**	**0.003**	**0.01**	**0.02**	**--**	**--**
ASS	**0.04**	**0.10**	**0.50**	**0.04**	**0.002**	**0.16**	**17.83**	**8.41**	**0.13**

Figure3.1. Optical emission spectrometer

3.3 Specimen dimension:

Material thickness is around 1.5 mm. the test coupon were cut as per guideline specified for this range of thickness in ‘recommended practice for test methods for evaluating the resistance spot welding behavior of automotive sheet steel materials(ANSI/AWS/SAE/D8.9-97) [1] all of the steel sheets were of the same batch for their respective thickness.

T (mm)	W (mm)	L (mm)
T < 0.8	16	76
0.8 – 1.3	19	76
1.3 – 2.5	25	102
2.5 – 3.3	32	127
3.3 – 4.8	38	127
T > 4.8	51	152

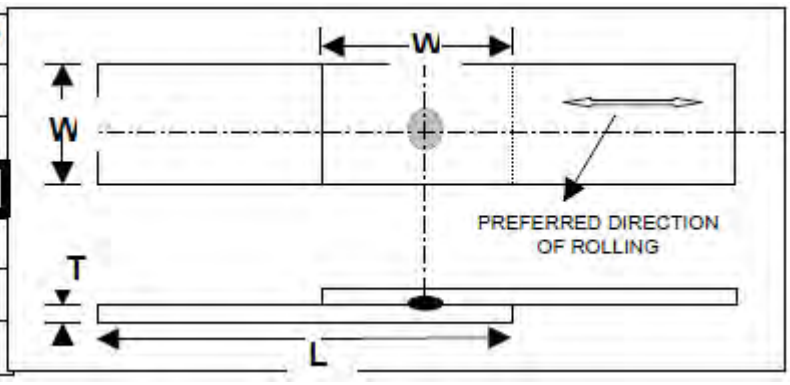

Figure3.2. Standard dimension of tensile test specimen as per ANSI/AWS/SAE/D8.9-97.

3.4 Welding equipment: Resistance spot welding set up:

The resistance spot welding samples are produced by using a 5 KVA pneumatically operated single phase resistance spot welding machine with constant current control and a frequency 50 HZ.

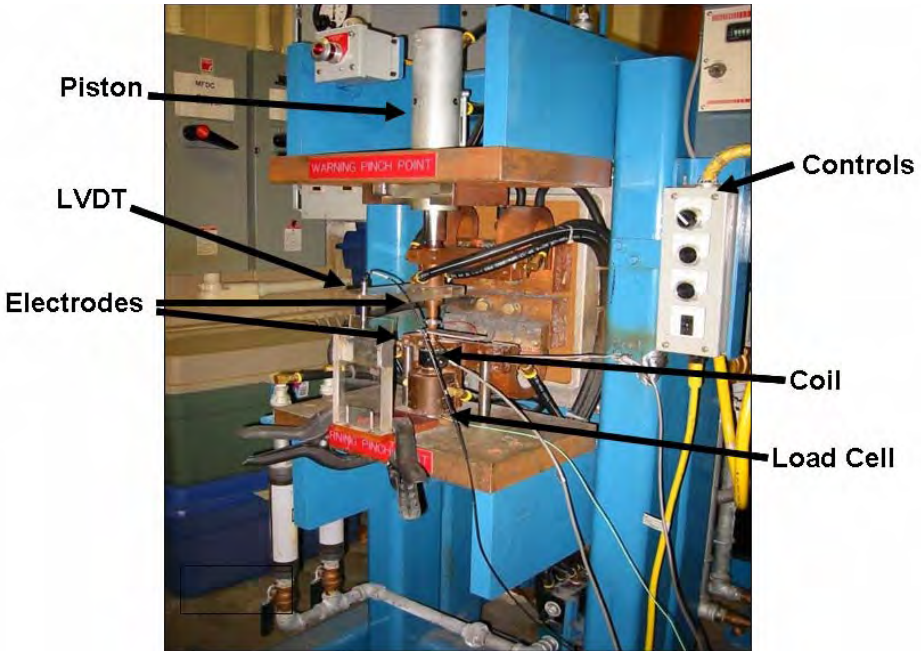

Figure3.3. Resistance Spot Welding Machine

Figure3.3. Show the resistance spot welding machine. Welding was conducted using 45µ truncated cone type electrode with 7 mm face diameter. Total number of welds per electrode was monitored to stay below the electrode degradation limits. Cooling water flow rate and holding time of the machine also followed AWS recommendation of 6 l/min and 5 cycles respectively.

3.5 Sample preparation for welding parameter optimization:

It is well known that expulsion reduces the strength of a spot weld due to the smaller size of the nugget formed and the porosity of the nugget. The welding parameters and the weld ability diagrams were determined in this study after several welding trial. Electrode force was kept constant during the test. Welding current and welding time were changed during weld ability studies. Welding current was increased step by step and welding time kept constant then the welding current was kept constant and welding time increased step by step. The process parameters are given below (Table 3.2).

Table 3.2: Parameters for welding dissimilar steels

Welding Current (KA)	Welding time (Cycles) 1 second= 50 cycles	Identified as
9	90	Sample 1
7	90	Sample 2
5	90	Sample 3
3	90	Sample 4
9	70	Sample 5
7	70	Sample 6
5	70	Sample 7
3	70	Sample 8
9	50	Sample 9
7	50	Sample 10
5	50	Sample 11
3	50	Sample 12
9	30	Sample 13
7	30	Sample 14
5	30	Sample 15
3	30	Sample 16

By using these parameters we prepared sixteen sets of samples. All these samples use for mechanical and metallographic experiment.

3.6 Determination of nugget diameter of spot welds:

For parameter optimization, the most crucial dimension to be determined is studying the nugget diameter of spot welded coupons and it plays the vital role in determining the mode of failure of the joint. Several standards are set to determine the nugget dimension for a particular sheet metal thickness. Several researchers have also proposed mathematical equation for the calculation of these standards and calculation were based upon the lap shear coupon configuration. American welding society (AWS), American national standards institute (ANSI) and Society of Automotive Engineers (SAE) jointly recommended the size of the spot weld nugget diameter for the steel according to the following equation

$$\mathbf{d = 4\sqrt{t}} \quad \ldots\ldots\ldots\ldots\ldots\ldots 3.1$$

Where d and t is the nugget diameter and sheet thickness in mm respectively.

For process parameter optimization of spot welded dissimilar metal, it is very important to find desirable nugget diameter of the weld sample like theoretical value and that is ensure the proper nugget diameter. One set of spot welded sample use for determining the diameter of the welding nugget. The measuring process was conducted by cutting of transvers section through the welding and measured the maximum length of the nugget and checks this size by optical microscopy and scanning electron microscopy of the cross section of the spot welded coupons. Dissimilar welded metal showed asymmetrical weld nugget which contain heat affected zone and complete fusion zone so measuring of weld nugget is not to easy we are trying to find weld nugget dimension by following Figure 3.4 and these results are ensure by hardness measurement at different point of the weld nugget.

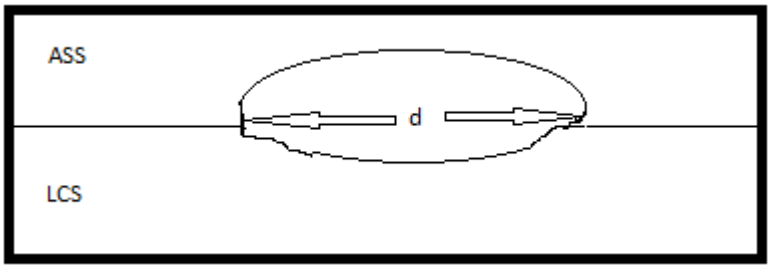

Figure 3.4: Measuring of Weld nugget (d).

3.7 Mechanical Testing

Several mechanical testing such as tensile test, micro hardness tests were performed to find out the properties of the resistance spot welded dissimilar metal. From the fractured sample we can study about failure mode of spot welded dissimilar metal.

3.7.1 Tensile Share test:

Joint mechanical properties at different process parameters were evaluated by measuring the maximum load to failure during overlap tensile shear testing. Care was taken to maintain co-planar alignment during mechanical testing. This test consists of pulling in tension to destruction on Instron 3369 universal testing machine (Figure 3.5). minimum four tests are performed randomly for every sets to determine final tensile properties.

Figure 3.5: Universal testing machine (Instron 3369).

Dimension of the tensile specimen (Figure 3.6) is 102 mm length and 25 mm width and this is follow AWS standard.

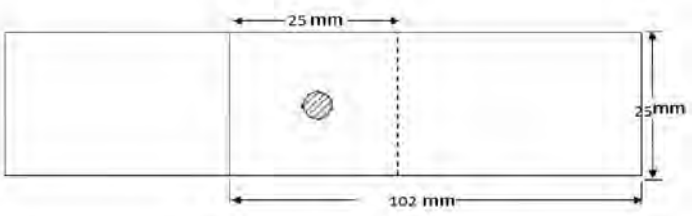

Figure 3.6: Dimension of the tensile test specimen

3.7.2 Failure mode analysis:

The fracture surface of the tensile test specimens were examined using by SEM fractography, optical electron microscopy and physical observation. Detailed examination of failure mechanism was also facilitated by interrupting the loading cycle during overlap shear testing. I.e. By halting the tensile testing machine when the welded section only partially failed. This technique allowed detailed examination of the nature of failure propagations during failure of particular joints. Finally, the projected cross sectional area of the bonded region was measured by digital image analysis.

3.7.3 Hardness Test:

To conduct the micro hardness test, a micro hardness testing machine Shimadju is used (figure 3.7). The basic equation to measure the hardness of any material is as follows

$$HV=1.854(F/d\ 2)\ldots\ldots\ldots\ldots\ldots\ldots\ldots 3.2$$

Where HV is the hardness value, F is the force and d is the average diagonal distance of the indentation in mm. The calibrated force is used for measuring hardness for the chosen material the distance between the consecutive indentations along the radial direction from the spot weld nugget for the hardness testing was taken as 1 mm. The test set up is shown in the following figure (Figure 3.8).

Figure3.7: Hardness testing machine

Figure3.8: Hardness testing of welded sample (a) testing set up (b) indentation marks

Using proper level of force the hardness value was measured in various directions around the spot welding nugget. In this experiment we use 500 gram load and 6 second for indentation time. Hardness value of the base metal is taken in around 5 mm apart from the heat affected zone.

3.8 Metallographic Examination:

Sample preparation is an essential part of microscopy and there are many techniques (and variations) that can be used. The approaches very commonly used to prepare specimens for analysis are as follows: The sample needs to be cut to size using one of the slicing methods outlined. The cut sample is either set in a mold or mounted externally on a polishing mount. This step is followed by a series of coarser to finer grinding on SiC grit paper. For optical microscopy and SEM, subsequent fine polish is done using alumina suspension. Polished samples are then cleaned thoroughly and etched chemically or thermally to reveal surface contrast.

During Sample preparation all welding dissimilar metals are cut through longitudinal direction of the weld nugget. Then all cross section are etched by appropriate etching reagent to distinguished the different phase in the fusion zone, heat affected zone and thermo mechanically affected zone of resistance spot welded dissimilar metal. Here we are using two different etching reagent one is 2% nital and another is aqua rezia.

3.8.1 Microscopy:

Optical microscope was used to observed metallographic samples and fracture surfaces respectively. Here we use **Optika** microscope (Figure 3.9) for metallographic observation and imaging of the structure.

Figure3.9: Optical microscope

3.8.2. Scanning Electron Image Analysis

The SEM can automatically perform image analysis and with the advanced of chemical characterization using Energy Dispersive X-ray (EDX) detector (Model No: XL-30). All cross sectional surface (heat affected zone, fusion zone), and fractured surface found form tensile test were observed in SEM. Nugget diameter also measured By SEM analysis. Dilution of chemical component like chromium, nickel etc in the fusion zone of dissimilar welded metal also analysis by EDX technique.

Operating condition:

1. Specimen was placed on the stage of the scanning electron microscope so that the specimen surface is perpendicular to the optical axis.
2. Images were examined by using magnifications of 10000X.
3. Images were chemically micro-analyzed by use of energy dispersive x-ray detector.

Chapter 4

Results and discussion

4.1 Macro structural observation:

Macroscopic view of the cross section of resistance welded dissimilar metal is shown in Figure 4.1. It is clear that weld nugget of the dissimilar metal welded coupon is of asymmetrical shape and also found that final solidification line shift from sheet/sheet interface in to the austenitic stainless steel side.

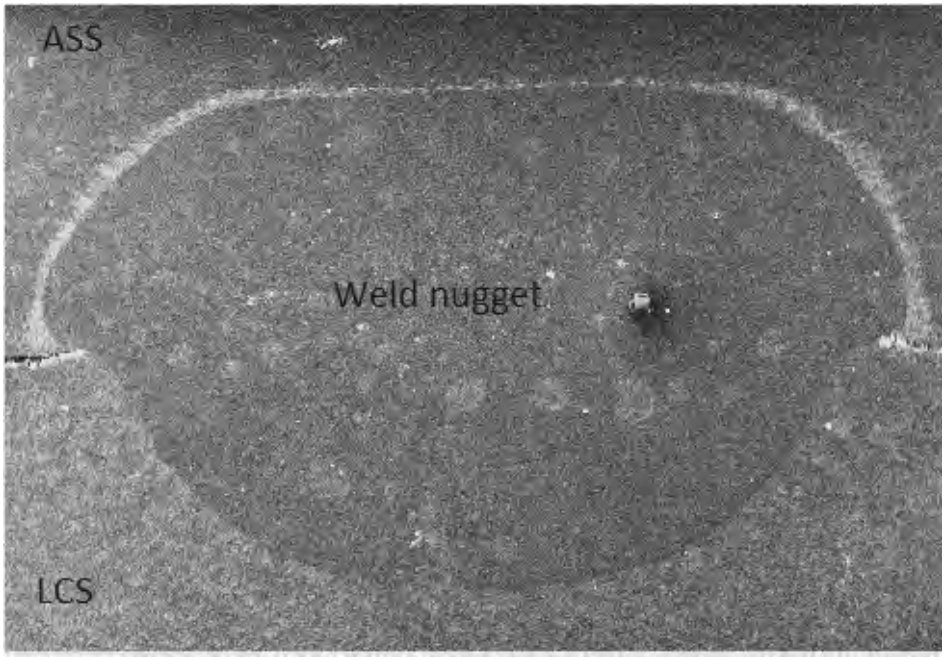

Figure: 4.1 Asymmetrical weld nuggets from dissimilar metal spot welding.

The fusion zone size and penetration depth of the austenitic stainless steel is higher than low carbon steel side. It can be seen that welding parameters have an important role on fusion zone size. An increase in welding current increases weld nugget size significantly at constant weld cycle but with respect to weld cycle no significant change occurs in fusion zone size, both of these discuses in section 4.2.

Different electrical resistance and thermal conductivity is found at different metal sheets and this is the main cause of asymmetrical weld nugget. Thermal expansion coefficient is another

property of the material which affect on welding property. So the different property of electrical resistivity, thermal conductivity and thermal expansion coefficient is the main cause of asymmetrical weld nugget. The Thermal conductivity coefficients are higher in low carbon steel (51.9 $Wm^{-1}K^{-1}$) as compare to austenitic stainless steel (16.2 $Wm^{-1}K^{-1}$). The electrical resistivity of low carbon steel is 1.59×10^{-7} Ω.m where as austenitic stainless steel value is 6.89×10^{-7} Ω.m. thermal expansion coefficient of austenitic stainless steel is 17.2×10^{-6} K^{-6} where as low carbon steel have lower thermal expansion coefficient 11.9×10^{-6} K^{-6}. Technically this phenomenon is called heat imbalance [20]. This heat imbalance makes asymmetrical weld nugget. This result was found by different researchers. Monsouri, Majid P [18] found that compared to similar welds, weld nugget of dissimilar SS/CS RSWs has two distinct feature: Asymmetrical shape (fusion zone of SS side is greater than that of for CS side due to its higher resistivity) and shifting of the final solidification line from sheet/sheet interface to the SS side. As a direct result, mechanical performance of dissimilar SS/CS is determined by FZ size of CS side.

4.2 Weld nugget dimension:

Resistance spot welding was done by using resistance heating and application of force without using filler metal. Dissimilar metals, austenitic stainless steel and low carbon steel were welded, so the weld nugget was asymmetrical in shape. The coupons were checked after spot welding to determine the weld nugget diameter (Figure 4.2). The checking process was conducted by optical microscopy and scanning electron microscopy [discussed in chapter 3 Section 3.3].

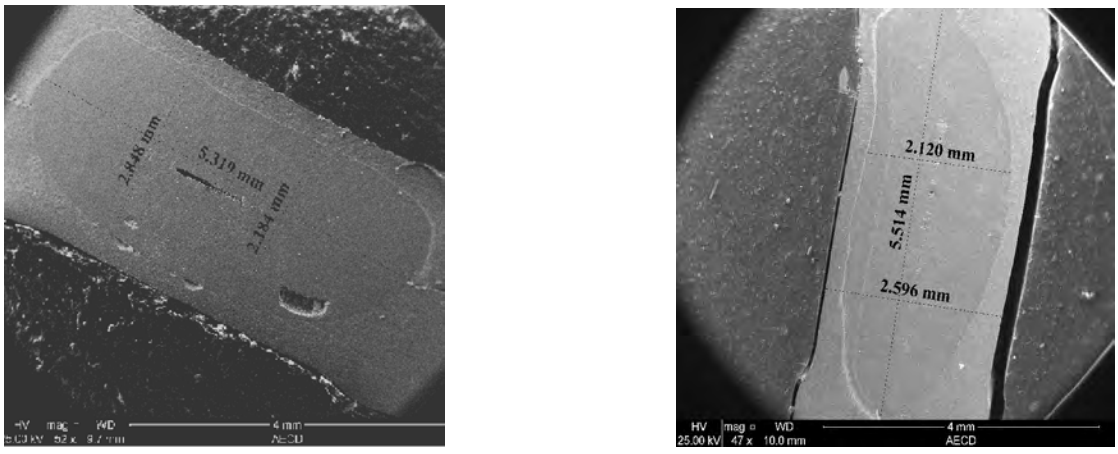

(a) (b)

Figure 4.2: Measuring process of weld nugget by Scanning electron microscopy.

(a) Sample S-3 (b) Sample S-13

Here we found different size of the weld nugget at different welding parameter. These results are shown in the figure 4.3 to 4.18.

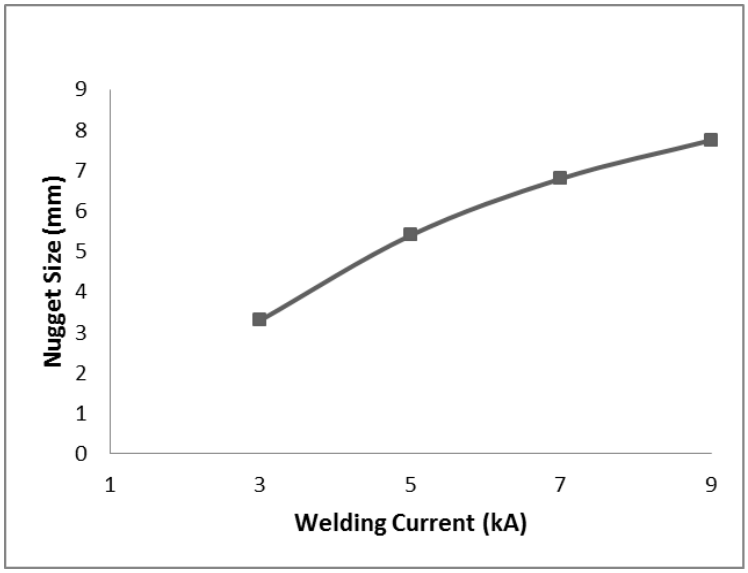

Constant weld Cycle: 90 cycle		
Sample No	Current KA	Nugget Size mm
S-1	9	7.75
S-2	7	6.8
S-3	5	5.4
S-4	3	3.3

Figure 4.3: Weld nugget dimension at 90 Cycle, but different weld current

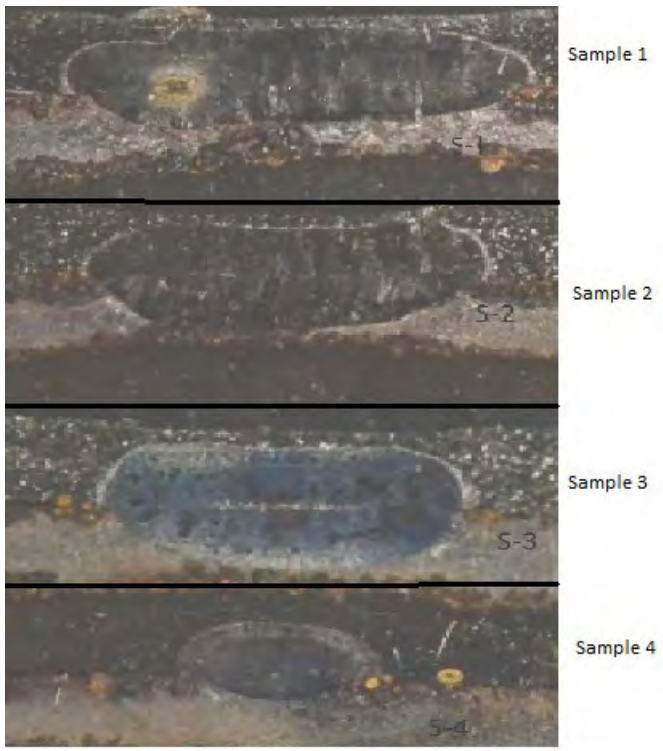

Figure: 4.4 Effect of welding current at constant weld cycle [90 cycles] in macroscopic view.

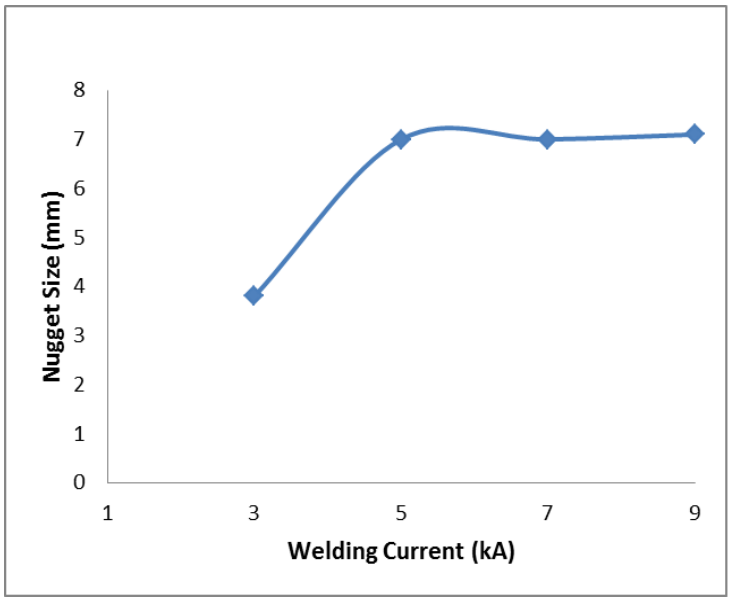

Constant weld Cycle: 70 cycle		
Sample No	Current KA	Nugget Size Mm
S-5	9	7.1
S-6	7	7
S-7	5	7
S-8	3	3.8

Figure 4.5: Weld nugget dimension at 70 Cycle but different weld current

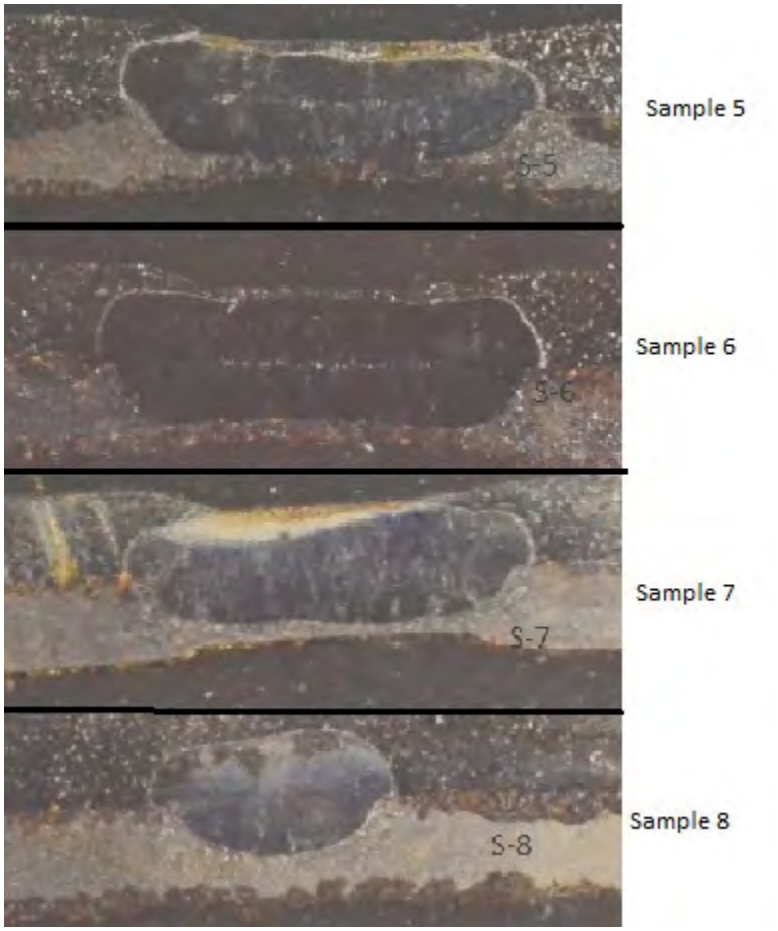

Figure: 4.6 Effect of welding current at constant weld cycle [70 cycles] in macroscopic view.

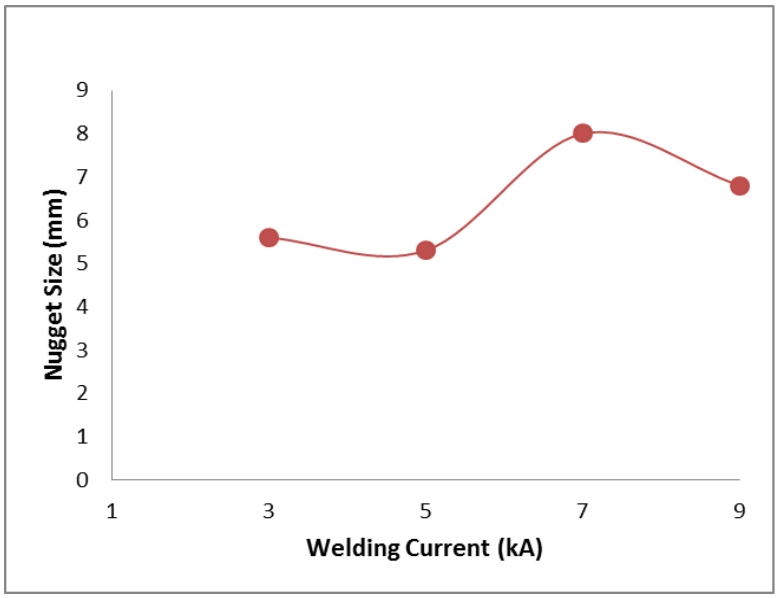

Constant weld Cycle: 50 cycle		
Sample No	Current KA	Nugget Size Mm
S-9	9	6.8
S-10	7	8
S-11	5	5.3
S-12	3	5.6

Figure 4.7: Weld nugget dimension at 50 Cycle but different weld current.

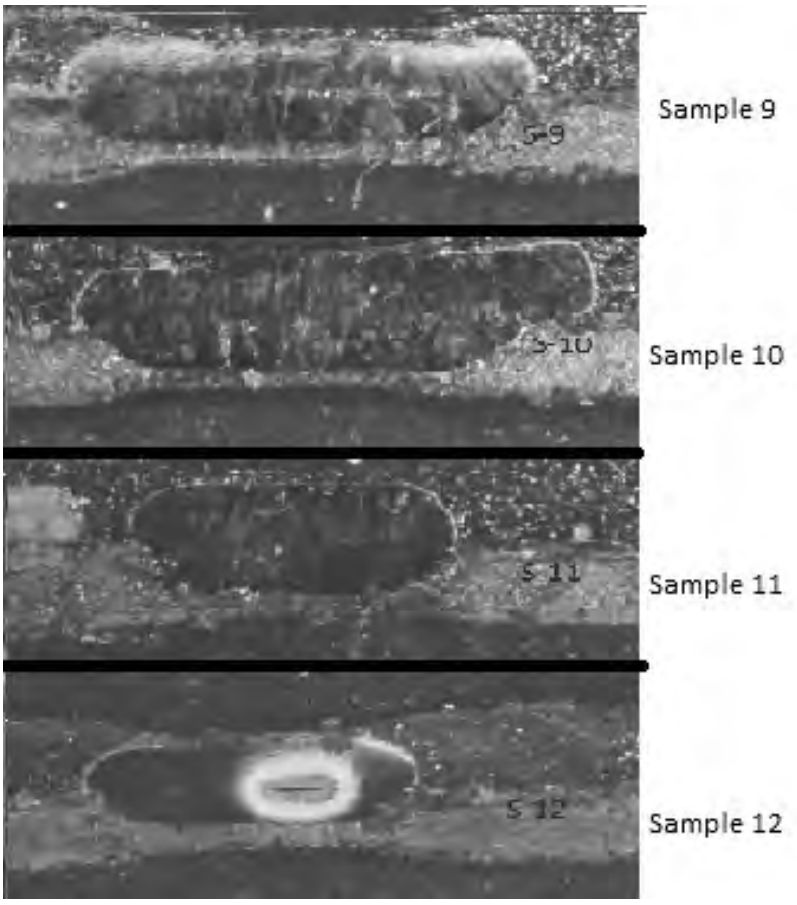

Figure: 4.8 Effect of welding current at constant weld cycle [50 cycles] in macroscopic view.

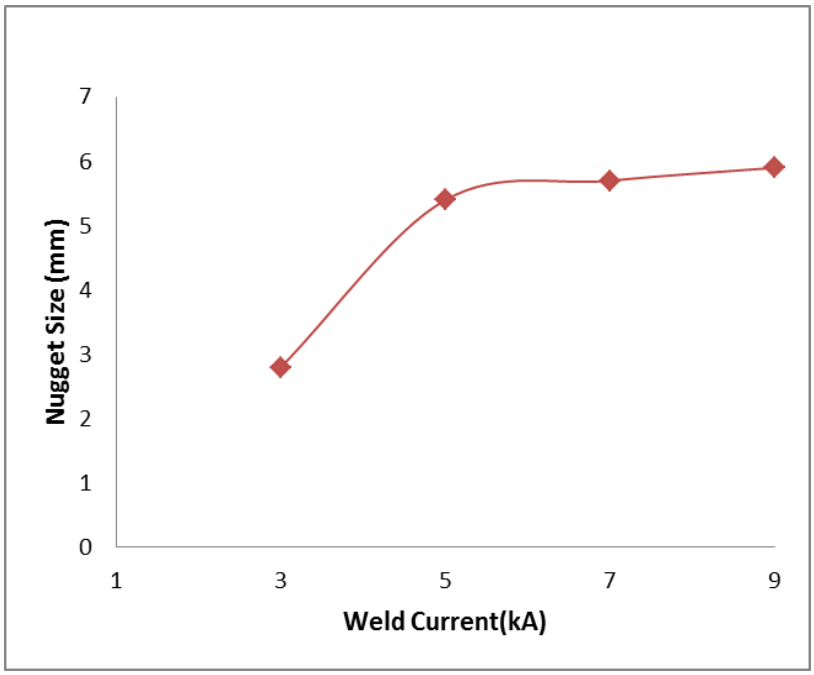

Constant weld Cycle: 30 cycle		
Sample No	Current KA	Nugget Size Mm
S-13	9	5.9
S-14	7	5.7
S-15	5	5.4
S-16	3	2.8

Figure 4.9: Weld nugget dimension at 30 Cycle but different weld current.

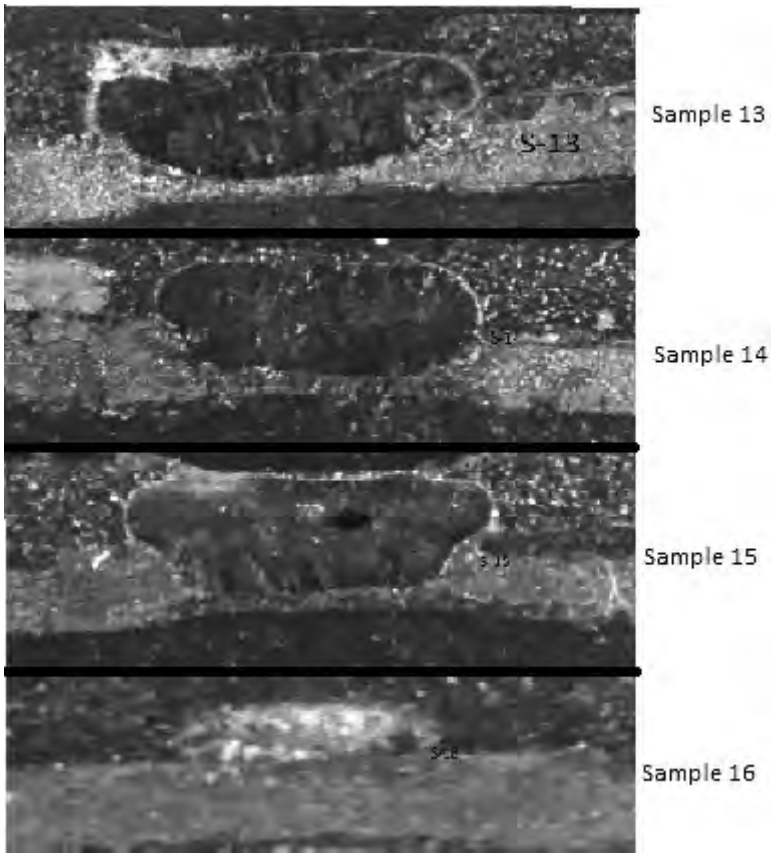

Figure: 4.10 Effect of welding current at constant weld cycle [30 cycles] in macroscopic view.

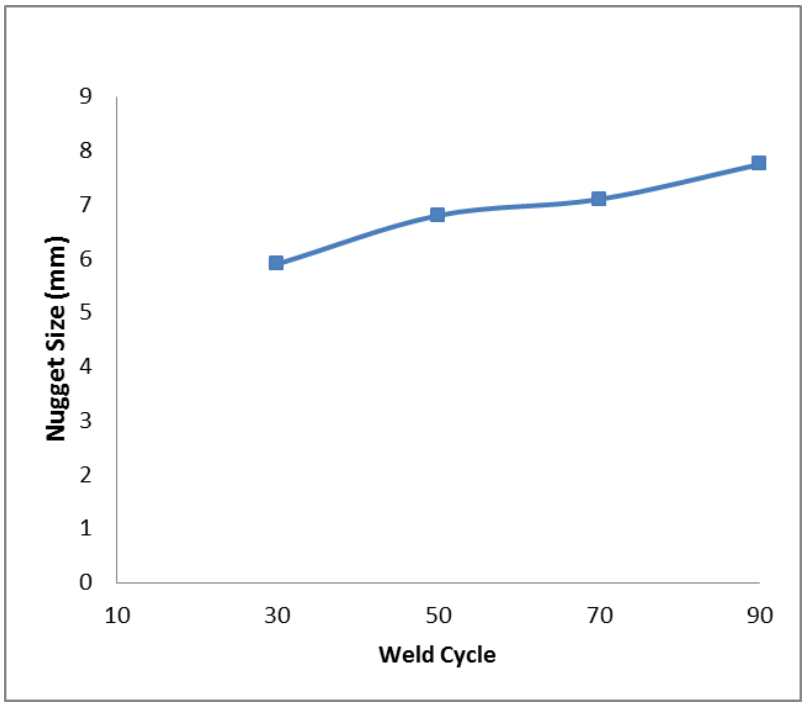

Constant weld Current: 9 kA		
Sample No	Time Cycle	Nugget Size mm
S-1	90	7.75
S-5	70	7.1
S-9	50	6.8
S-13	30	5.9

Figure 4.11: Weld nugget dimension at 9 kA but different weld Cycle.

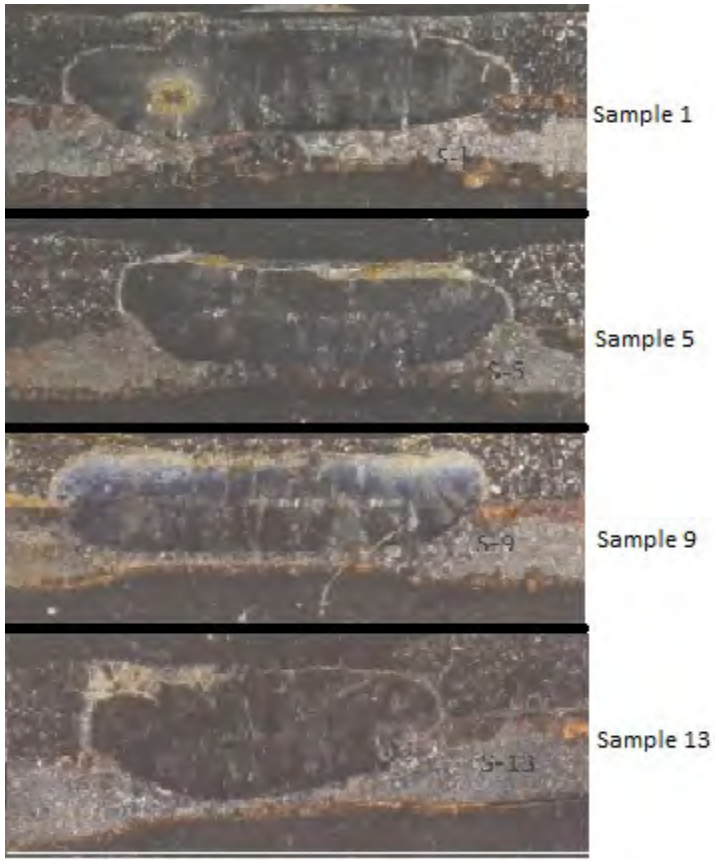

Figure: 4.12 Effect of welding cycle at constant weld current [9 kA] in macroscopic view.

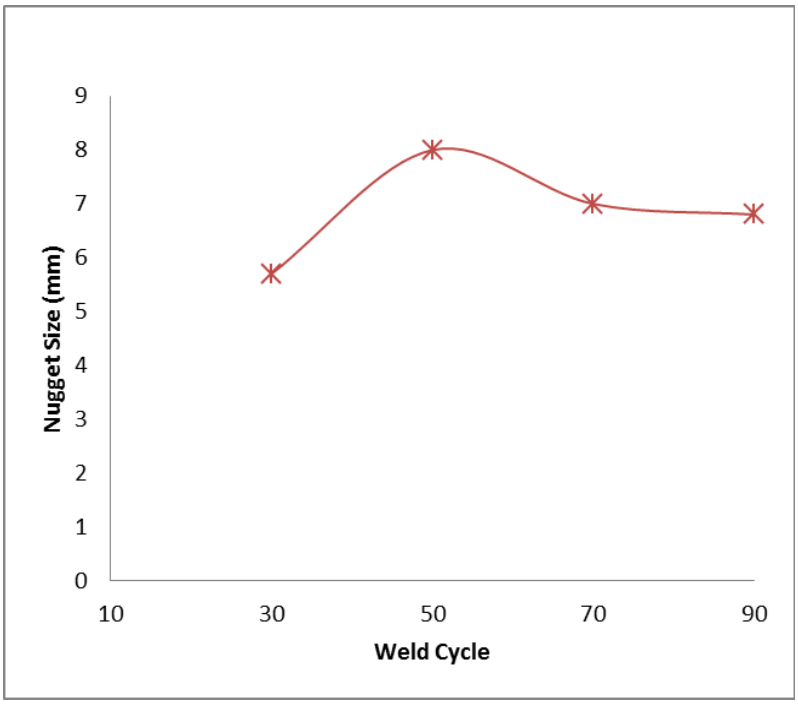

Constant weld Current: 7 kA		
Sample No	Time Cycle	Nugget Size mm
S-2	90	6.8
S-6	70	7
S-10	50	8
S-14	30	5.7

Figure 4.13: Weld nugget dimension at 7 kA but different weld Cycle.

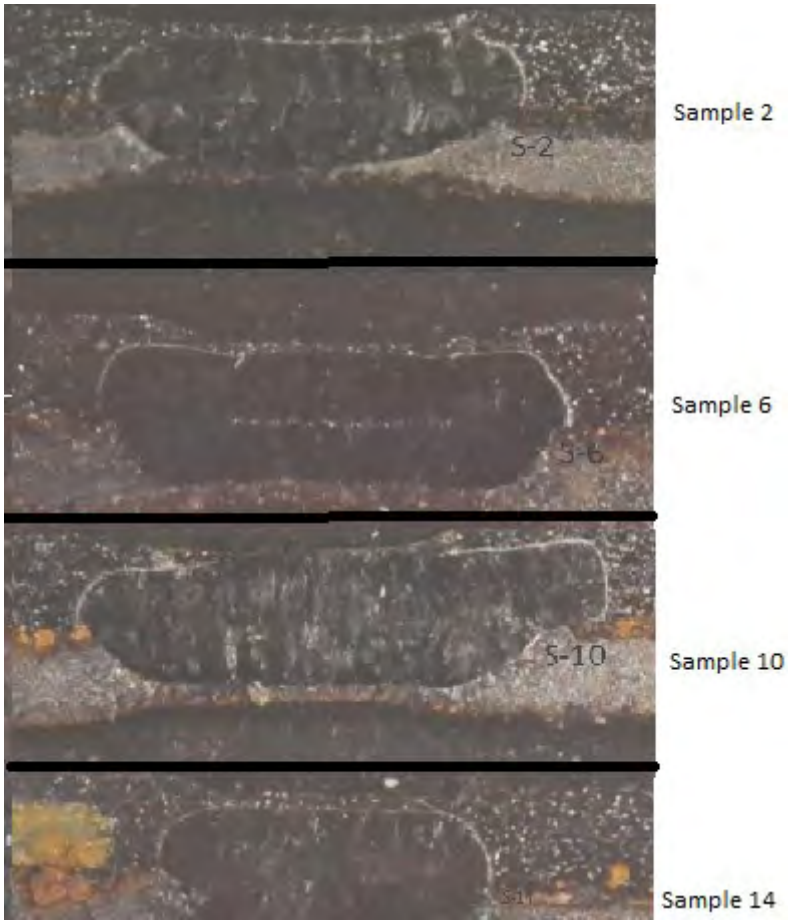

Figure: 4.14 Effect of welding cycle at constant weld current [7 kA] in macroscopic view.

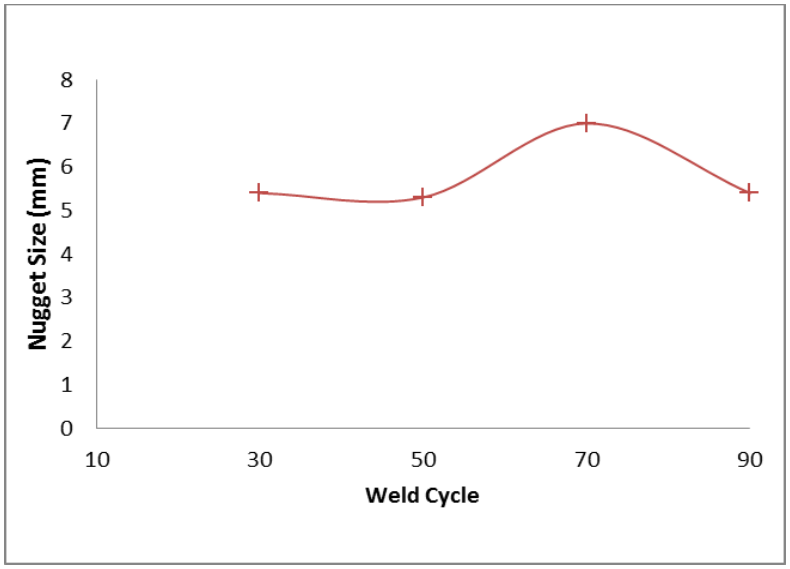

Constant weld Current: 5 kA		
Sample No	Time Cycle	Nugget Size mm
S-3	90	5.4
S-7	70	7
S-11	50	5.3
S-15	30	5.4

Figure 4.15: Weld nugget dimension at 5 kA but different weld Cycle.

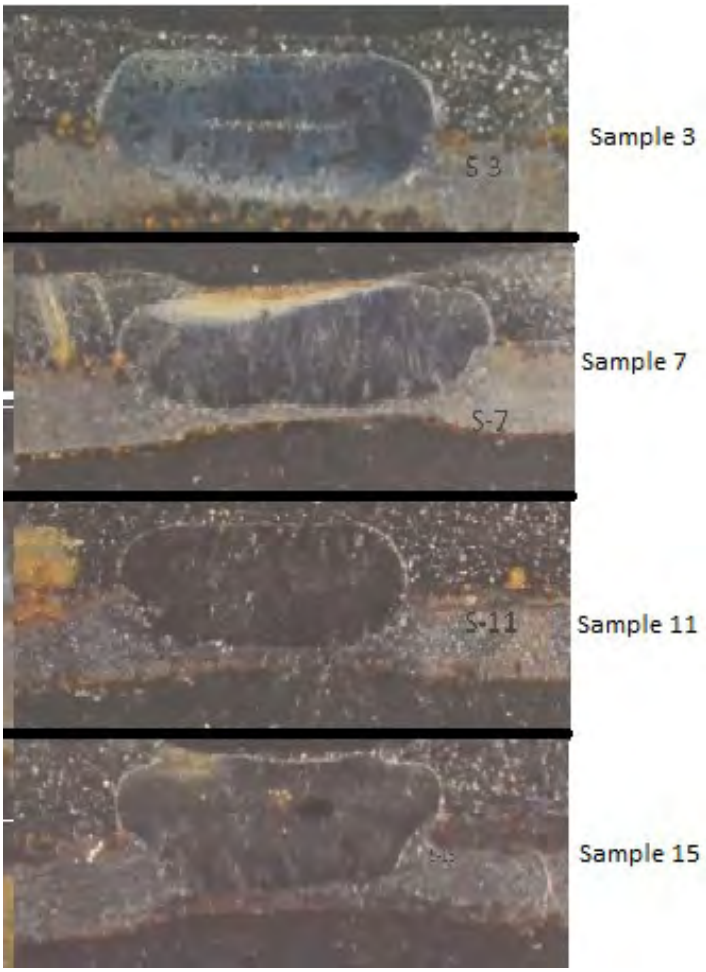

Figure: 4.16 Effect of welding cycle at constant weld current [5 kA] in macroscopic view.

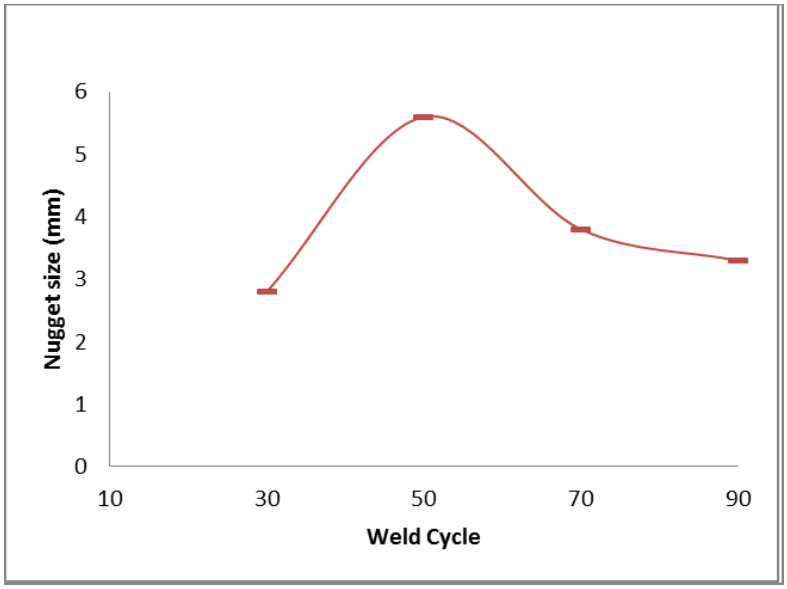

Constant weld Current: 3 kA		
Sample No	Time Cycle	Nugget Size mm
S-4	90	3.3
S-8	70	3.8
S-12	50	5.6
S-16	30	2.8

Figure 4.17: Weld nugget dimension at 3 kA but different weld Cycle.

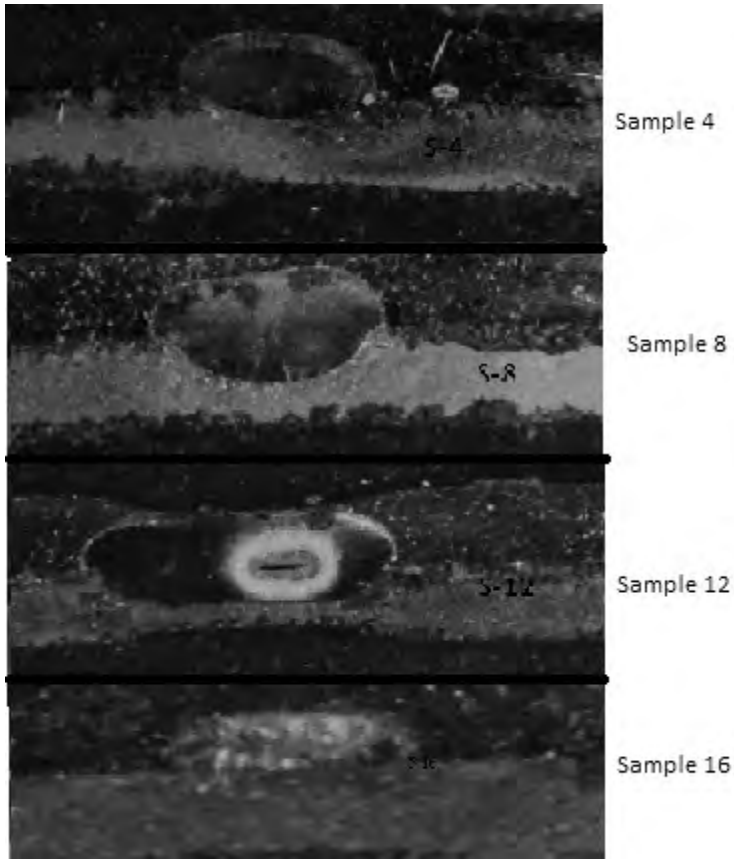

Figure: 4.18 Effect of welding cycle at constant weld current 3 kA in macroscopic view.

From all of these figures we can draw a final discussion. From Figure 4.3 to Figure 4.10, we found that at constant weld cycle an increase in weld current increases the weld nugget size. From figure 4.11 to figure 4.18, we found that at constant welding current weld cycle cannot

make a significant direction of changing weld nugget but lower weld cycle make smaller weld nugget and large weld cycle make large weld nugget.

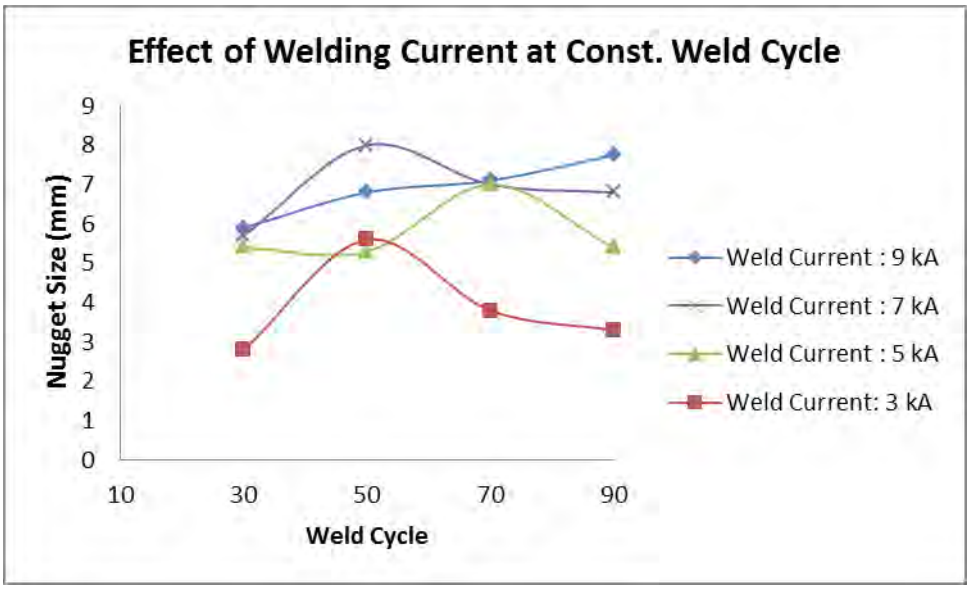

Figure 4.19: Effect of welding current at constant welding cycle.

Figure 4.19 shows that at constant welding cycle by increasing welding current at higher weld cycle 90 cycles and lower weld cycle 30 cycles weld nugget size is increase significantly. But at cycle 70 and cycle 50 weld nugget sizes are not changed with any directions.

Figure 4.20 shows that only at higher welding current an increasing welding cycle increase the weld nugget size. At lower current weld cycle have no significant effect on weld nugget size. Weld nugget size is determined by heat input and heat input rate. Generated heat at joint spot is controlled by welding current and by welding cycle. At higher welding cycle nugget size is not uniform because at this time expulsion may occur.

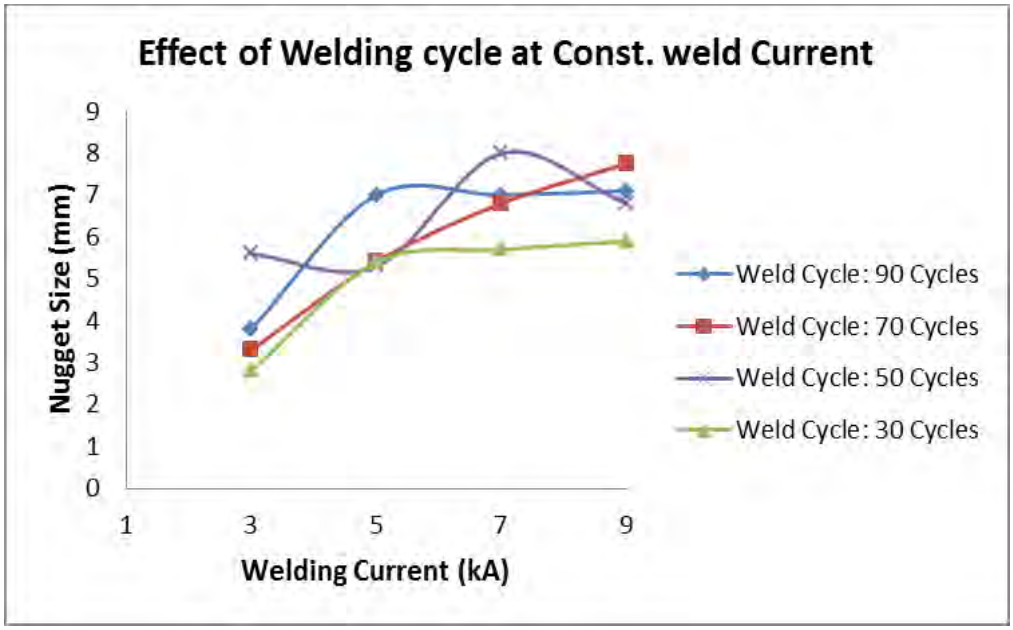

Figure 4.20: Effect of welding Cycle at constant welding Current.

According to J.E.Gould [21], weld nugget growth as a function of welding current and welding time occurs at four stages, as follow:

I. Incubation stage: no melting occurs and weld nugget is not formed,

II. Nugget formation and rapid nugget growth stage

III. Slow nugget growth rate stage, and

IV. Expulsion

Indeed, weld nugget growth rate is affected by two phenomena: increase in electric resistance due to increasing the metals temperature and decrease in electric resistance due weld nugget formation and growth. At early stages of weld growth, which weld nugget is small, resistance increase due to heating material (because of welding current or welding cycle) overcomes resistance decrease weld nugget growth. However, increasing weld nugget diameter increases the effect of resistance decrease caused by weld nugget growth. Therefore, weld nugget growth rate decreases by further increase in welding current or welding cycle.

4.3 Micro structural observation:

Figure 4.21 shows the three different zones of the welded joint. These are

1. Base metal (BM) which remained unaffected during the welding process.
2. Heat affected zone (HAZ) which experienced solid state microstructural alteration during thermal cycle of welding.
3. Fusion zone (FZ) or weld nugget which experienced melting and solidification during thermal cycle of welding.

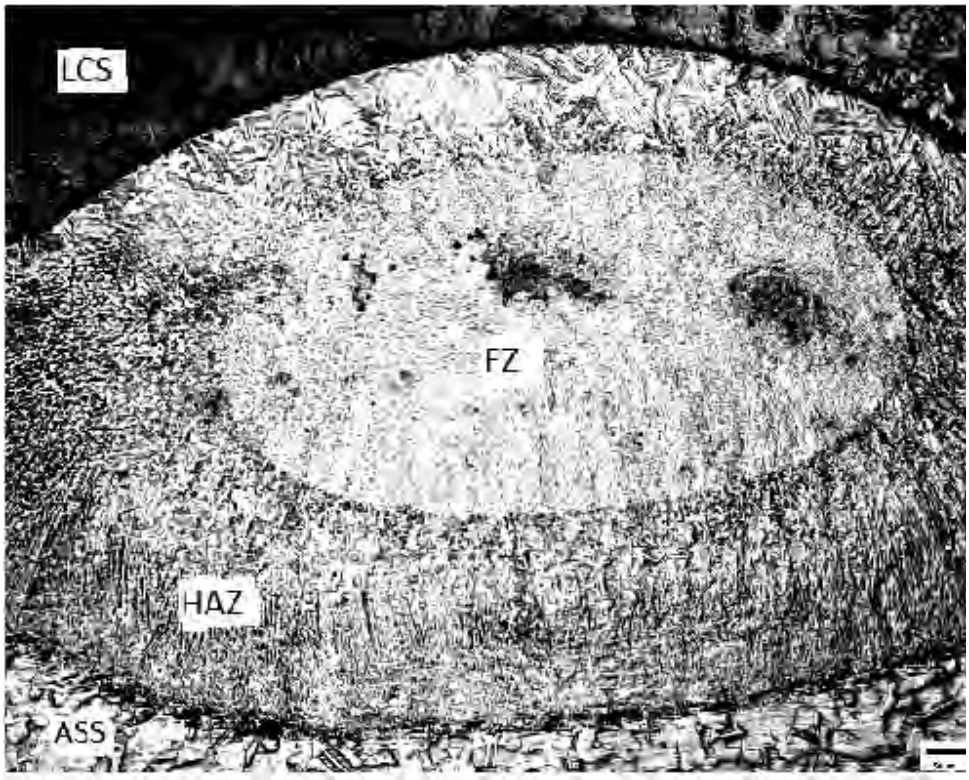

Figure 4.21: Microstructure of welded coupon of RSW of dissimilar (ASS/LCS) metal, (5X).

In these experiments, two different metals, ASS and LCS were welded which have two different microstructures. Two different characteristics in base metal were observed. Heat affected zone also have different characteristics in the fusion zone adjacent to the base metal but a complex micro structure in the fusion zone was observed. Different welding parameter was used in this experiment but there is no significant structural change could be found in this microstructural observation, it affects only geometrical characteristics. Different welding

parameters create different sizes of weld nuggets and also enhance heat affected zone size. We are discussing the microstructural part by using following line diagram. From this figure 4.22 we found base metal (unaffected zone (a)), heat affected zone (transition zone (b), refined zone (c)), fusion zone.

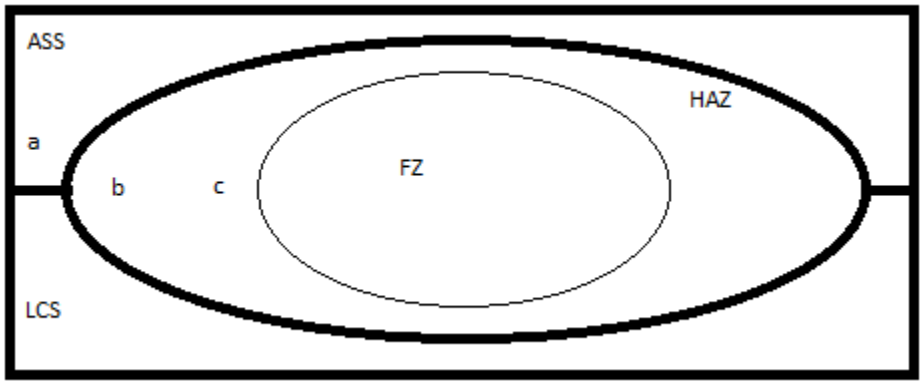

Figure 4.22: Line diagram of the welded coupon.

4.3.1 Base metal

In base metal, different structure can be observed in both LCS side and ASS side. The unaffected zone in low carbon steel side represents the typical grain structure of the parent low carbon steel which has not been heated to a high enough temperature to reach the critical range, hence its structure is unchanged (Figure 4.23). This figure show unaffected zone consisting large amount of ferrite with very low amount of pearlite.

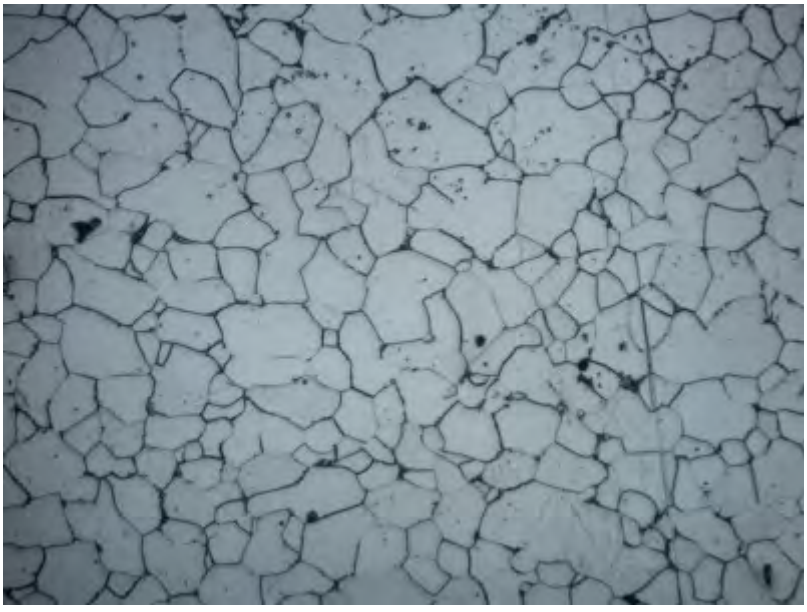

Figure 4.23: Unaffected zone in the low carbon steel side, 50X.

Analysis of microstructure in austenitic stainless steel shows no change in base metal near to the weld nugget. Base metal of austenitic stainless steel is twins structure which shown in figure 4.24.

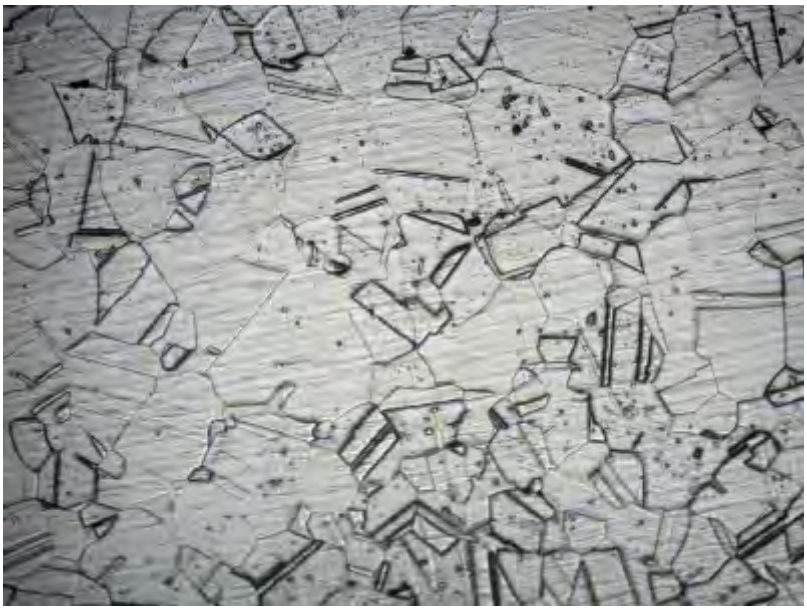

Figure 4.24: Base metal of the austenitic stainless steel, 10X.

4.3.2. Heat affected zone

In the outer side of the fusion zone is the heat affected zone. Microstructure is more heterogeneous in heat affected zone than in the fusion zone. The material in the heat affected zone experiences a peak temperature and a cooling rate which are inversely proportional to its distance from the final fusion line. The heat affected zone microstructure near the fusion zone boundary of the low carbon steel side consists of martensite, grain boundary ferrite and widmanstatten ferrite (Figure 4.25).

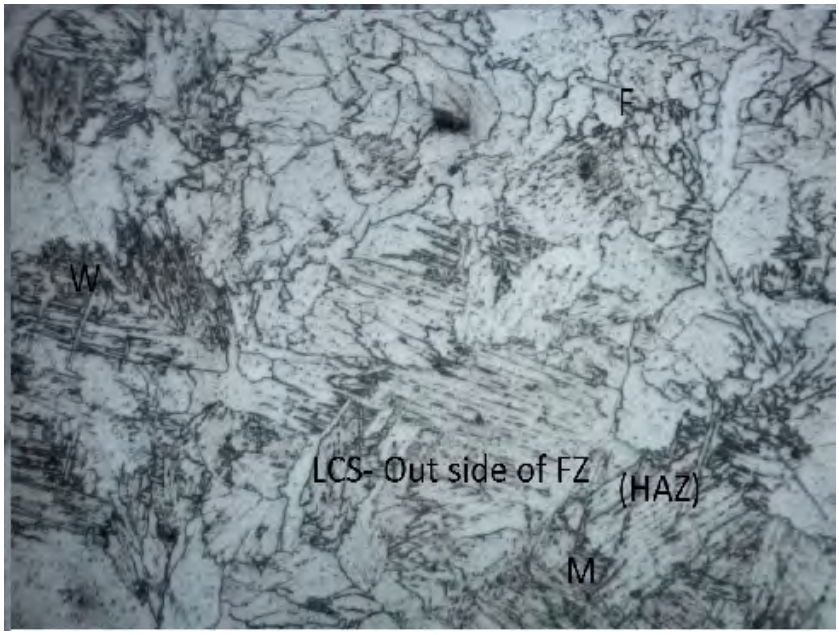

Figure 4.25: heat affected zone in low carbon steel side, 50X.

Figure 4.26 shows large region of pearlite and smaller grains of ferrite. Examination of the pearlite at higher magnification showed a finer structure that existed in the original pearlite areas because of the rate of cooling prevailed.

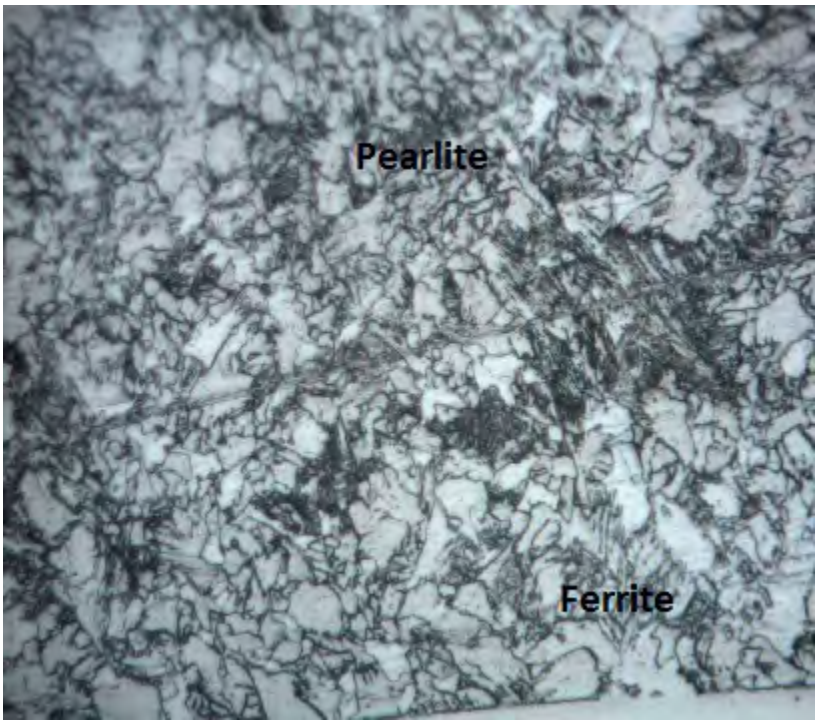

Figure 4.26: Fine pearlite outside of the fusion zone, 50X.

The very coarse structure near the fusion zone is shown in the Figure 4.27.

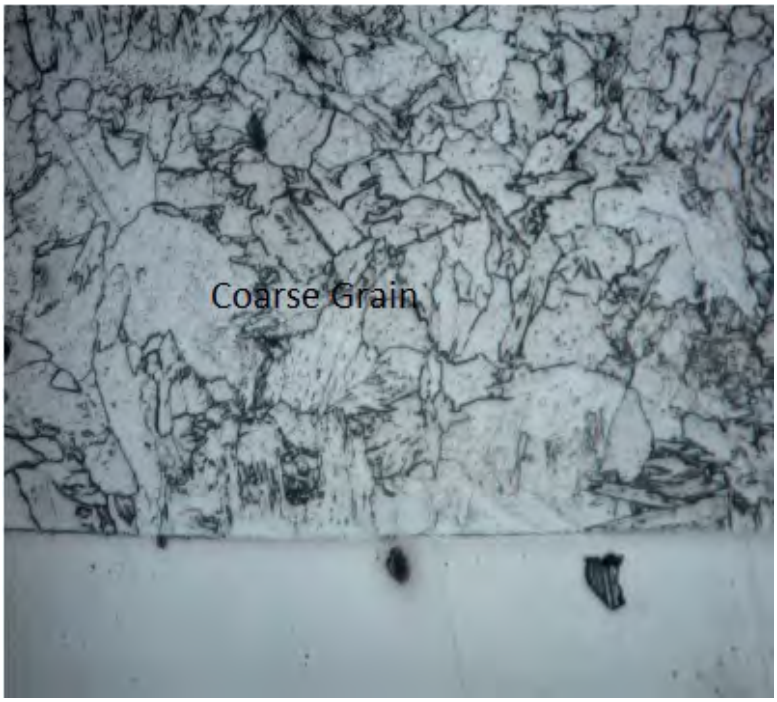

Figure 4.27: Coarse grain near to fusion zone at the low carbon steel side, 50X.

In the transition zone, temperature ranges exist between the A_1 and A_3 transformation temperature where partial allotropic recrystallization takes place. This structure is shown in the Figure 4.28.

Figure 4.28: Transition Zone in the low carbon steel side, 50X.

In transition zone the ferrite grains have not been altered but the pearlite region have been made much finer. This change is produced by heating into the critical range which transformed the pearlite into austenite and by subsequent cooling reform the pearlite. Complete recrystallization is shown in Figure 4.29. In which ferrite and pearlite areas are both much finer forming from the austenite that existed at a temperature just above upper critical temperature. This zone is called refined zone which present near the fusion zone. These entire three zone showing in the Figure 4.30.

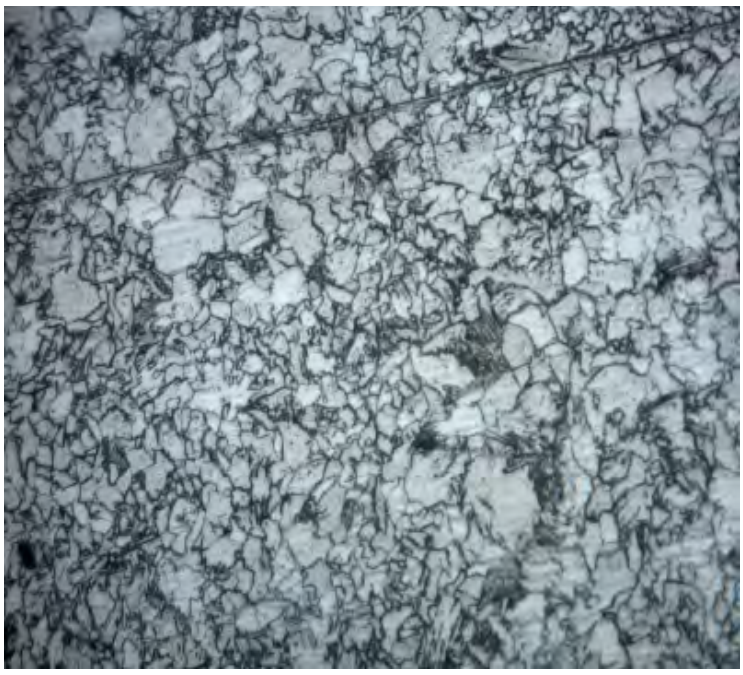

Figure 4.29: Refined zone in low carbon steel side, 50X.

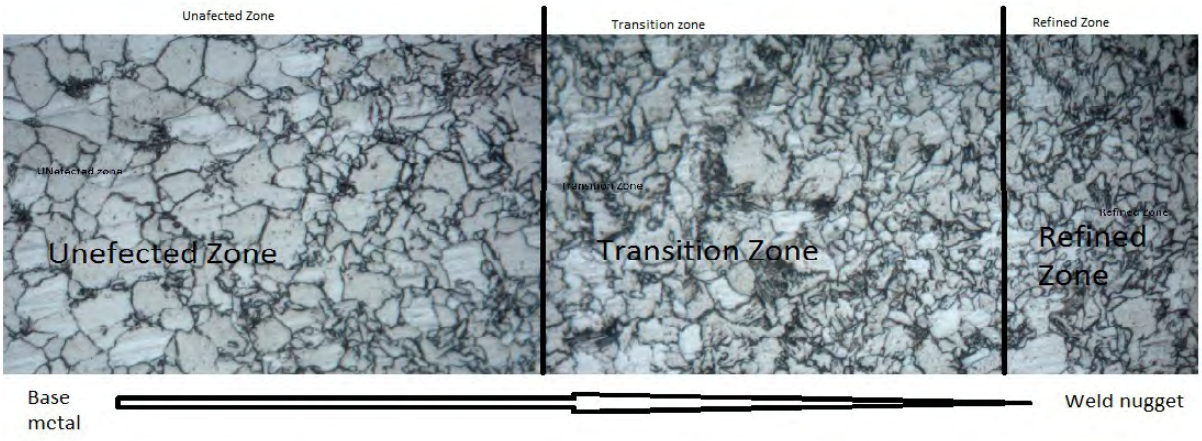

Figure 4.30 microstructure of the low carbon steel base metal near to the weld nugget, 50X.

Adjacent to the weld nugget austenitic stainless steel has not transformed (Figure 4.31). Only very small size of transition zone is present near to the welding nugget.

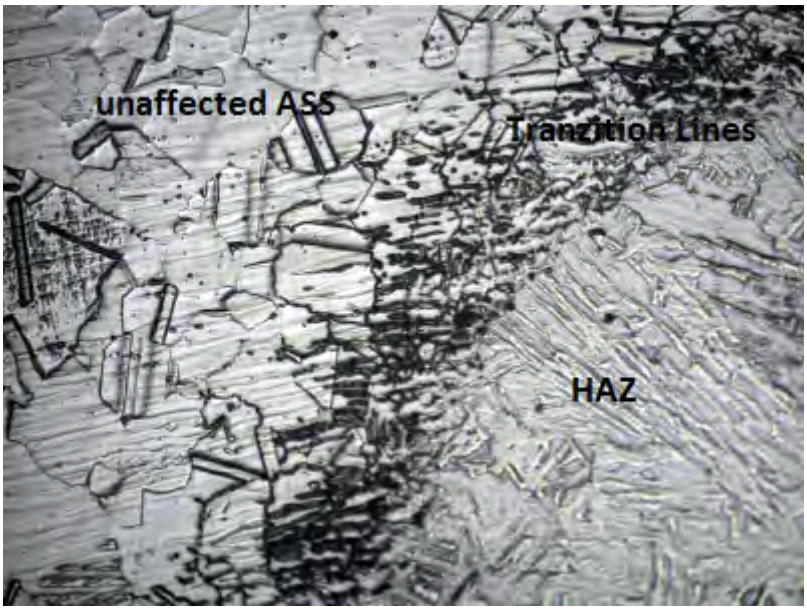

Figure 4.31: Un-transformable base metal (Transition Zone) of ASS, 20X.

The structure is of widmanstatten type with lines of ferrite breaking up the pearlite area. This structure is common in low carbon steel in which transformation occurs form large austenite grains during medium fast rate of cooling.

In case of the austenitic stainless steel no phase change occurs in the heat affected zone. However grain structure of this region was affected by welding. Some grain growth was observed adjacent to weld nugget. It is worth mentioning that the extent of grain growth for austenitic stainless steel is a lot less than ferritic steel. The structure shows widmanstatten structure with in austenite matrix (Figure 4.32 & 4.35) and lamellar form extending base metal austenitic stainless steel to fusion zone.

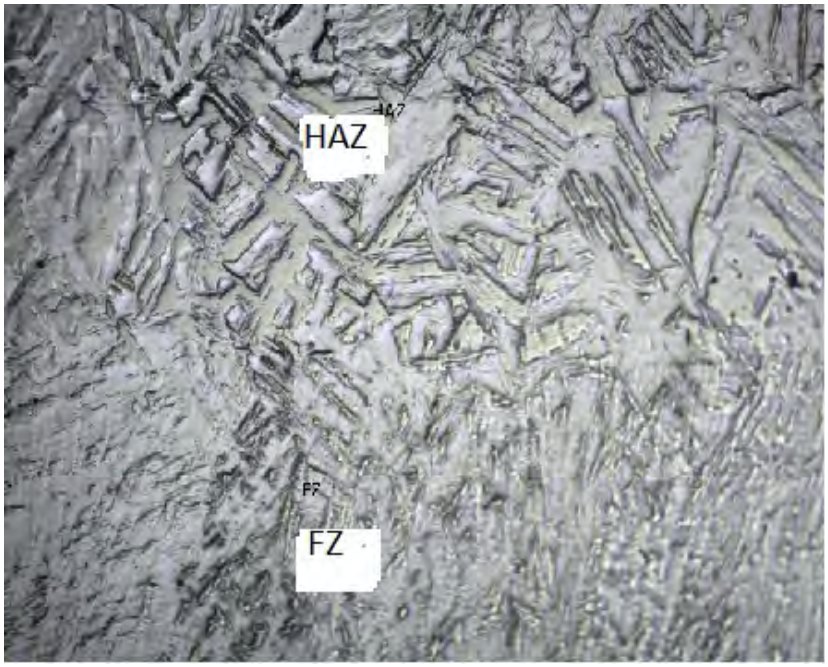

Figure 4.32: Heat affected zone in austenitic stainless steel side, 10X.

4.3.3. Fusion zone

In the fusion zone or weld nugget, a different structure neither low carbon steel nor austenitic stainless steel can be seen. This is like cast microstructure. Some amount of grain boundary phase, such as proeutectoid (grain boundary ferrite), widmanstatten ferrite and polygonal ferrite present in the weld nugget microstructure. Figure 4.33 shows microstructure of weld structure of austenitic stainless steel. Of the surface weld is dendritic with excess delta ferrite in austenite matrix. The low carbon steel has a structure consisting of fine ferrite and pearlite.

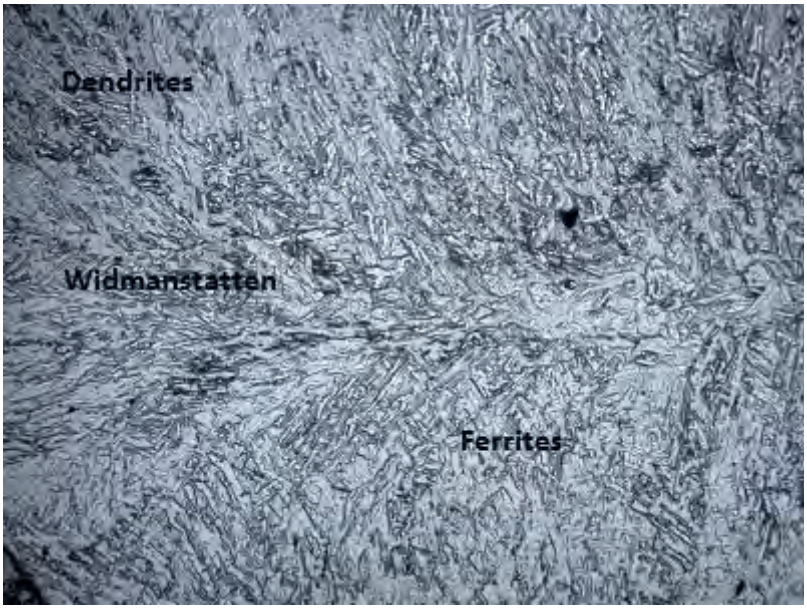

Figure 4.33: Weld nugget cast structure, 10X.

Despite of low carbon content martensite phase was formed due to high cooling rate of resistance spot welding process. Here also coarse columnar grain was found. In figure 4.34 one can see that acicular low carbon martensite.

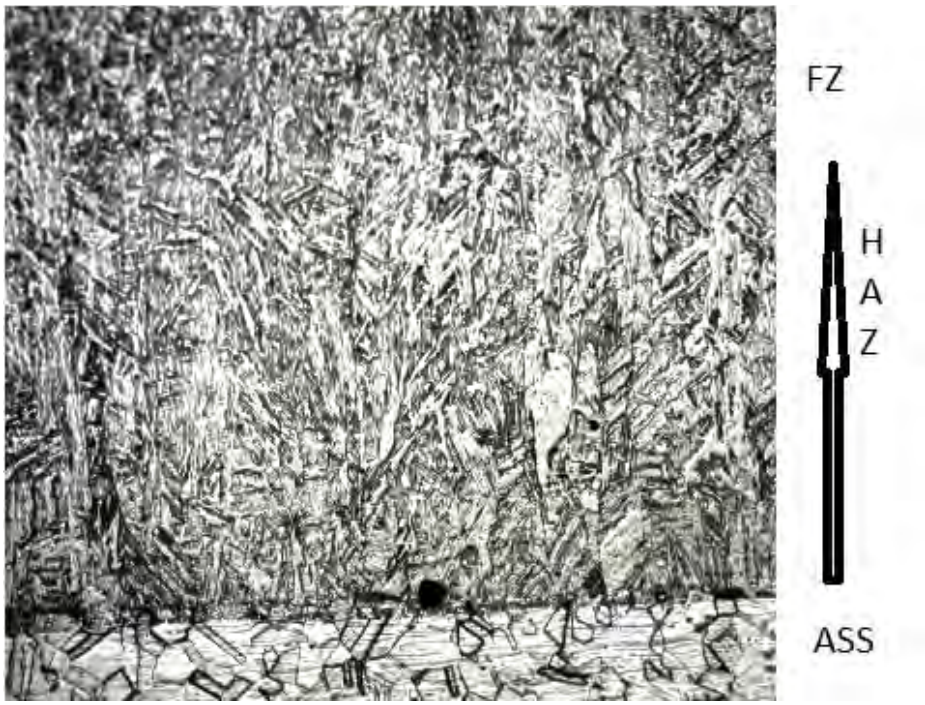

Figure 4.34: coarse columnar grain of weld nugget, 20X.

P.Marashi [22] examined the microstructure of the welded nugget of a dissimilar joint between galvanized steel and stainless steel using schaeffler diagram. He found the structure

fully martensitic and it was supported by higher hardness. It should be noted that changing of the welding current has no significant effect on weld microstructure, it is only affects on geometrical characteristics of weld nugget. Mansouri [18] found the heat affected zone of carbon steel side experienced significant microstructure alteration as indicated by hardness profile. However, it should be noted that, austenitic stainless steel base metal is not transformable, no phase transformation occurs in the heat affected zone. However, grain structure of this region is affected by welding process. Some grain growth was observed adjacent to the weld nugget. Hasanbasoglu and Kacar[23] found that weld nugget has columnar structure. An increase in energy input caused coarsening of the microstructure of weld nugget and also heat affected zone. It can be noted that grain growth occur due to the heat transfer. Therefore, the of heat affected zone grain growth region was found wider on low carbon steel side of weldment that have higher thermal coefficient compared with stainless steel.

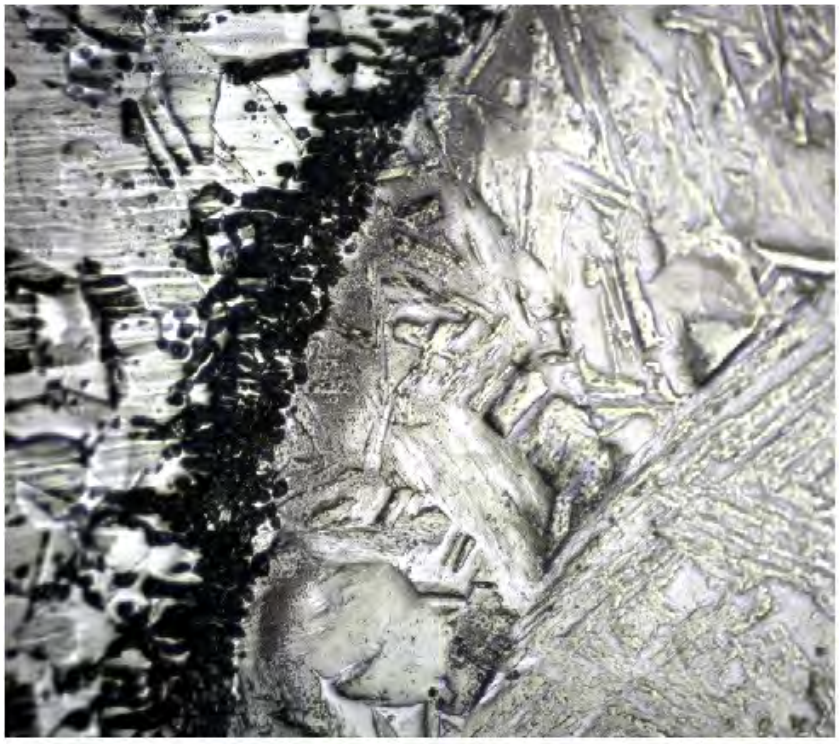

Figure 4.35: austenitic stainless steel with heat affected zone and fusion zone, 20X.

4.4 SEM observation

Some images taken by scanning electron microscope are given below in Figure 4.36 to 4.42.

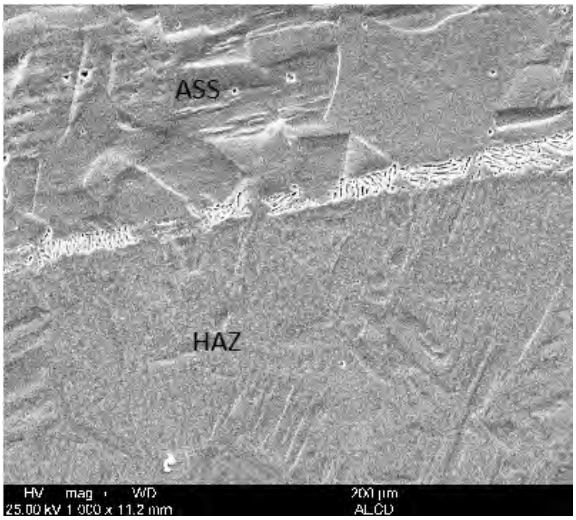

Figure 4.36: ASS with HAZ

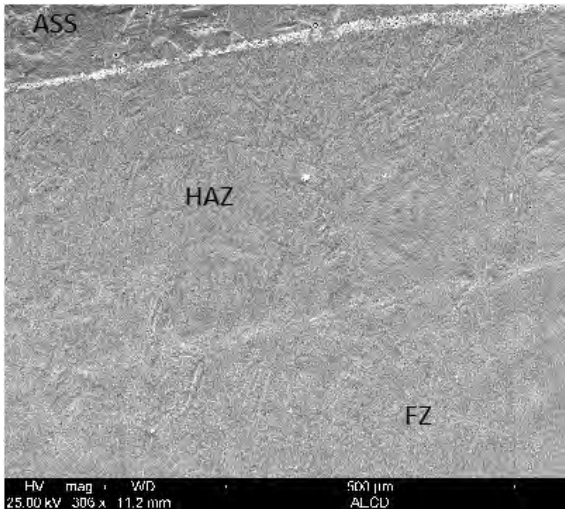

Figure 4.37: ASS with HAZ and FZ

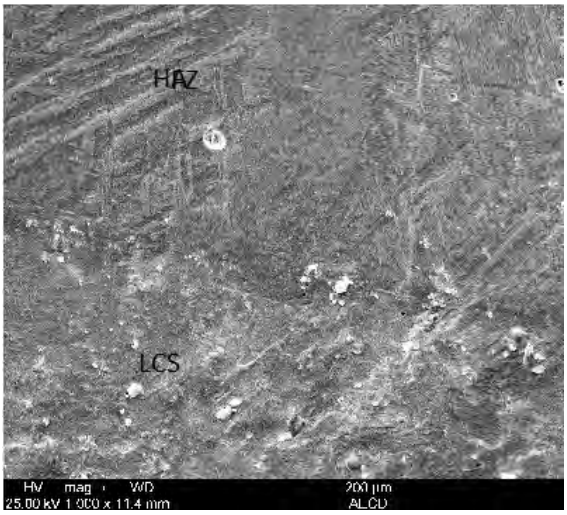

Figure 4.37: LCS with HAZ

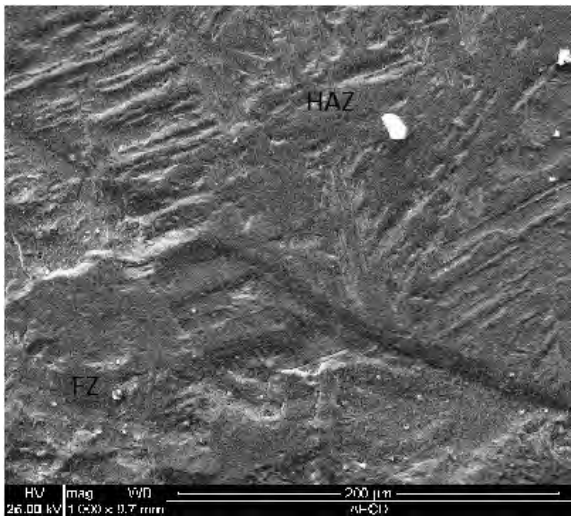

Figure 4.38: HAZ with FZ in LCS side

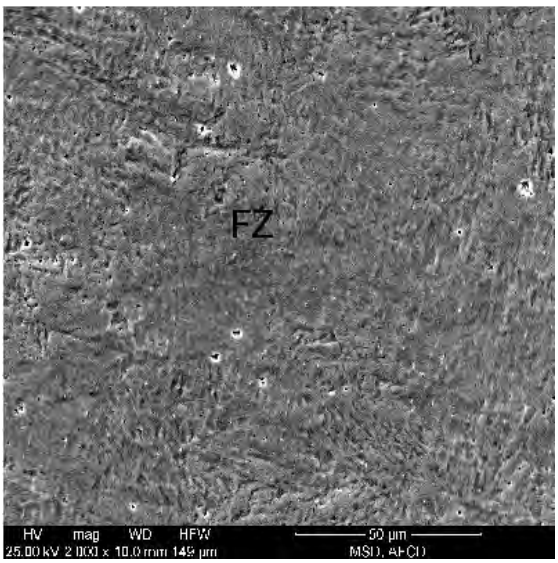

Figure 4.39: Fusion zone

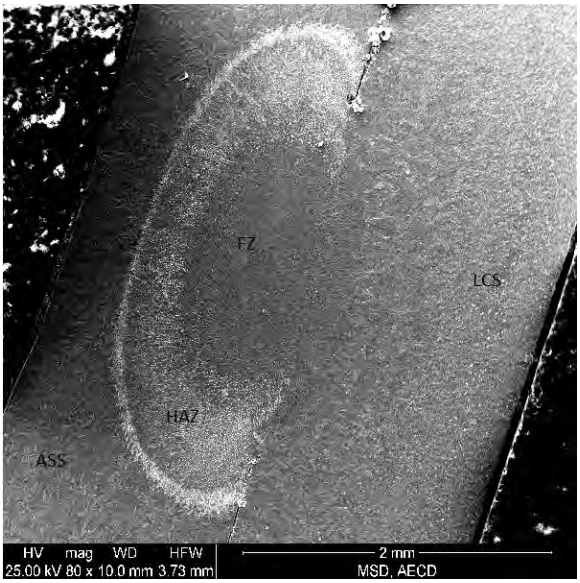

Figure 4.40: Cross section of weld coupon

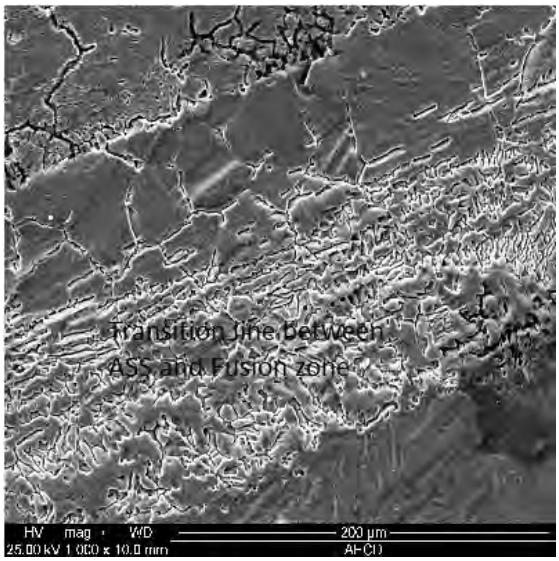

Figure 4.41: Transition line between HAZ and ASS.

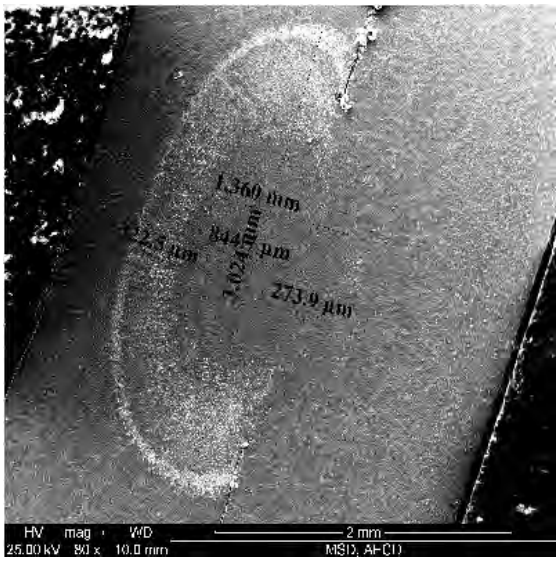

Figure 4.42: Measurement of Nugget size and HAZ.

4.5 Hardness measurement

The hardness test was performed in a micro hardness testing machine. The detail test setup is given in section 3.7.3. By using proper level of force the hardness value was measured in different directions in the base metal (around 5 mm of HAZ) and around the weld nugget.

Here a vertical hardness profile is observed as a function of welding current and welding cycle. These results are shown in figure 4.43 to 4.50.

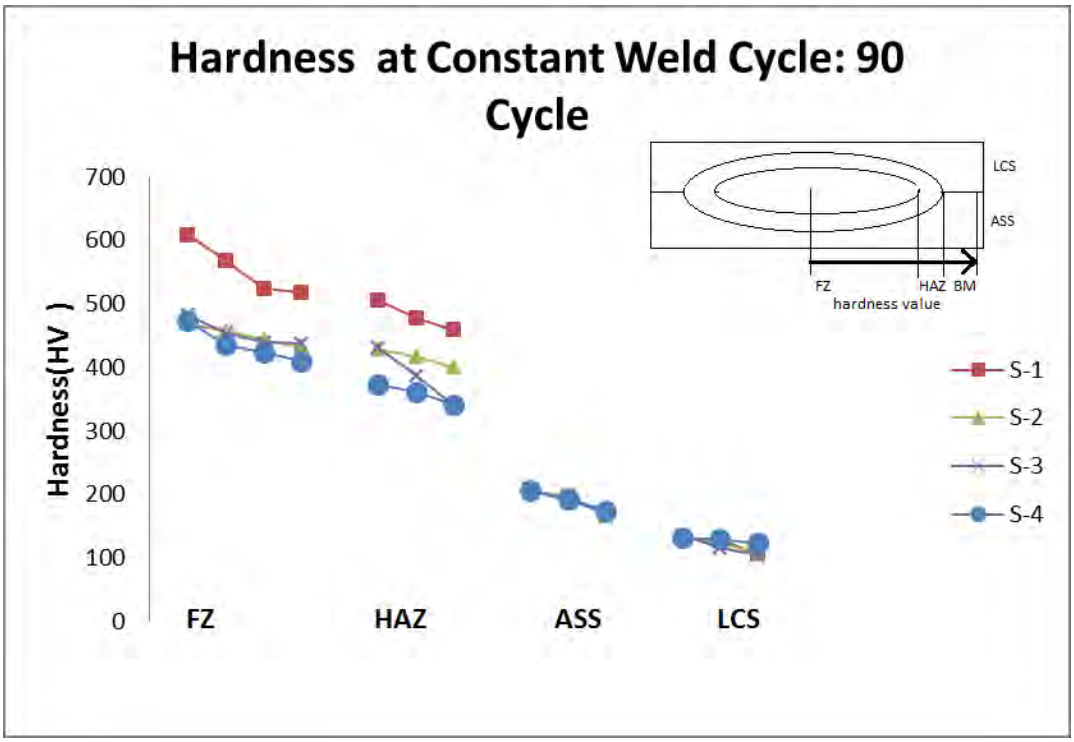

Figure 4.43: Effect of welding current on hardness at constant weld cycle (90 Cycles)

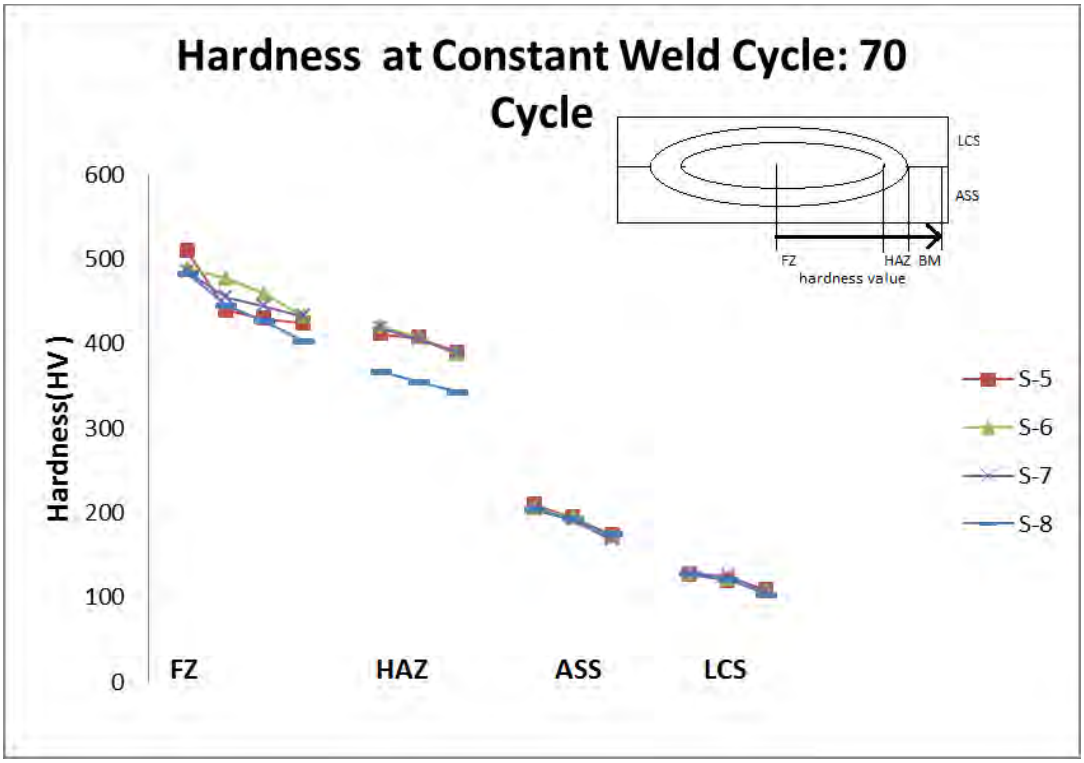

Figure 4.44: Effect of welding current on hardness at constant weld cycle (70 Cycles)

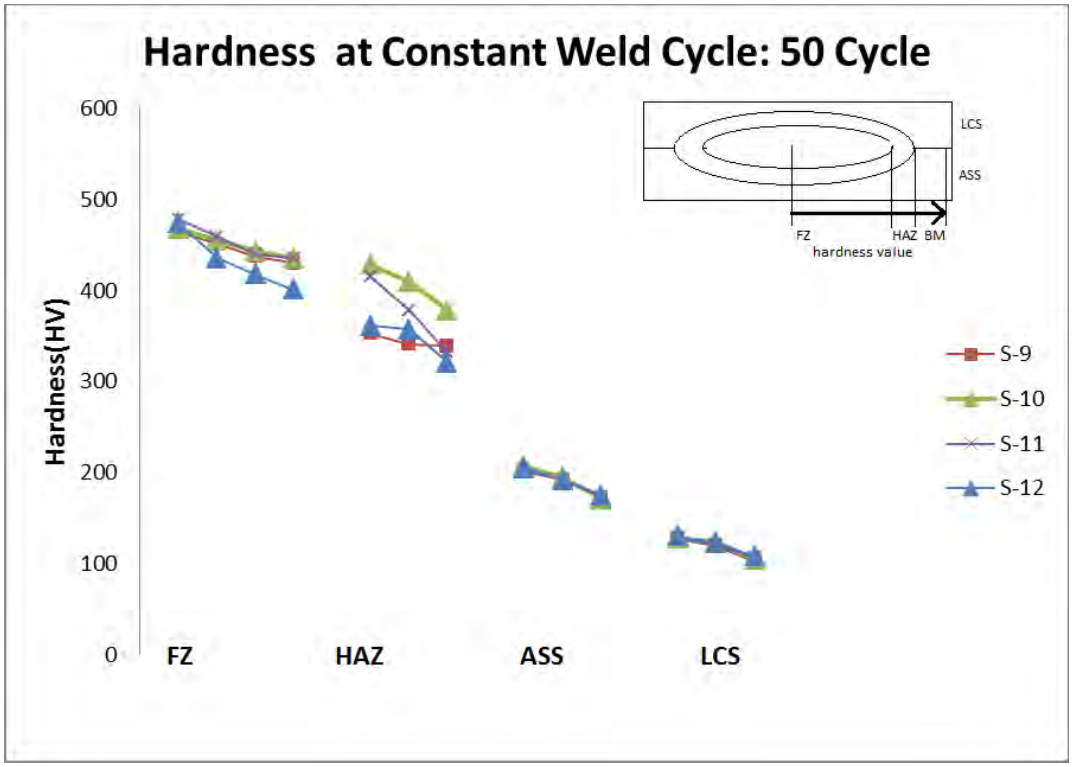

Figure 4.45: Effect of welding current on hardness at constant weld cycle (50 Cycles)

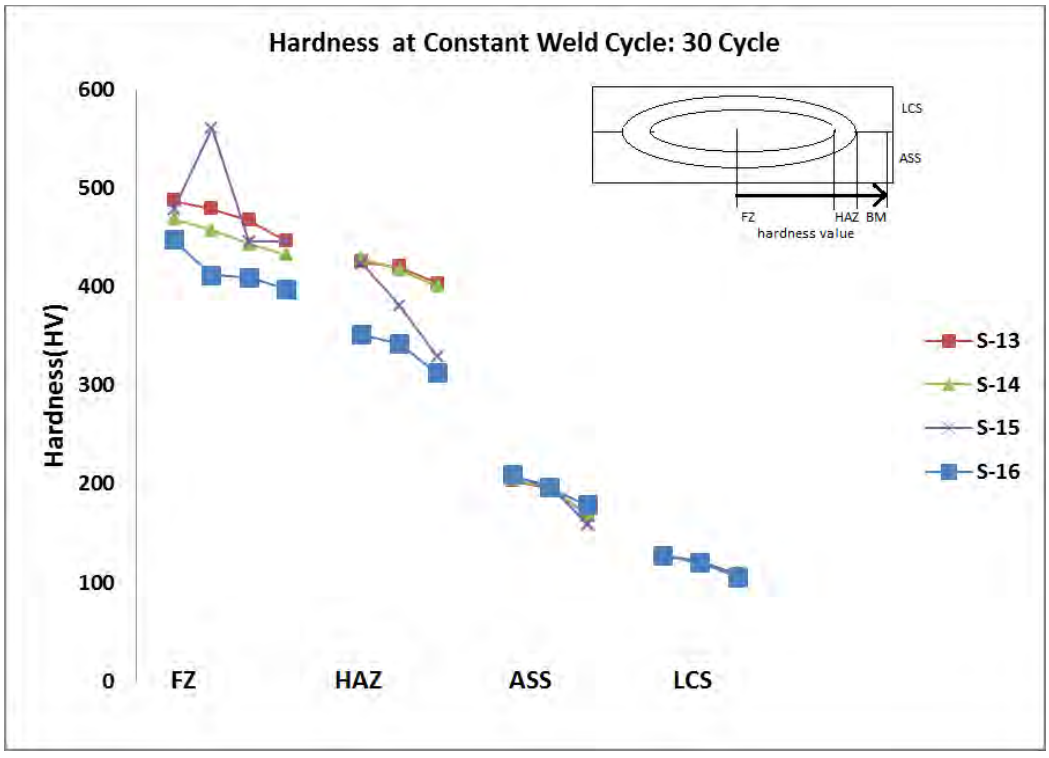

Figure 4.46: Effect of welding current on hardness at constant weld cycle (30 Cycles)

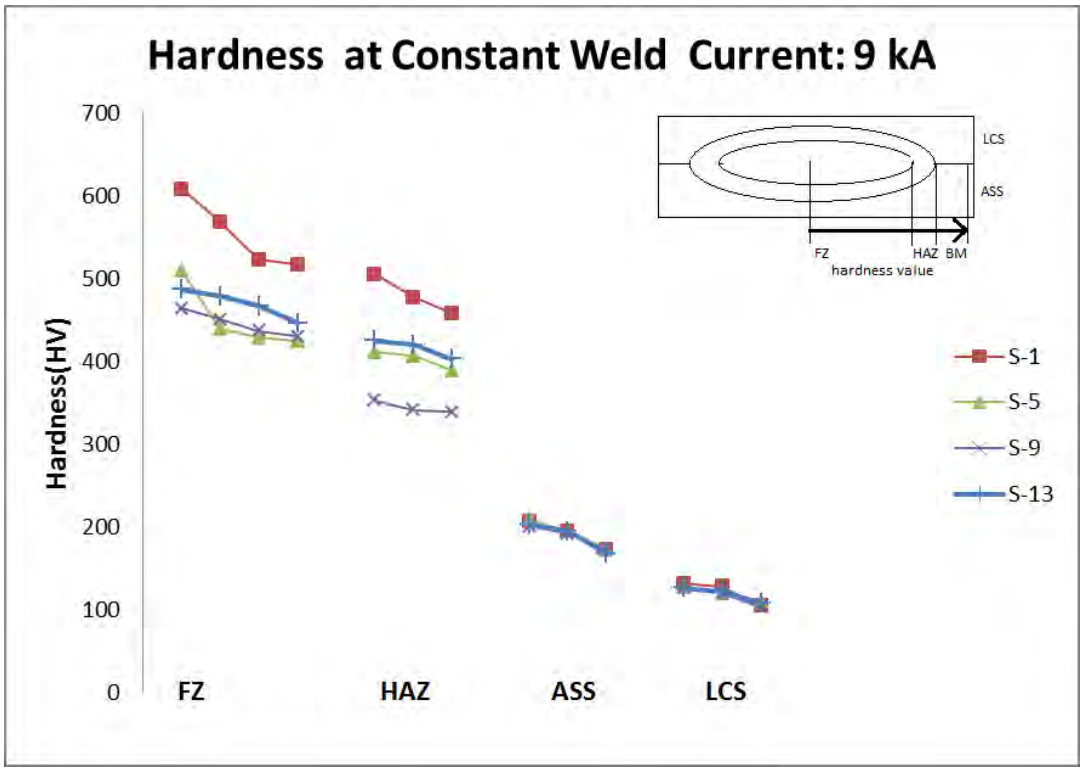

Figure 4.47: Effect of welding cycle on hardness at constant weld current (9 kA)

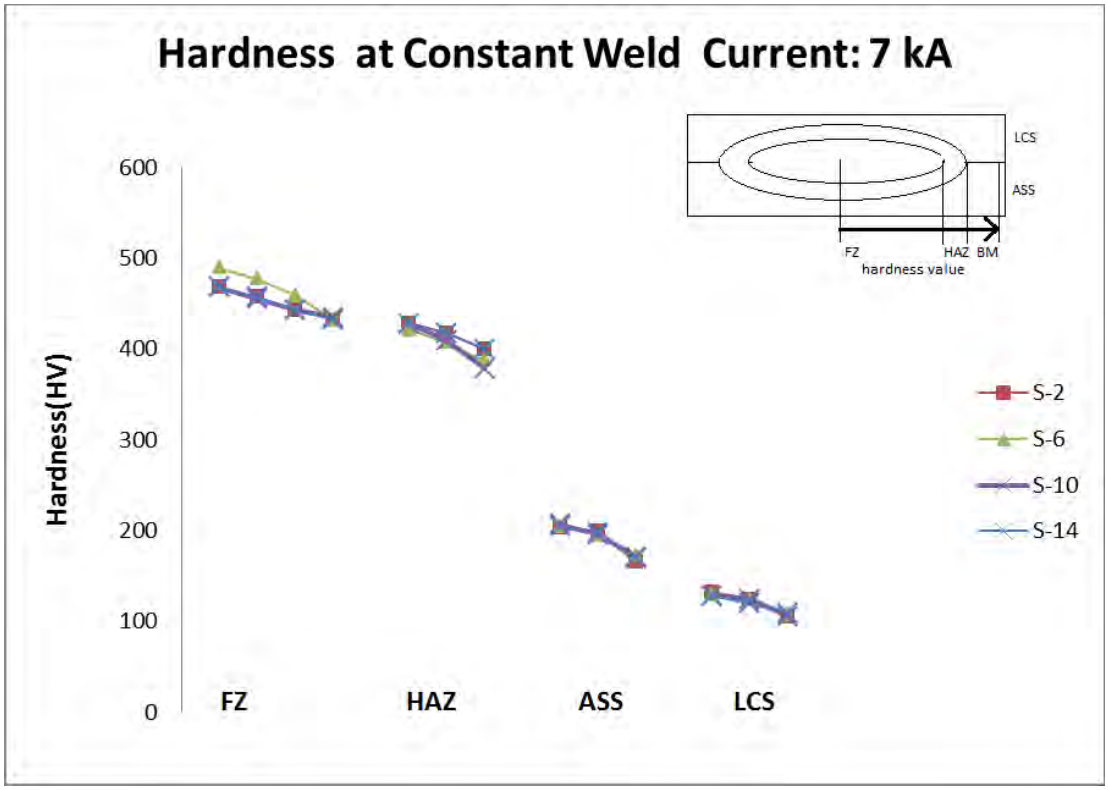

Figure 4.48: Effect of welding current on hardness at constant weld cycle (7 kA)

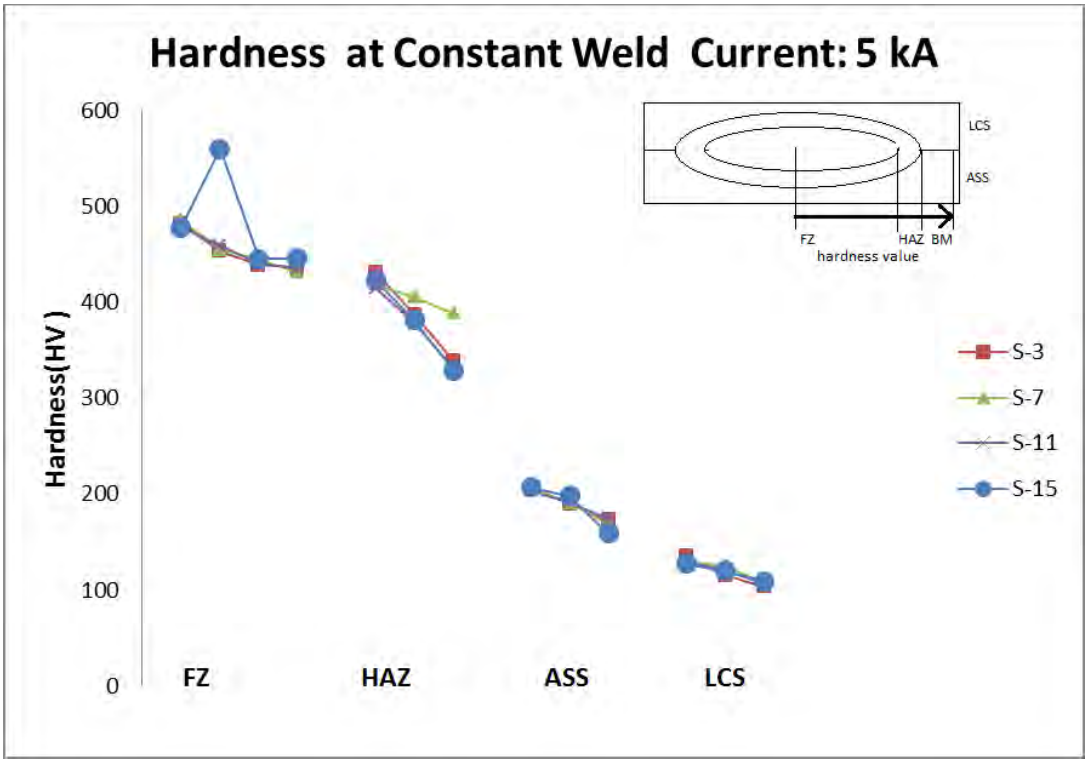

Figure 4.49: Effect of welding current on hardness at constant weld cycle (5 kA)

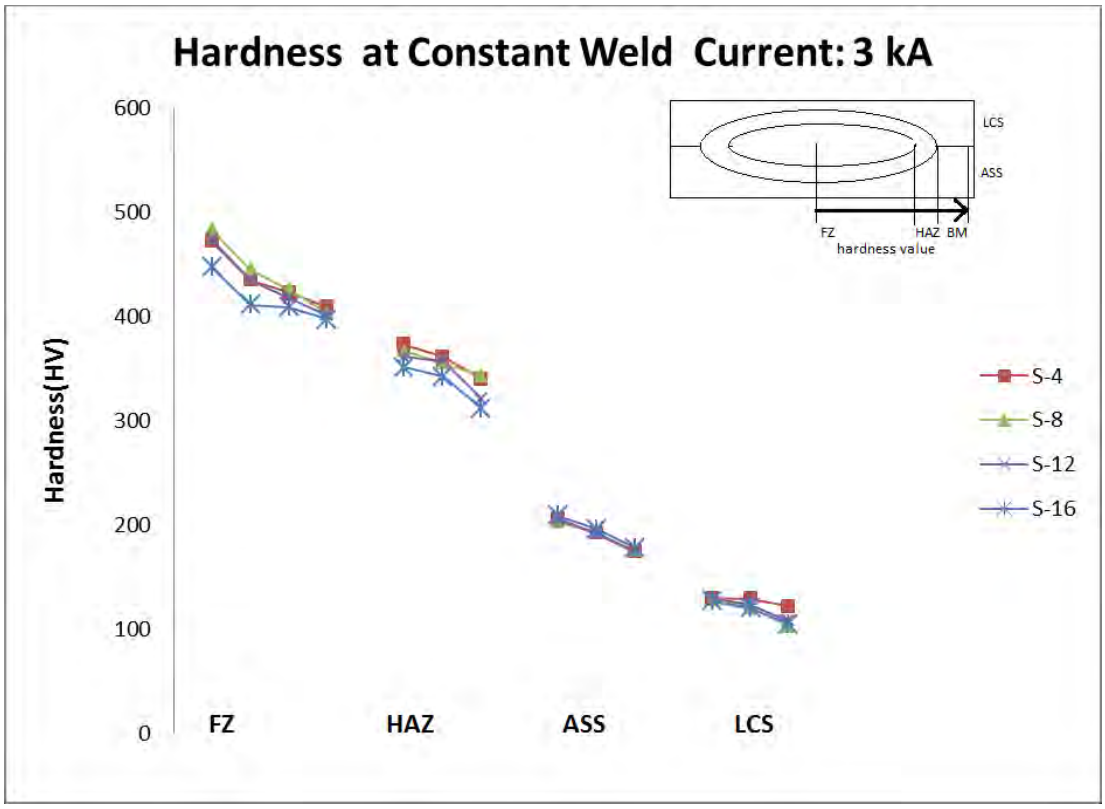

Figure 4.50: Effect of welding current on hardness at constant weld cycle (3 kA)

Average hardness **(HV)** values are given below (Table 4.1).

Table 4.1 hardness **(HV)** values

Sample No	Micro hardness (Average)			
	Base. LCS	HAZ	FZ	Base. ASS
S-1	122	480	554	191
S-2	120	415	450	189
S-3	118	386	453	190
S-4	127	358	435	191
S-5	119	402	450	192
S-6	120	405	464	191
S-7	121	404	454	188
S-8	117	355	439	190
S-9	117	344	446	188
S-10	119	405	450	191
S-11	119	375	453	190
S-12	120	346	432	191
S-13	119	416	470	189
S-14	119	415	450	190
S-15	119	378	482	188
S-16	117	335	416	194

From the figure 4.43 to 4.50 and table 4.1, it can be seen that hardness in the fusion zone is maximum and it is 2.5 times than the hardness of low carbon steel and around 2 times than that of austenitic stainless steel. Hardness of the heat affected zone is higher than base metal. Higher hardness value of the weld nugget is because of martensite formation. Weld parameters have some definite effect on hardness property. Figures 4.43 to 4.46 show that at higher welding current hardness value is higher and it is lower at lower welding current. Figures 4.47 to 4.50 show that weld cycle does have not significant effect on hardness value. M. Pouranvari [19] found that the hardness of the weld nugget is much higher than the hardness of the both base metals. The higher hardness of the weld nugget can be attributed to martensite formation in this zone. R.K Rajkumar [24] found that the welded areas increased in hardness due to the nature of the hardness properties. The hardness of the both side increased and the values are seemed very close to carbon steel values as the fusion process combines these materials. Besides, the hardness increments or decrements are never once being proportional in the distribution as it fluctuated up and down.

M.Alenius [25] found that the micro hardness values of the weld nugget were high due to the martensite microstructure of the weld nugget. He also suggested that nitrogen content has a large effect on the hardness of the martensite and that is also important.

4.6 Tensile properties:

Resistance spot welding is a important welding process for sheet metal welding where filler metal is not in use. Welding is done by resistance heating so material charecteristics and welding process parameter is important for welding quality. Avarage tensile test results are given in Table 4.2.

Table 4.2: Tensile test results are given below.

Sample No	Current (kA)	Time (Cycle)	Maximum Load (KN)	Maximum UTS (MPa)
S-1	9	90	11.24	299.6
S-2	7	90	11.23	299.6
S-3	5	90	10.17	271.1
S-4	3	90	4.845	129.2
S-5	9	70	11.89	317
S-6	7	70	11.79	314.4
S-7	5	70	10.96	292.3
S-8	3	70	6.887	183.7
S-9	9	50	11.22	299.3
S-10	7	50	11.6	309.3
S-11	5	50	10.25	273.4
S-12	3	50	7.257	193.5
S-13	9	30	11.39	303.7
S-14	7	30	10.94	291.7
S-15	5	30	9.872	263.2
S-16	3	30	1.166	31.09

All of these results are shown in figure below.

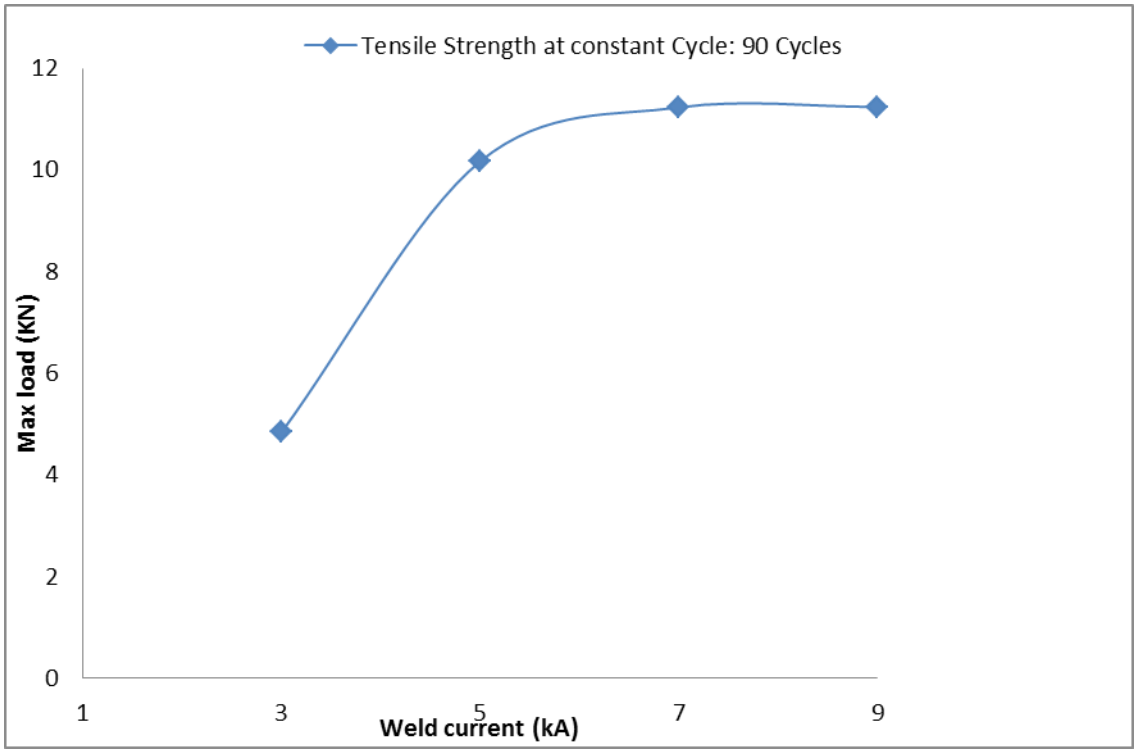

Figure 4.51 Effect of welding current on tensile strength at constant weld cycle: 90 cycles

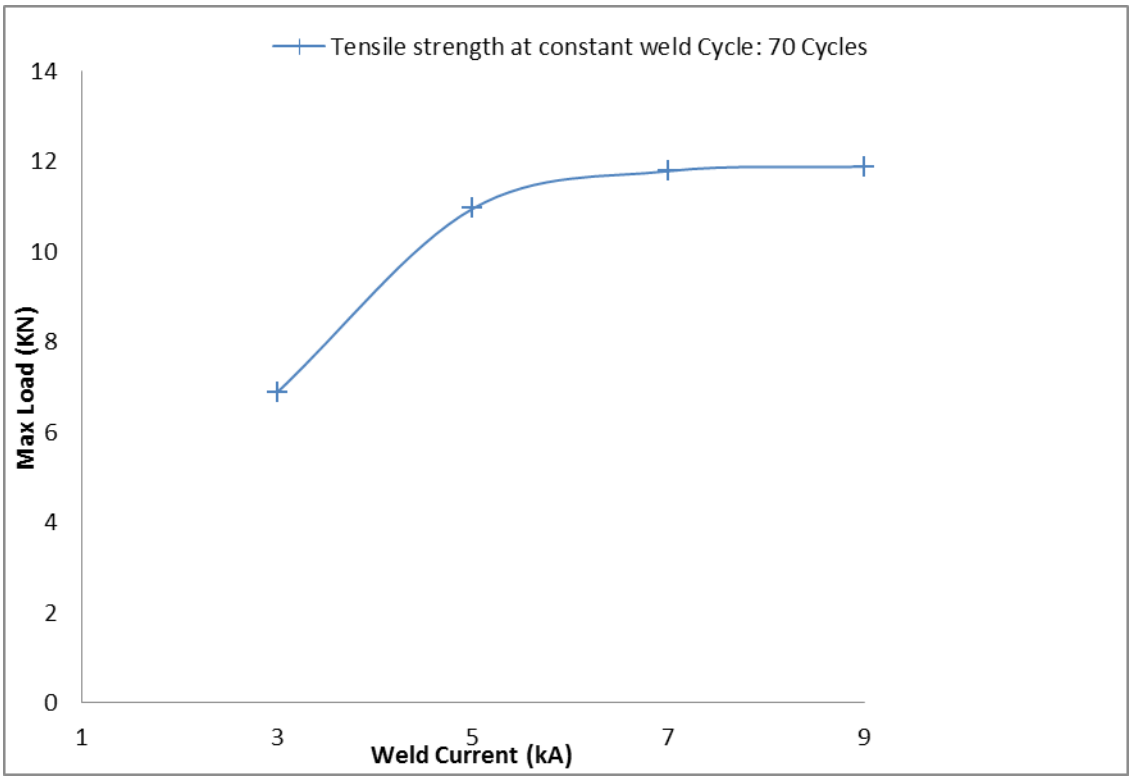

Figure 4.52: Effect of welding current on tensile strength at constant weld cycle: 70 cycles

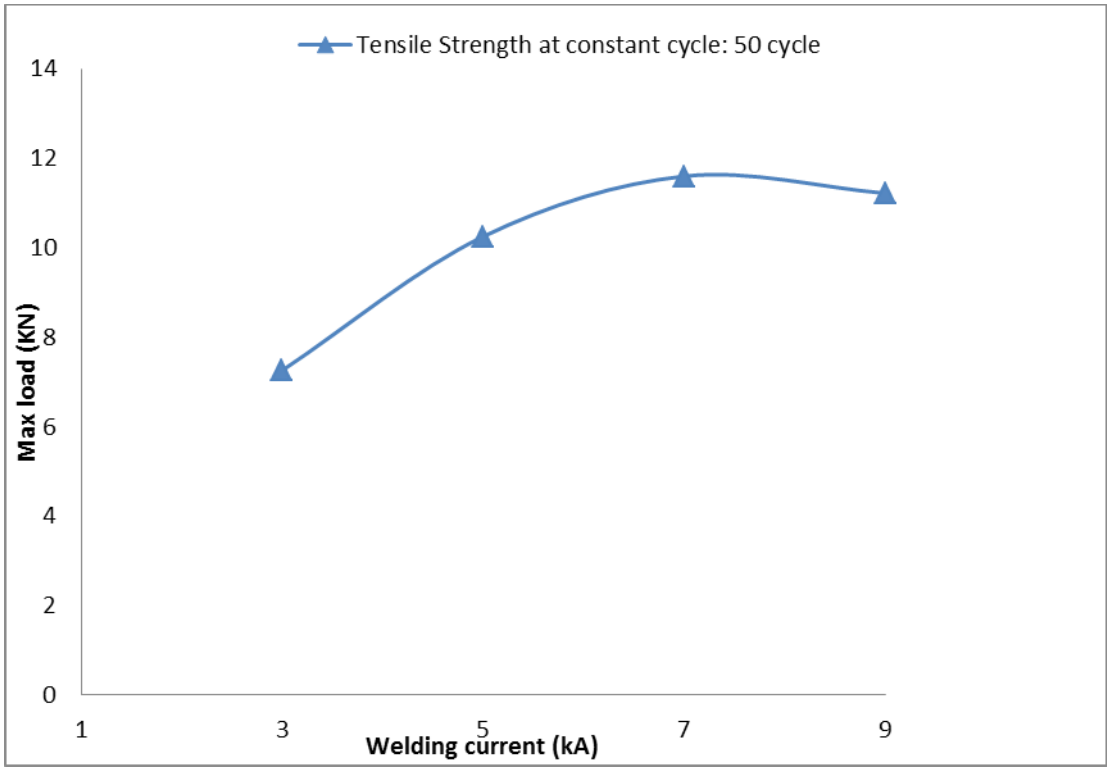

Figure 4.53: Effect of welding current on tensile strength at constant weld cycle: 50 cycles

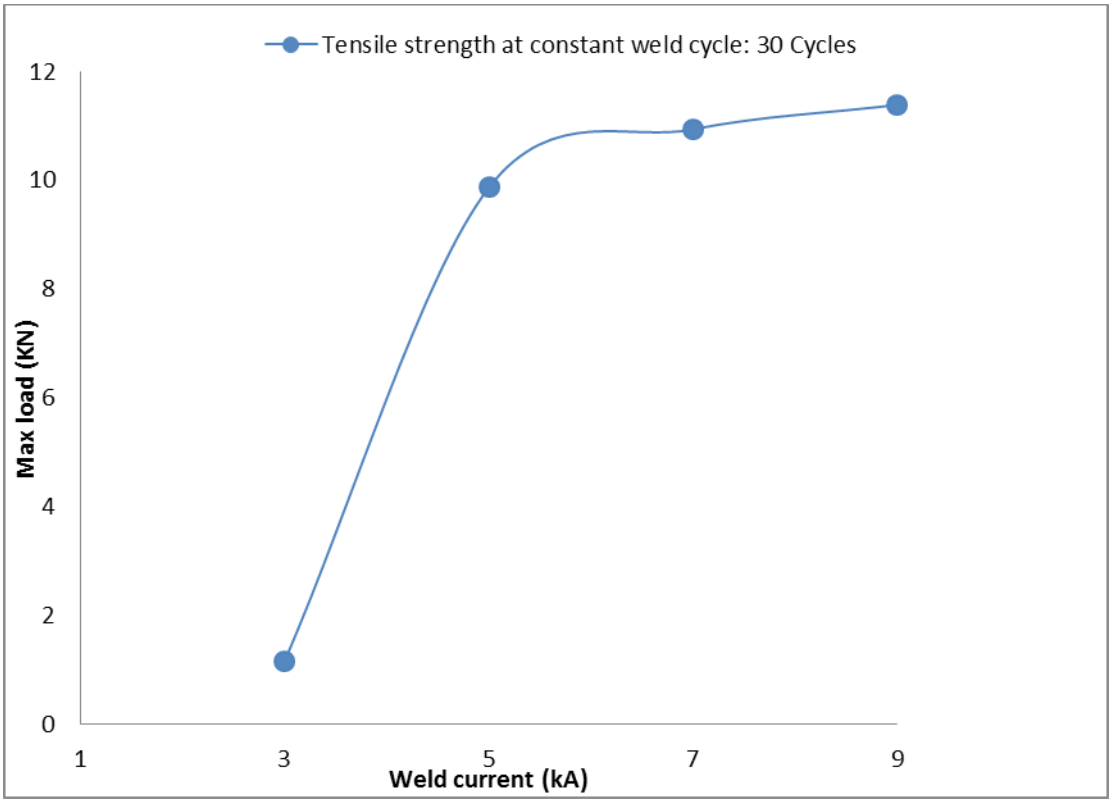

Figure 4.54: Effect of welding current on tensile strength at constant weld cycle: 30 cycles

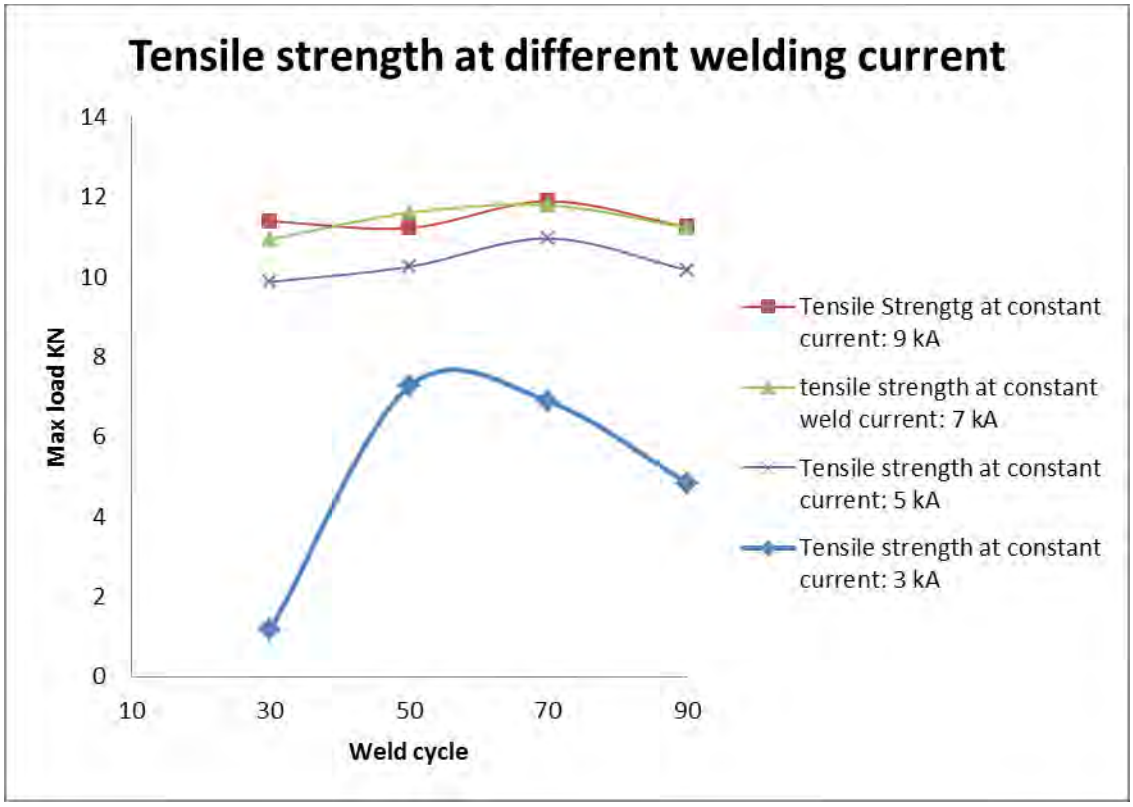

Figure 4.55: Effect of welding current at different weld cycle on tensile strength.

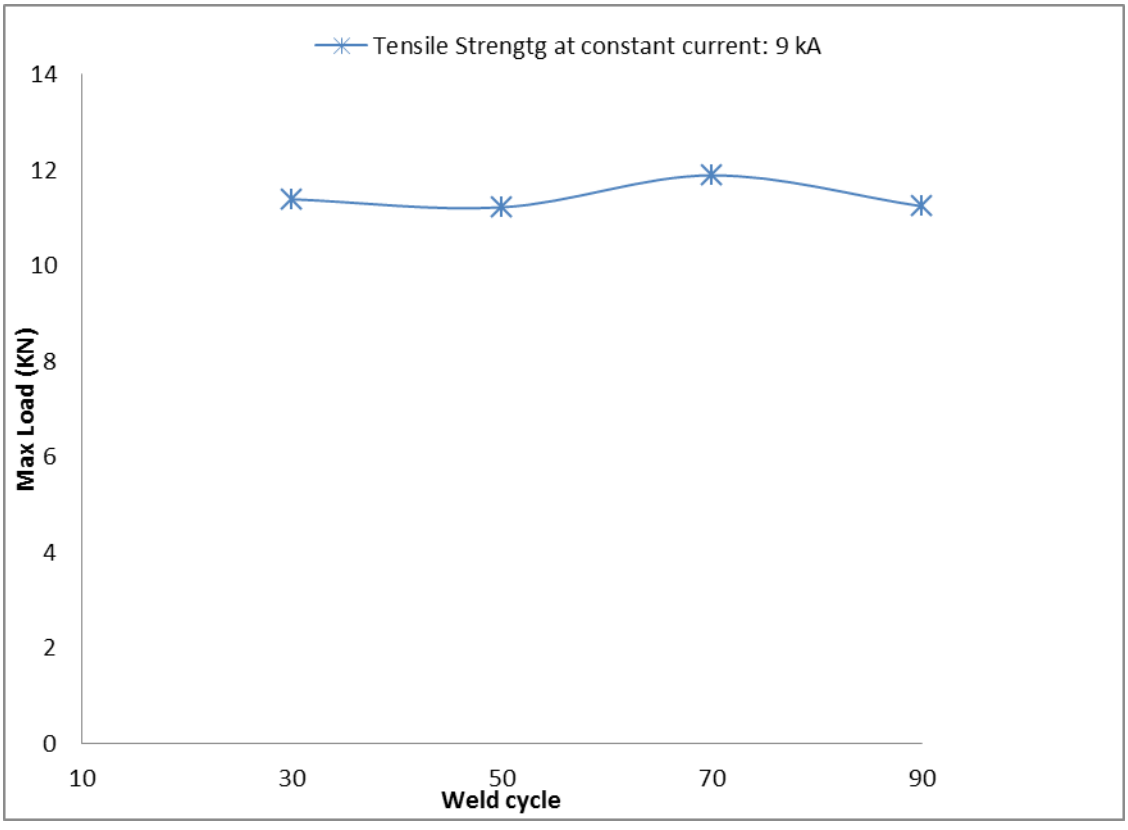

Figure 4.56: Effect of welding cycle on tensile strength at constant welding current: 9 kA

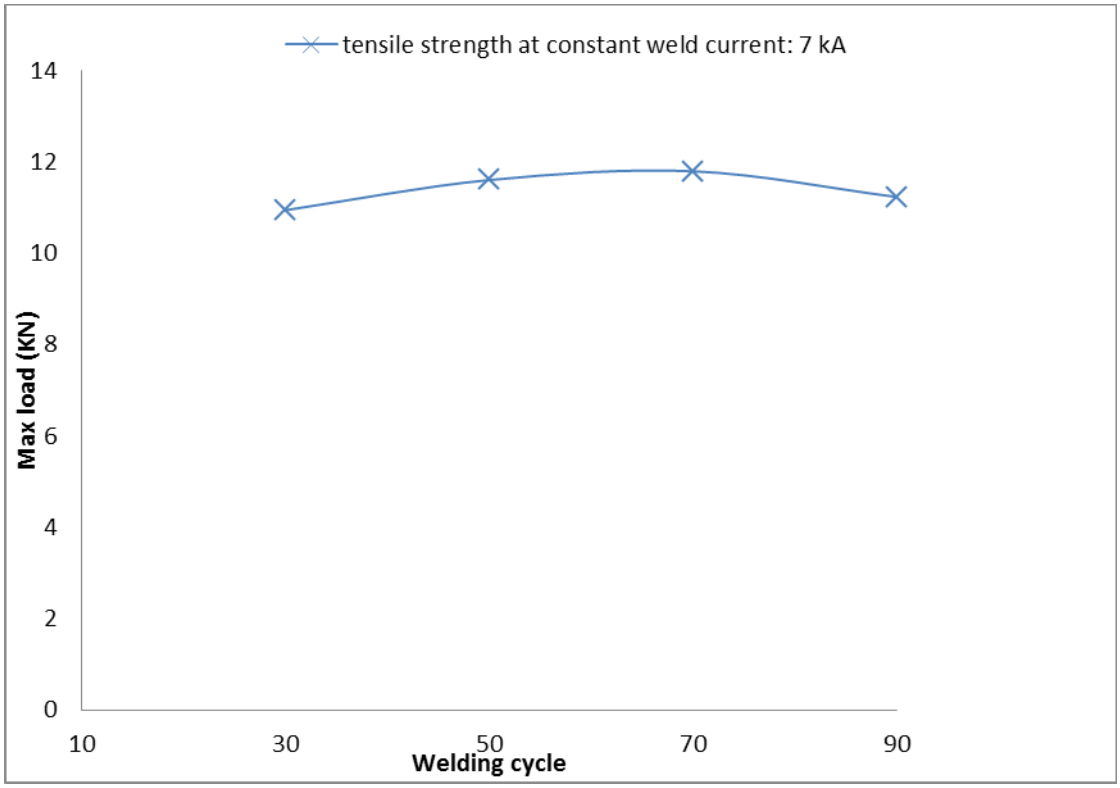

Figure 4.57: Effect of welding cycle on tensile strength at constant welding current: 7 kA

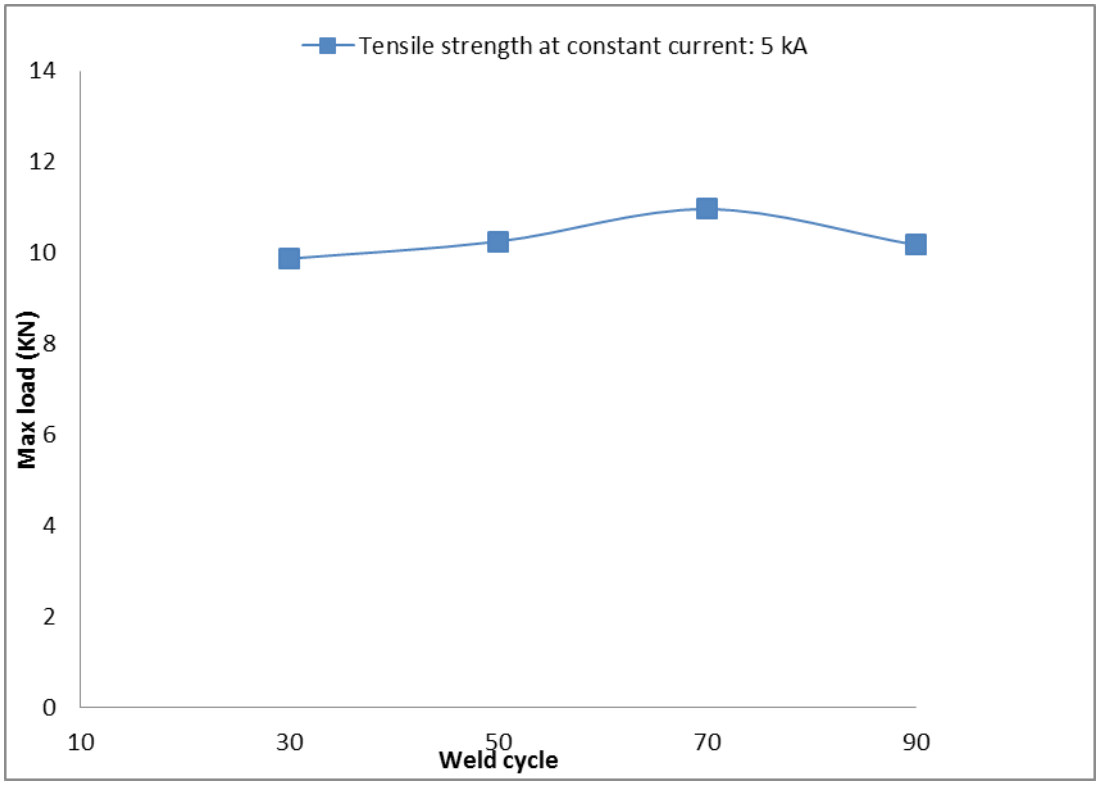

Figure 4.58: Effect of welding cycle on tensile strength at constant welding current: 5 kA

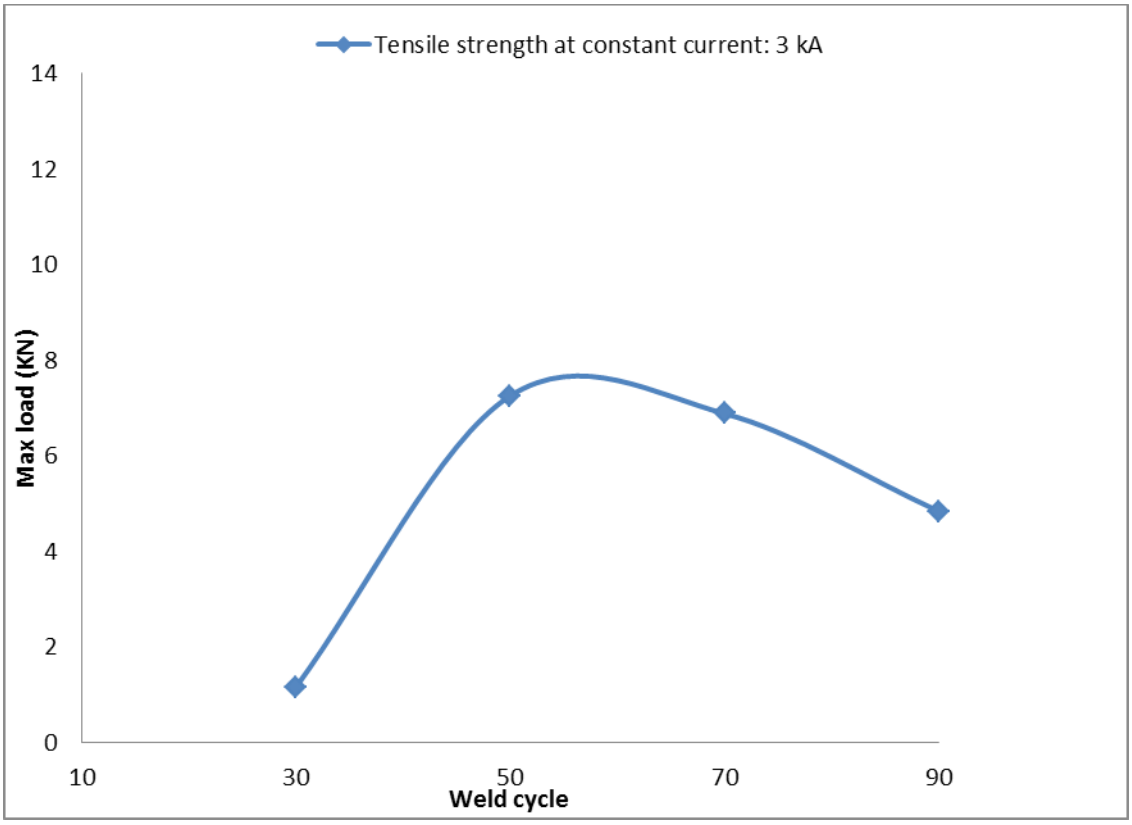

Figure 4.59: Effect of welding cycle on tensile strength at constant welding current: 3 kA

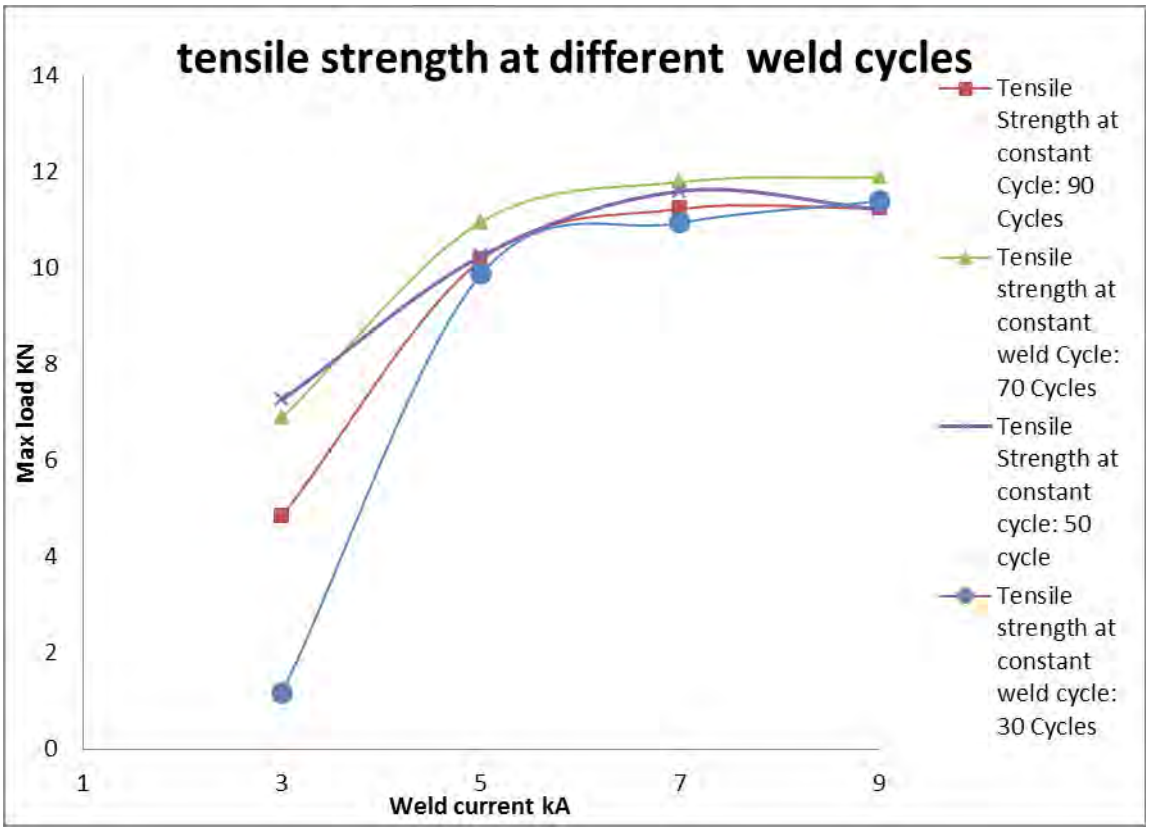

Figure 4.60: Effect of weld cycle at different weld current on tensile strength

Figures 4.51 to 4.54 show that at constant welding cycle an increase in welding current increases the maximum tensile load. At lower current this value is very low which is not suitable for working condition. At maximum welding current welding coupon tear at the base material which means weld nugget has higher strength than base metal. Figure 4.55 showed that at constant welding cycle, welding current have an important effect on tensile strength.

Figures 4.56 to 4.59, it can be seen that at constant welding current there is no significant effect of welding cycle on tensile strength. Figure 4.60 show at 70 cycles welding nugget has the maximum tensile strength.

The entire result can be explained by weld nugget size. Increasing welding current and welding cycle increase the heat input in the welded coupon. And the increased heat input incresase the nugget size of the welded coupon. That is the main controlling factor that determine tensile strength.

M. Pouranvari[26] found that in addition to peak load, maximum energy should be considered to more precisely describe spot welds mechanical behavior and performance. Excessive electrode pressure can reduce both peak load and maximum energy considerably. Holding time does not significantly affect peck loadand maximum energy for investigated material. Increasing welding time and welding currentto some extent, increase both peak load and maximum energy. Although expulsion might not decrease spot weld load carring capasity. It could reduce their energy absorption capability.

4.7 EDX test results:

The energy dispersive X-ray (EDX) test results are presented below.

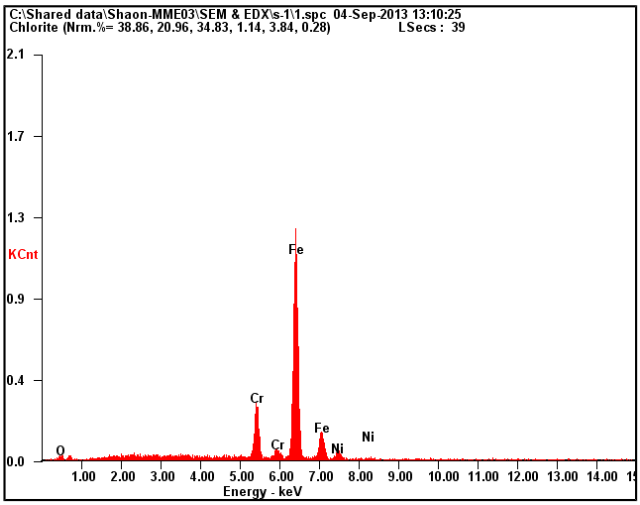

(a)

Element	Wt %	At %
CrK	11.48	12.27
FeK	82.66	82.20
NiK	05.85	05.54

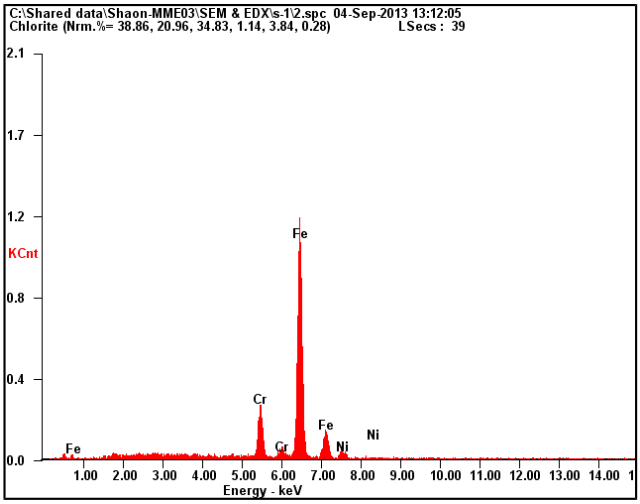

(b)

Element	Wt %	At %
CrK	10.82	11.57
FeK	83.64	83.20
NiK	05.54	05.24

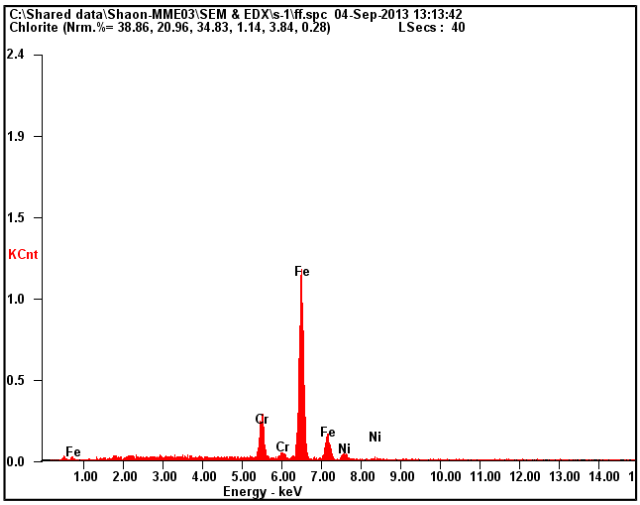

(c)

Element	Wt %	At %
CrK	10.38	11.09
FeK	84.35	83.92
NiK	05.28	04.99

Figure 4.61: EDX result of S-1 (a) ASS side (b) FZ (c) LCS side

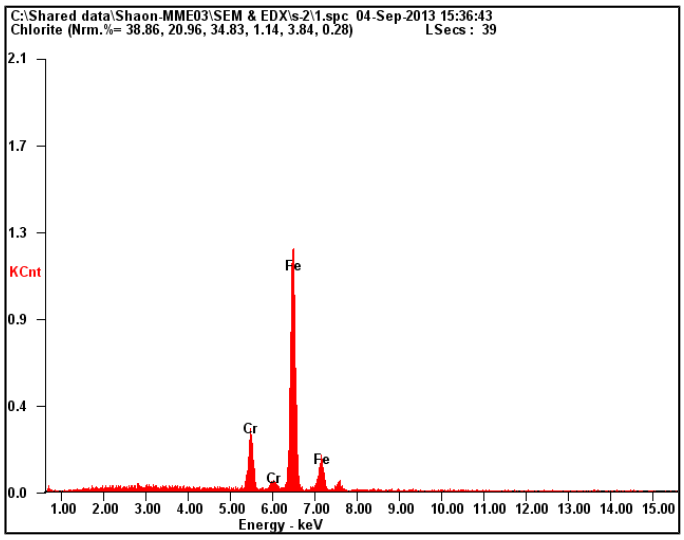

Element	Wt %	At %
CrK	10.99	11.74
FeK	83.11	82.67
NiK	05.90	05.59

(a)

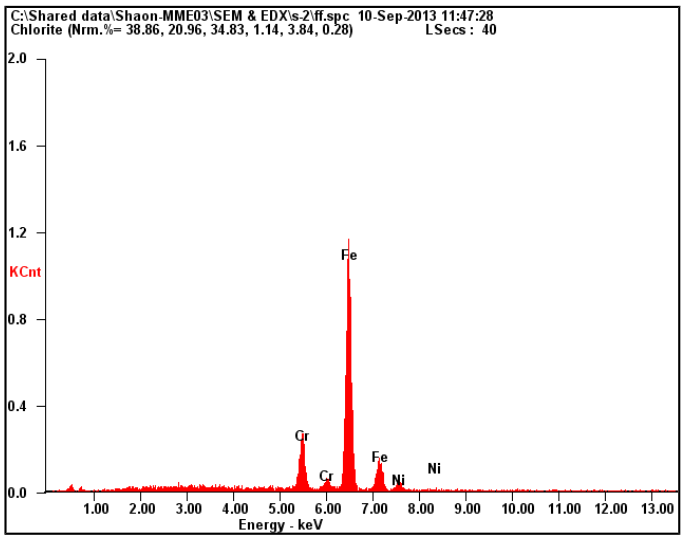

Element	Wt %	At %
CrK	10.76	11.49
FeK	83.65	83.21
NiK	05.60	05.30

(b)

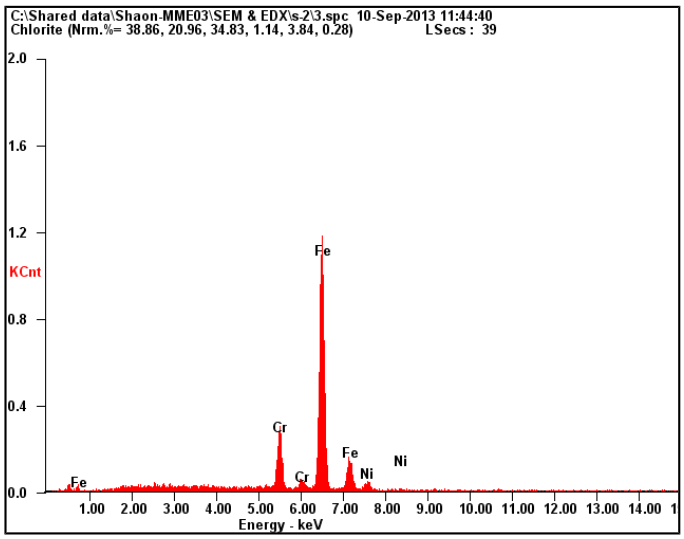

Element	Wt %	At %
CrK	10.52	11.25
FeK	83.52	83.12
NiK	05.95	05.64

(c)

Figure 4.62: EDX result of S-2 (a) ASS side (b) FZ (c) LCS side

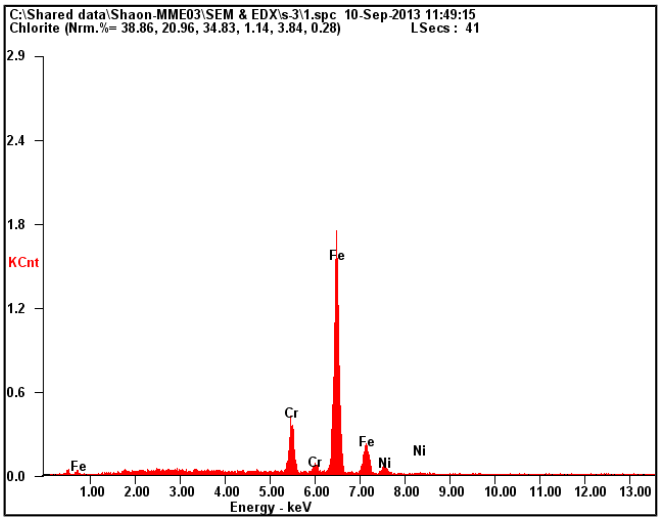

(a)

Element	Wt %	At %
CrK	10.75	11.49
FeK	83.79	83.35
NiK	05.46	05.16

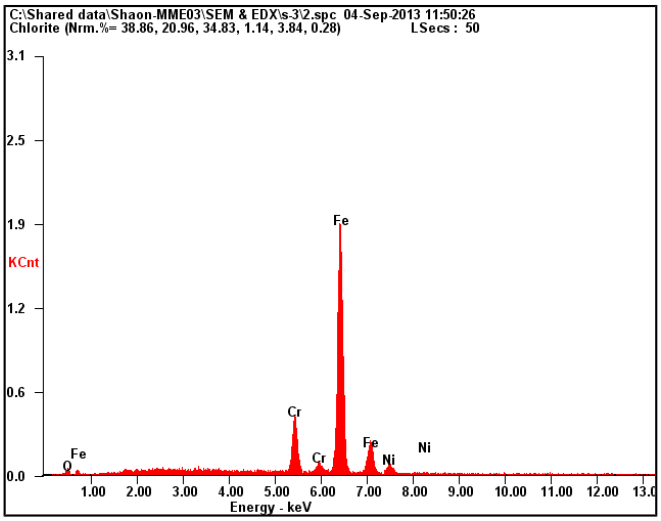

(b)

Element	Wt %	At %
CrK	10.34	11.05
FeK	83.65	83.25
NiK	06.02	05.70

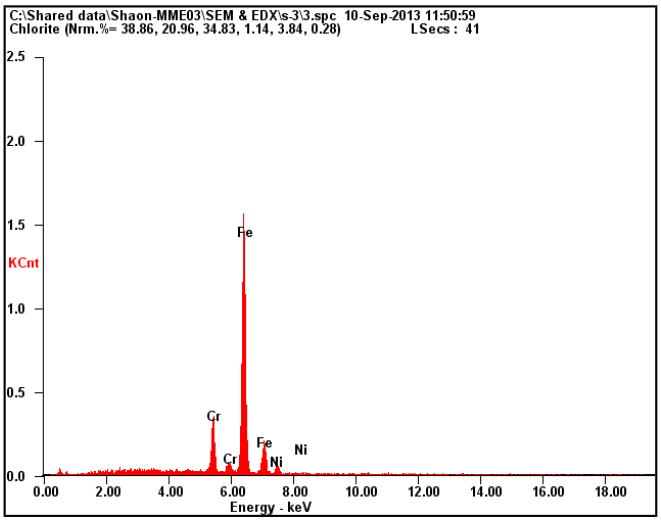

(c)

Element	Wt %	At %
CrK	09.85	10.53
FeK	84.55	84.17
NiK	05.60	05.30

Figure 4.63: EDX result of S-3 (a) ASS side (b) FZ (c) LCS side

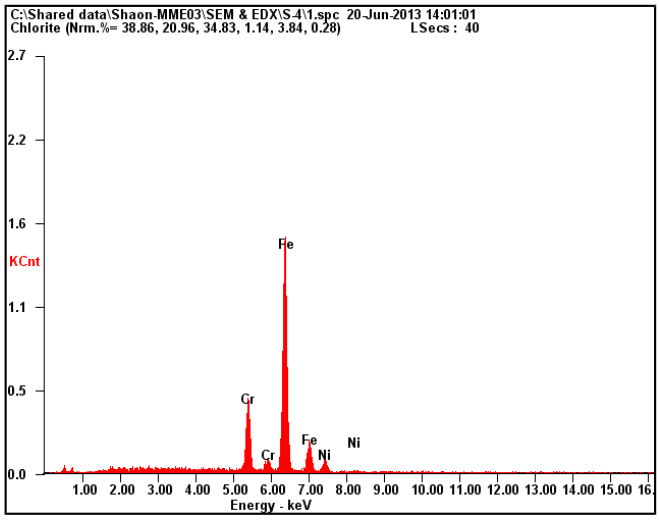

Element	Wt %	At %
CrK	15.31	16.31
FeK	78.05	77.42
NiK	06.64	06.26

(a)

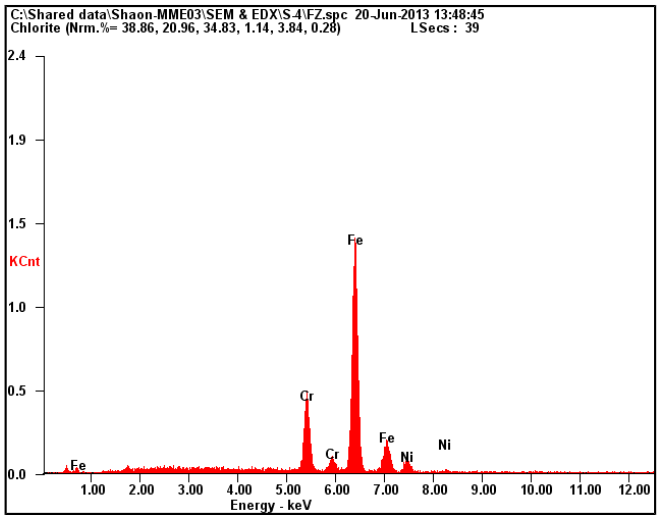

Element	Wt %	At %
CrK	15.28	16.28
FeK	77.58	76.97
NiK	07.15	06.74

(b)

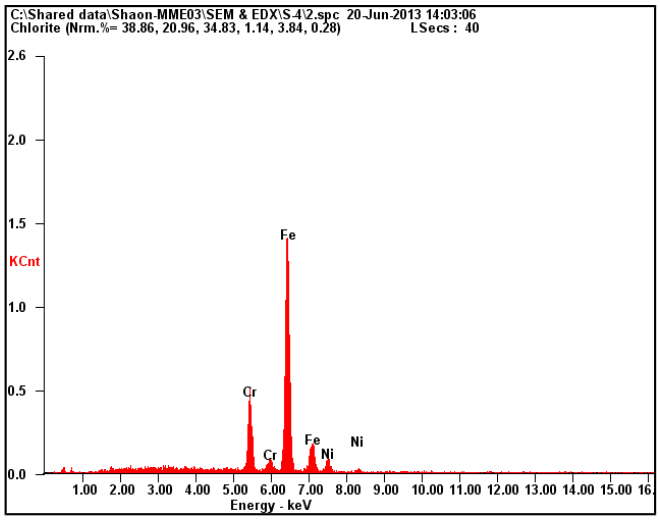

Element	Wt %	At %
CrK	15.22	16.21
FeK	79.29	78.62
NiK	05.49	05.18

(c)

Figure 4.64: EDX result of S-4 (a) ASS side (b) FZ (c) LCS side

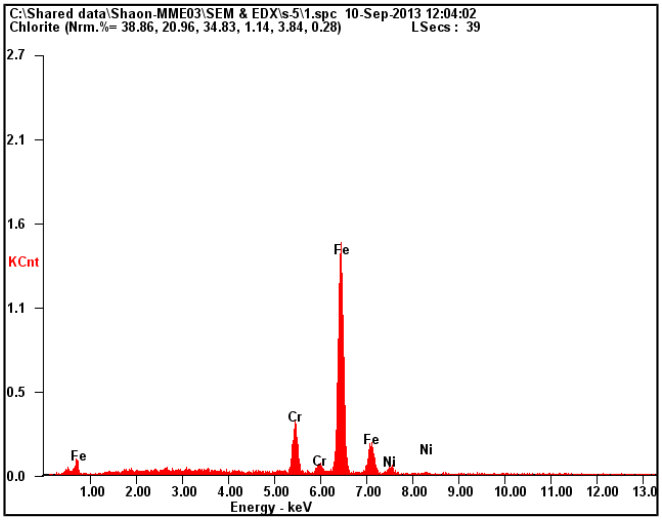

(a)

Element	Wt %	At %
CrK	10.43	11.15
FeK	84.06	83.64
NiK	05.50	05.21

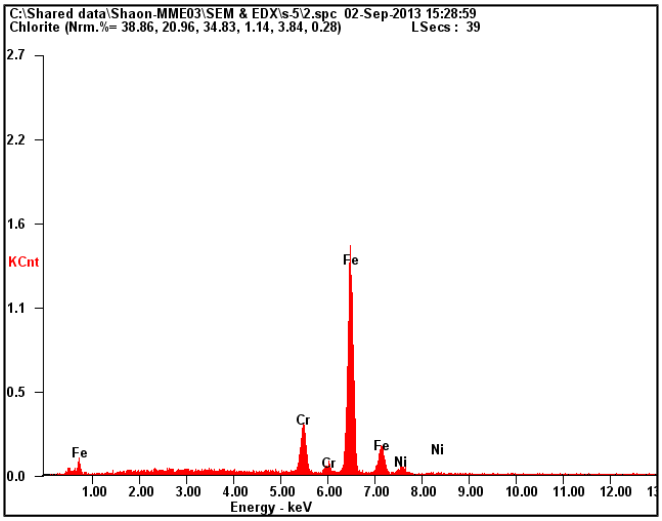

(b)

Element	Wt %	At %
CrK	10.82	11.56
FeK	83.76	83.32
NiK	05.42	05.13

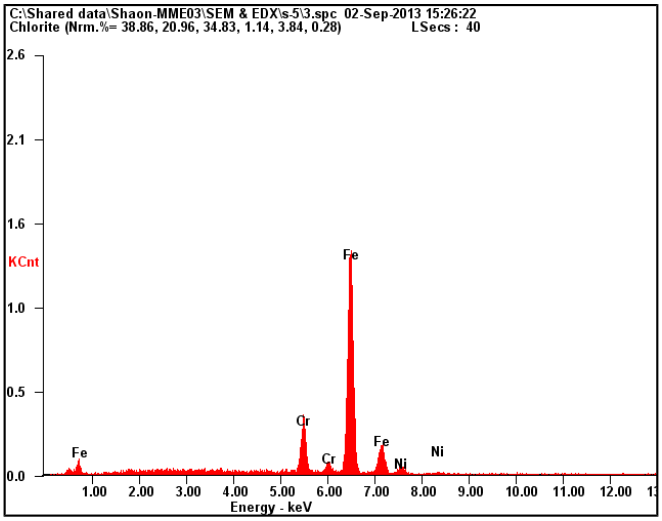

(c)

Element	Wt %	At %
CrK	10.28	10.98
FeK	84.33	83.91
NiK	05.39	05.10

Figure 4.65: EDX result of S-5 (a) ASS side (b) FZ (c) LCS side

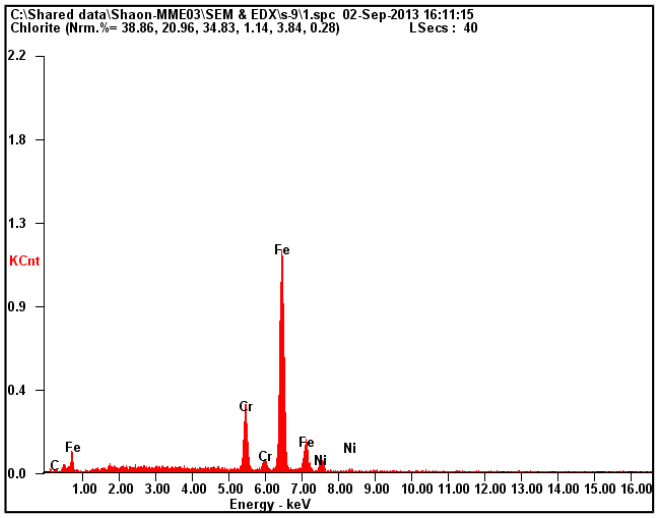

(a)

Element	Wt %	At %
CrK	12.27	13.11
FeK	80.90	80.44
NiK	06.82	06.45

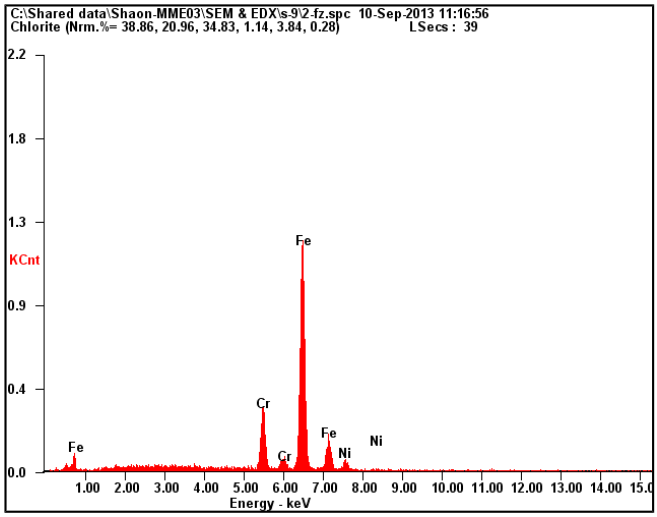

(b)

Element	Wt %	At %
CrK	12.06	12.88
FeK	81.90	81.41
NiK	06.04	05.71

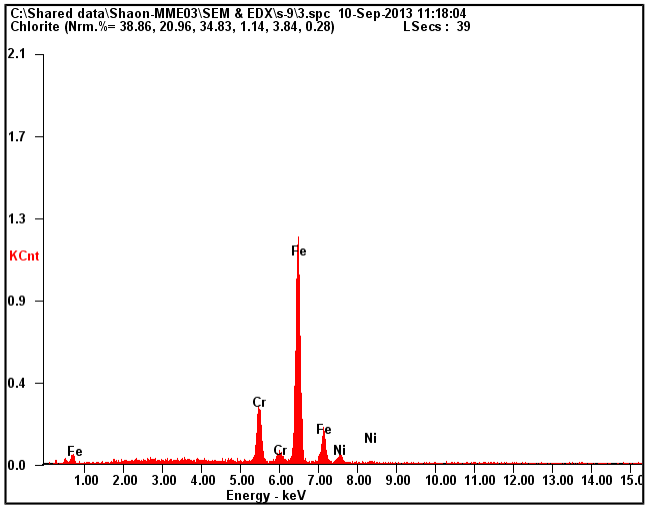

(c)

Element	Wt %	At %
CrK	11.34	12.11
FeK	83.10	82.63
NiK	05.56	05.26

Figure 4.66: EDX result of S-9 (a) ASS side (b) FZ (c) LCS side

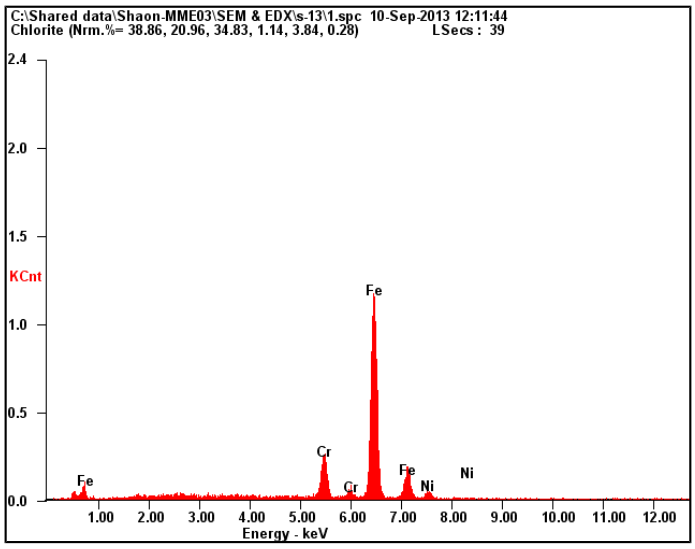

(a)

Element	Wt %	At %
CrK	10.09	10.78
FeK	84.48	84.07
NiK	05.44	05.15

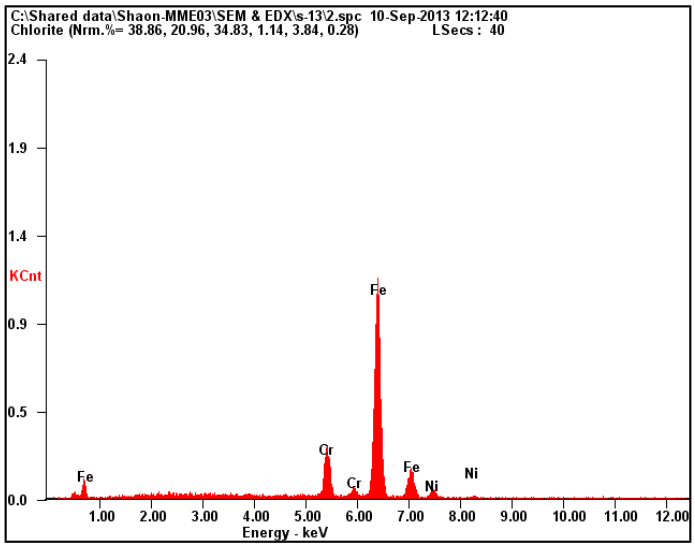

(b)

Element	Wt %	At %
CrK	10.08	10.78
FeK	84.12	83.73
NiK	05.80	05.49

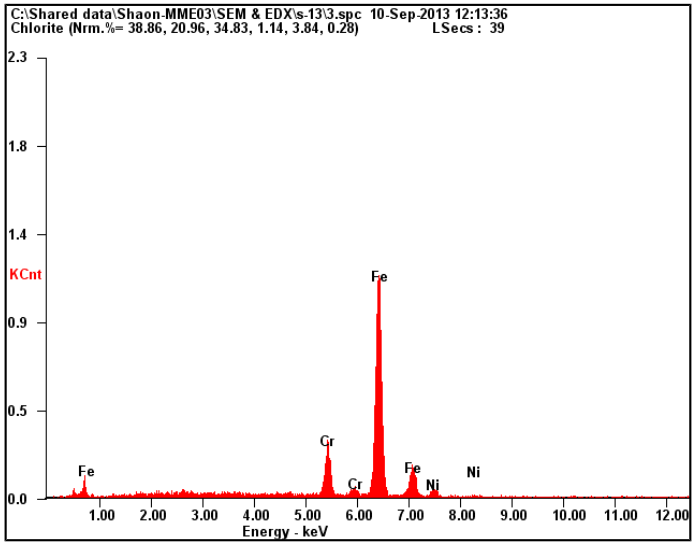

(c)

Element	Wt %	At %
CrK	10.03	10.72
FeK	84.45	84.05
NiK	05.52	05.22

Figure4.67: EDX result of S-13 (a) ASS side (b) FZ (c) LCS side

EDX results are given below (Table 4.3)

Table 4.3 EDX results summary

Sample	Current	Time	Chromium (%Wt)			Nickel (%Wt)		
No	(kA)	(Cycle)	ASS side	FZ	LCS side	ASS side	FZ	LCS side
S-1	9	90	11.48	10.82	10.38	5.85	5.54	5.28
S-2	7	90	10.99	10.76	10.52	5.90	5.60	5.95
S-3	5	90	10.75	10.34	9.85	5.46	6.02	5.60
S-4	3	90	15.31	15.28	15.22	6.64	7.15	5.49
S-5	9	70	10.43	10.82	10.28	5.50	5.42	5.39
S-9	9	50	12.27	12.06	11.34	6.82	6.04	5.56
S-13	9	30	10.09	10.08	10.03	5.44	5.80	5.52

It can be seen from Figures 4.61to 4.67 and Table 4.3 by the energy dispersive X-ray test (EDX detection) that the chromium is diluted from austenitic stainless steel to fusion zone. This dilution depends on heat input of the welded coupon. In these entire figure we found chromium content dilute from austenitic stainless steel to low carbon steel side. So chromium content of the austenitic steel side is maximum than in the center of the fusion zone. In the low carbon steel side of the fusion zone, chromium content is lower. At higher temperature this dilution rate of the chromium content is higher. Here also found that at lower heat input chromium content is maximum at fusion zone. Nickel content at center of the fusion zone is higher.

4.8 Failure Mode analyses

The modes of failure of resistance spot welded dissimilar metals joints at different welding parameters were investigated. Three different types of failure mode could be noticed. These are

1. Tearing of base metal.
2. Pull out failure mode.
3. Interfacial failure mode.

The failure locations and the schematics of the predictive characteristics curves for respective causes are given below.

4.8.1 Tearing of base metal

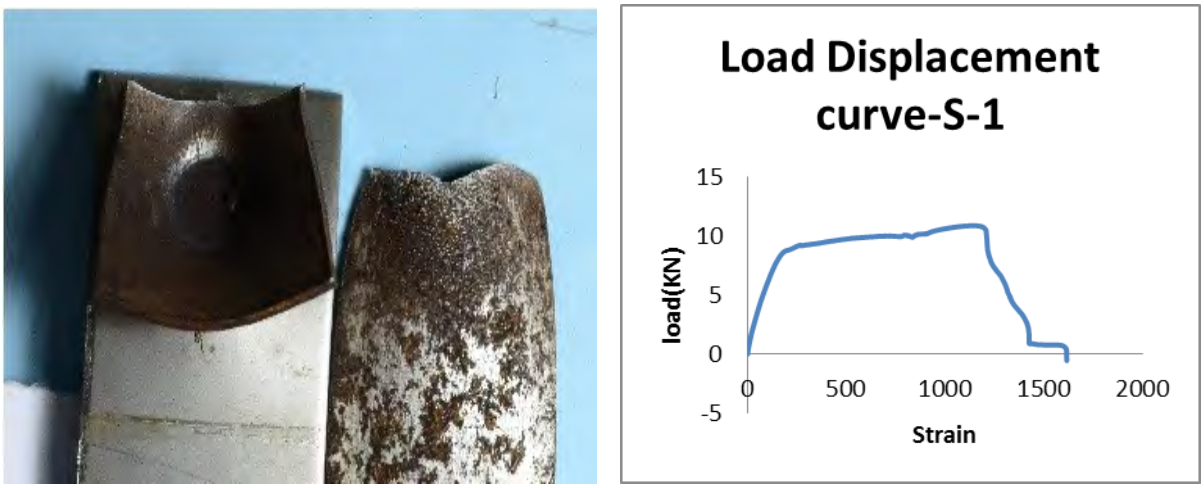

Figure 4.68: failure modes of S-1.

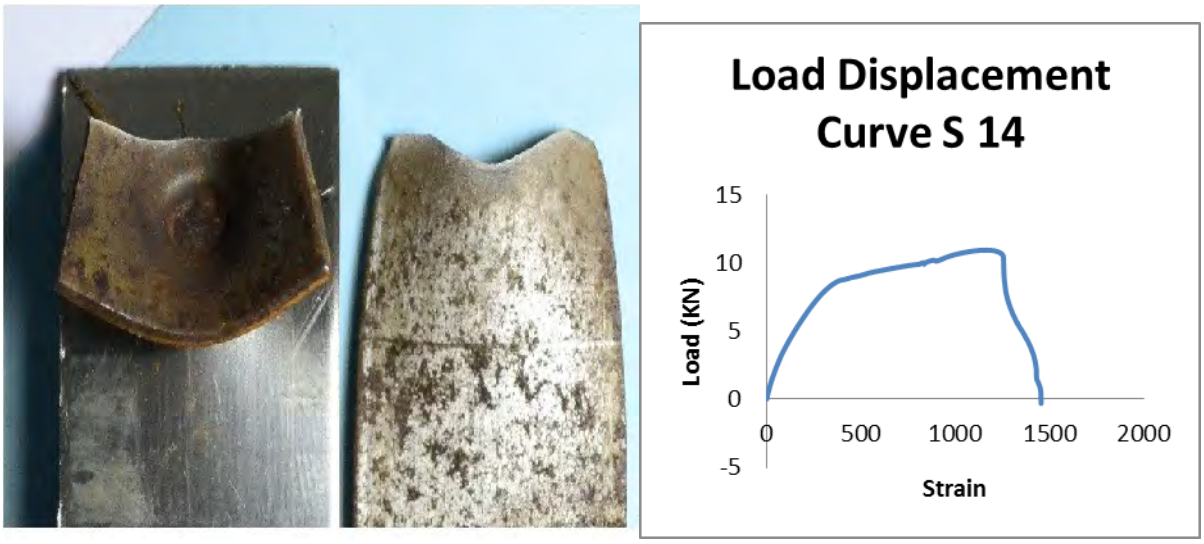

Figure 4.69: Failure mode of S-14

Figures 4.68 and 4.69 show that, the failure locations are in the base metal of the low carbon steel side which is not close enough to the nugget location. The cause of this type of failure is mainly in specimen size (length, width, overlap region) corresponds with process parameters. From analyze of tensile curve of this group of samples have behaved like low carbon steel. Strength of the welded zone is higher than the welded base material so the material tears far away from the welded nugget. So the main cause of this failure is excessive welding current and welding time. For proper spot welding and process parameter optimization this must be considered.

4.8.2 Pull out failure mode

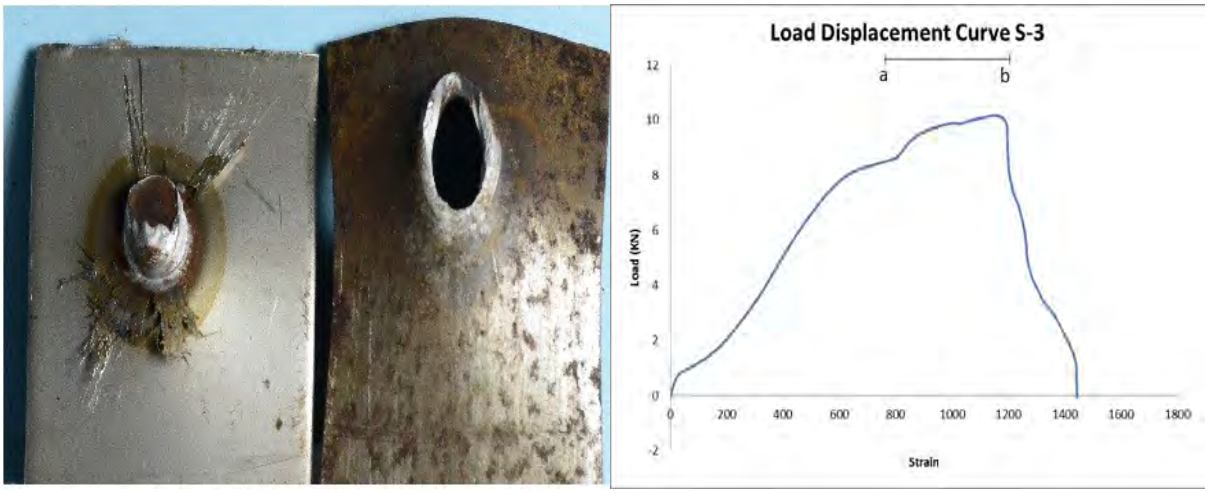

Figure 4.70: Failure mode of sample S-3

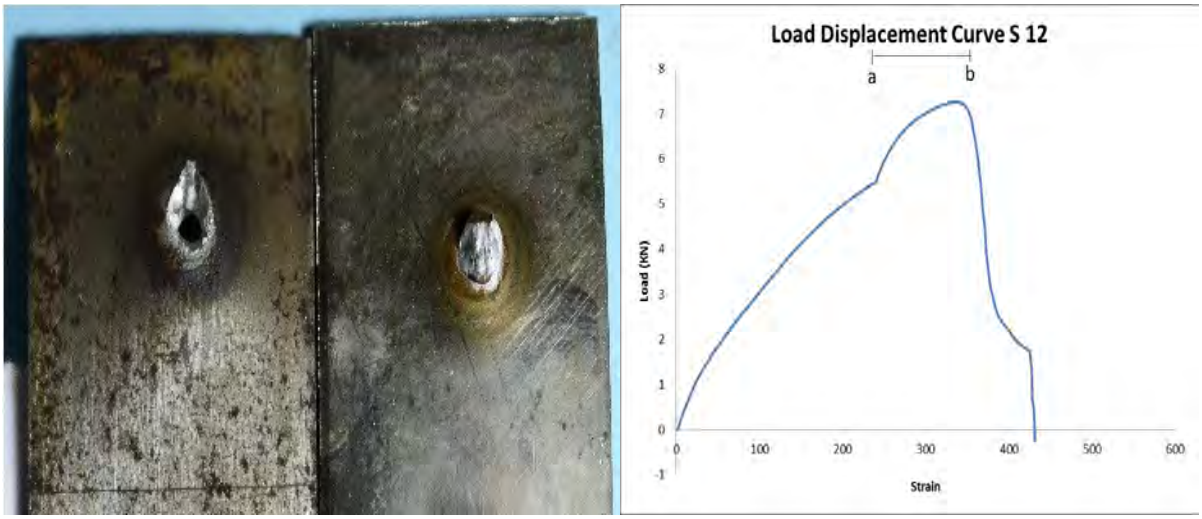

Figure 4.71: Failure mode of sample S-12

Figures 4.70 and 4.71 show welded nugget pullout failure where spot weld nugget gets out of the welded coupon. Because the nugget pulls out happens, it leaves behind a circular impression of the failure in the low carbon steel side.

Here we also found in the Figure 4.72 that welded coupon fails near to the nugget location and the material tears apart from the coupons.

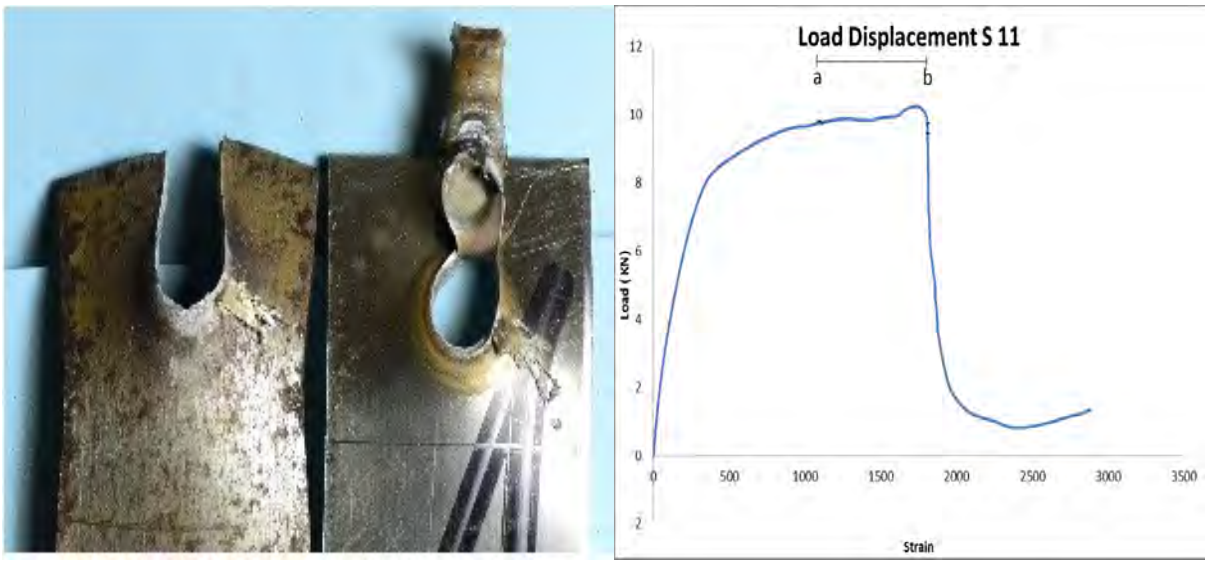

Figure 4.72: Failure mode of sample S-11

Nugget pullout failure occurred within a reasonable combination of the weld nugget diameter, thickness of the sheet metal and width of the testing samples correspondence with process parameters. From the tensile test we found in pullout failure mode that materials absorb higher energy than others so it gives a signal to fracture.

4.8.3 Interfacial failure mode

Another type of failure mode is interfacial failure mode where the coupons are detached from each other at the spot weld joint. This type of the failure occurs depends on the geometric dimension of the spot welding coupons. When considered in nugget diameter, it is shown that most of the interfacial failure occurs in case of the smaller nugget diameter with highest sheet thickness and this is for not proper welding current. These type of weld failure mode shown in below (Figure 4.73, 4.74 and 4.75).

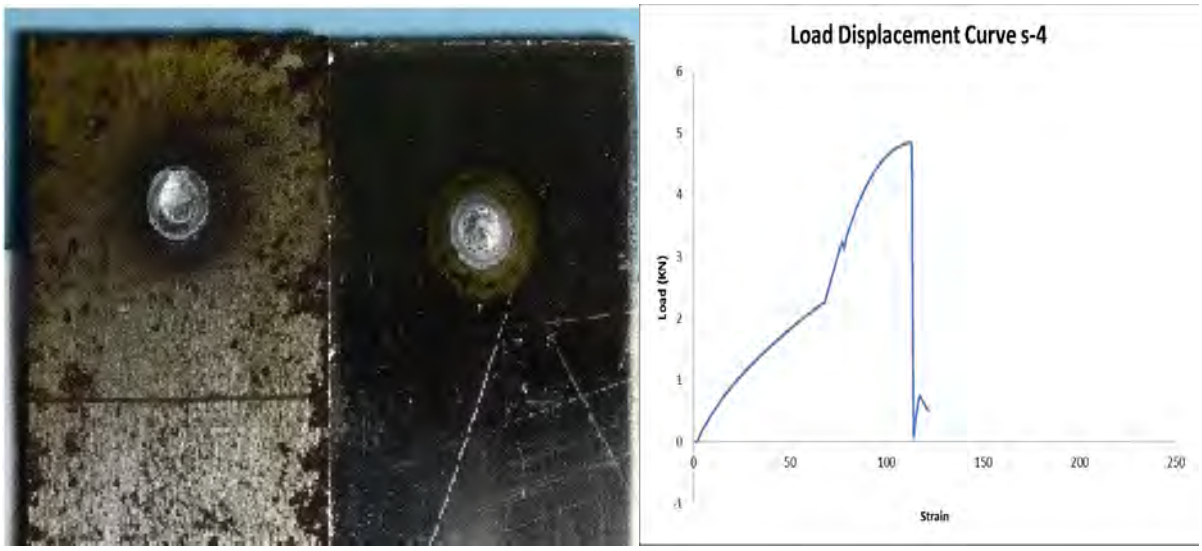

Figure 4.73: failure mode of sample S-4

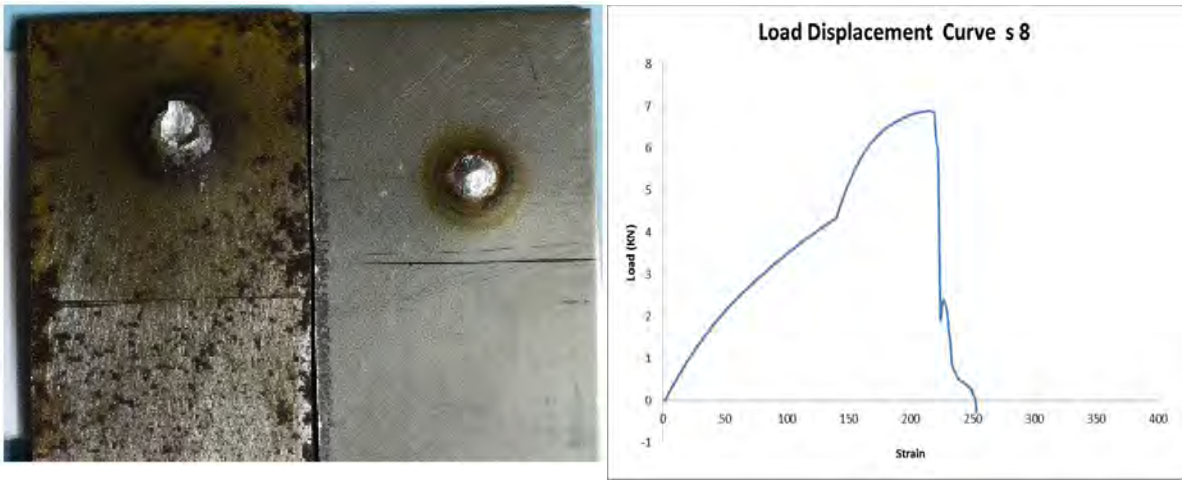

Figure 4.74: failure mode of sample S-8

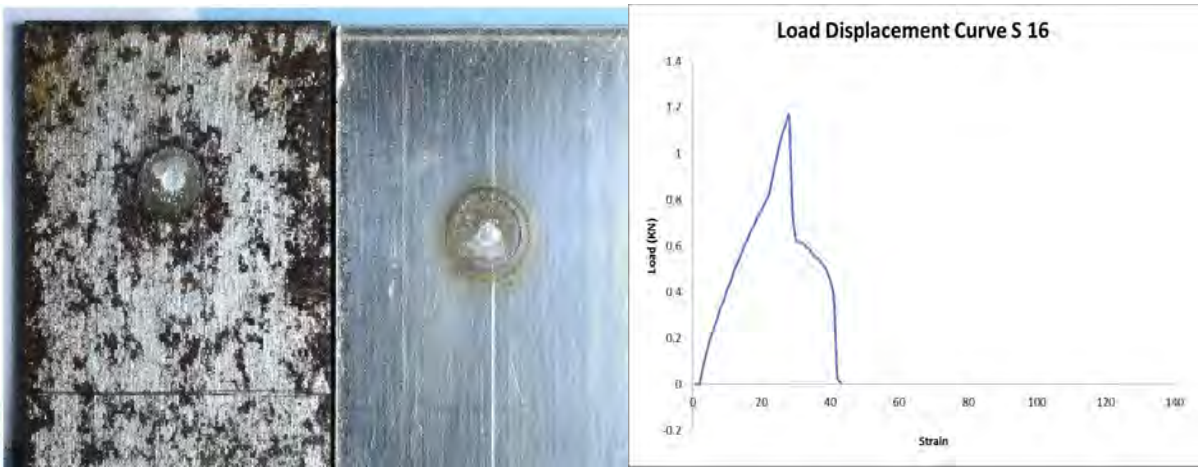

Figure 4.75: Failure mode of sample S-16

M. Pouranvari [25] found that spot welds fail in two modes: interfacial and pullout. In interfacial failure mode failure occurs by crack propagation through weld nugget, while in pull out mode, failure occurs by weld nugget being completely or partially pulled out from the metal sheet. Failure mode has strong effect on weld peak load and maximum energy. Maximum energy and maximum load have less value for interfacial failure mode compare to pullout failure mode. Interfacial failure mode show no plastic deformation while pullout failure mode accompanied by considerable plastic deformation. At low welding current and low welding cycle failure occurs in interfacial failure mode. Increasing welding current and welding time increases weld nugget diameter and thus changes the failure mode to pullout mode. Holding time does not affect weld nugget size and failure mode. P. Marashi [18] found that fusion zone size and the failure mode are the most critical factors in the weld quality in terms of peak load and energy absorption which is governed by the welding parameters such as welding current, welding cycle, welding force. Spot weld strength in the pullout failure mode is controlled by the strength and fusion zone size of the galvanized steel side. The hardness of the fusion zone which is governed by the dilution between two base metals, and fusion zone size of galvanized carbon steel side govern failure mode. For spot welds made at low welding current, low fusion zone hardness and small fusion zone size led to experiencing interfacial mode during tensile shear test. While for spot welds made at high welding currents, higher hardness of fusion zone due to matrtensite formation and larger fusion zone led to experiencing pullout failure mode during tensile shear test. Summary of the failure mode for all tested samples are given below table.

Table 4.4 Summary of failure analysis.

Sample No	Current KA	Time Cycle	Nugget Size Mm	Failure mode
S-1	9	90	7.75	Metal tear away from nugget
S-2	7	90	6.8	Metal tear away from nugget
S-3	5	90	5.4	Button Shape Pullout Failure
S-4	3	90	3.3	Interfacial Failure
S-5	9	70	7.1	Metal tear away from nugget
S-6	7	70	7	Metal tear away from nugget
S-7	5	70	7	Metal tear away from nugget
S-8	3	70	3.8	Interfacial Failure
S-9	9	50	6.8	Metal tear away from nugget
S-10	7	50	8	Metal tear away from nugget
S-11	5	50	5.3	Pullout apart from coupon
S-12	3	50	5.6	Button Shape Pullout Failure
S-13	9	30	5.9	Metal tear away from nugget
S-14	7	30	5.7	Pullout apart from coupon
S-15	5	30	5.4	Pullout apart from coupon
S-16	3	30	2.8	Interfacial Failure

So we found that fusion zone size is the key physical attribute properties of the resistance spot welds. The effect of welding current and welding time is important for fusion zone size. Figure 4.76 show that a reduction in welding current reduces fusion zone size because a reduction in current reduces heat generation in the sheet/sheet interface. All failure analysis shows failure occurs by tearing of low carbon steel side from spot welded dissimilar metal in all condition.

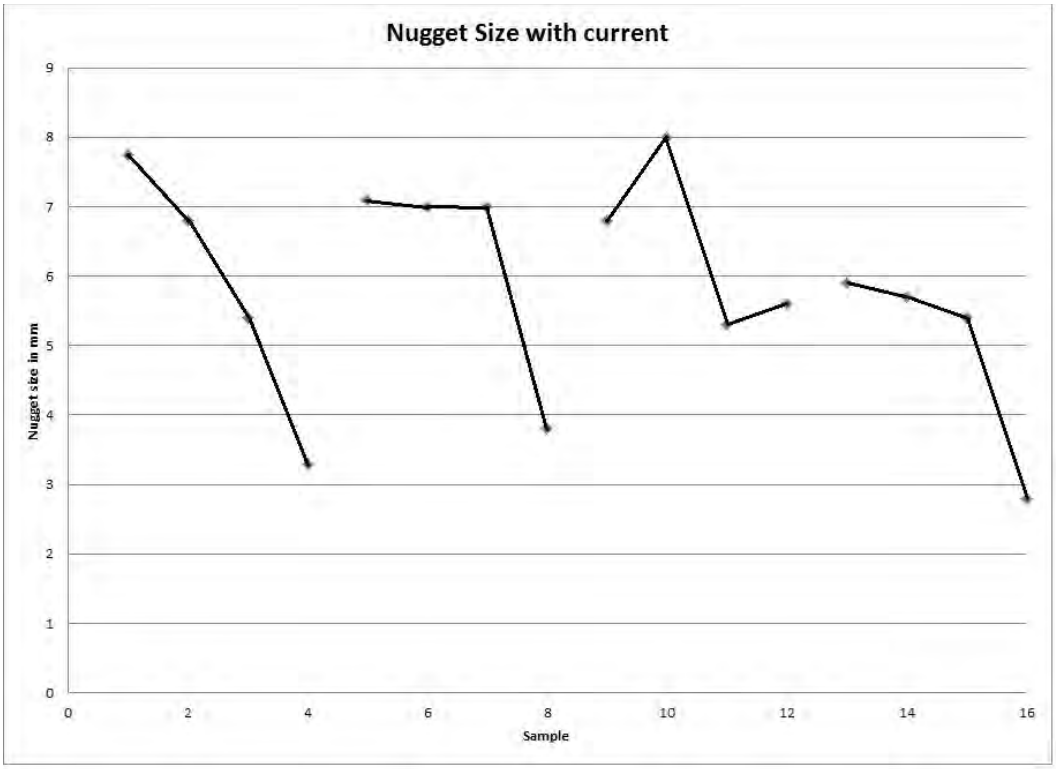

Figure 4.76: Nugget size decrease with decreasing welding current.

In the interfacial failure mode SEM image (Figure 4.77) of the fracture surface shows dimples. It is fact that during tensile test the tendency to fail in the brittle manner is high but the presence of dimples in the fracture surface indicates the failure was ductile in nature. This is due to fact that both of the two metal uses in this experiment was soft material with large plastic deformation before final fracture. In the pullout failure mode stress at the nugget circumference is the main driving force and it is also ductile fracture with elongated dimples along with loading direction (Figure 4.78).

Hence the nugget pullout failure mode is determined as the most desirable failure mode for the resistance spot welds. It absorbs much energy before failure and gives signal before fracture. The failure mode is changed from interfacial to pullout out failure mode by increasing current but excessive current may cause higher strength from base material which is not desirable for spot welding. So 5 to 6 KA current is suitable for this type of dissimilar metal spot welding where pullout failure found.

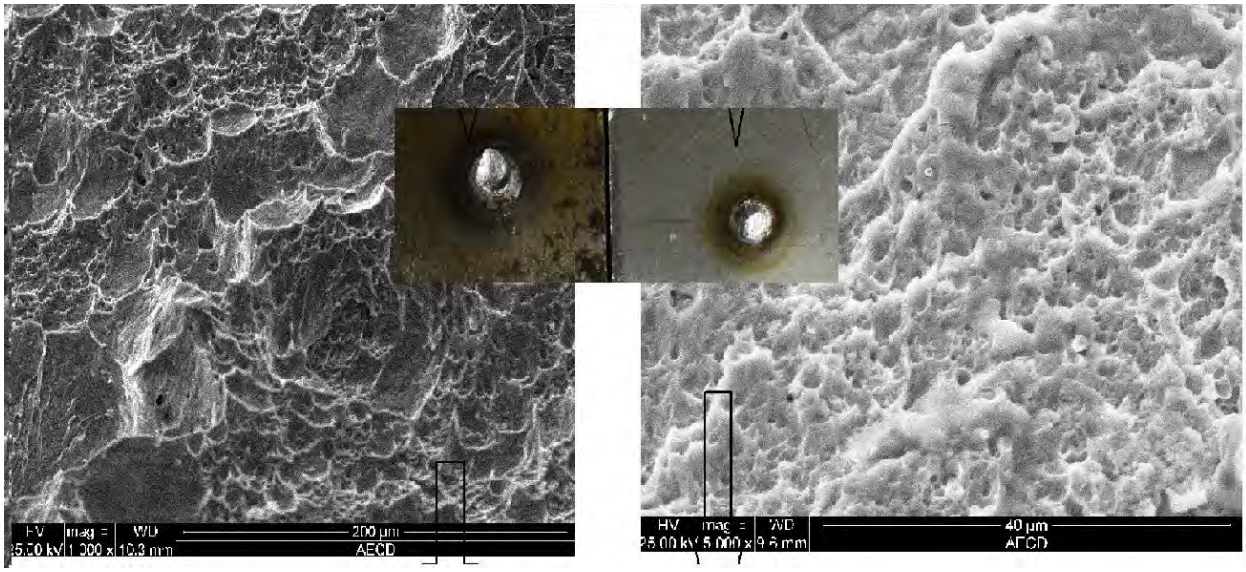

Figure 4.77: SEM image of the interfacial failure mode.

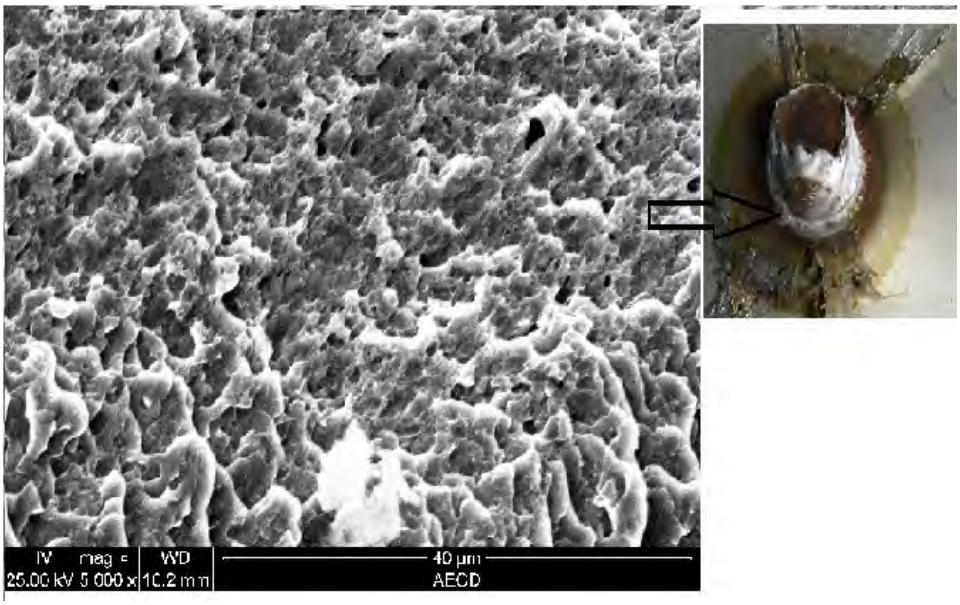

Figure 4.78: SEM image of the pullout failure mode.

4.9 Parameter optimization:

For process parameter optimization of dissimilar metal some point should be considered.

Fusion zone size is the most important phenomenon in determination of mechanical properties of resistance spot welding. Larger the fusion zone size, higher the strength of the spot welded sample. Fusion zone size depends on material characteristics, welding current, welding time and also on welding force. Generally higher the heat input larger the fusion

zone size but excessive heat input makes the weld nugget too large which is not appreciable for mechanical property.

Severe expulsion should be prevented during welding. An increase in heat input increases the temperature in the interface of the electrode and metal interface so higher the temperature expulsion may occur. This expulsion reduces the fusion zone size and also reduces the strength of the weld.

The welding parameter should be adjusted such that the pullout failure modes obtain during mechanical testing. Pullout failure mode is most desirable failure mode during their service life. A complex loading condition including shear, tensile, compression, bending or torsion stresses are introduce in spot welded metal and pullout failure mode give maximum safety of the system.

The discussion and analyses all of results of the experiments indicate that optimum fusion zone size is 5 mm to 6 mm and the theoretical value for 1.5 mm thick sheet metal is minimum 5 mm (from Eqn 3.1). It was found that the optimum welding tensile load is around 10 KN for this dissimilar combination and for maximum loading condition we need 5 to 7 KA current.

Chapter 5

Conclusion

5.1 Summary and Conclusion

In this research work Resistance spot welding is done between two different types of sheet metals. Here low carbon steel and austenitic stainless steel sheets are used. Welding parameters are varied welding current and welding cycle. After resistance spot welding, the size of the welding nugget is measured from macrograph and analyses the effect of welding parameters. Optical microscopy, EDX and SEM were taken at different location of the weld nugget. Various mechanical tests like micro hardness testing, tensile testing were performed to observe the effect of welding parameters. Here also the failure modes of the fracture samples were described from tensile shear testing. Lastly, we are trying to optimize the process parameter of the resistance spot welded dissimilar metal.

From this research work the following conclusion were made

- **Welding nugget**

Weld nugget size increases at increasing welding current at constant welding cycle but at constant welding current welding cycle has no significant changes of weld nugget size. The size of the weld nugget can be controlled by heat input and heat input rate. So welding current and welding cycle is the important parameter for determining weld nugget size. It is also considered that higher heat input produce expulsion which make deformed weld nugget and not acceptable in working condition.

- **Macrograph**

Asymmetrical weld nugget is found by welding of dissimilar materials. Final solidification line is shifted from sheet/sheet interface into the austenitic stainless steel side. The main reason of this properties is heat imbalance, this is because different heat conductivity, electrical resistivity and thermal expansion coefficient of austenitic stainless steel and low carbon steel.

- **Optical micrograph and scanning electron microscopy**

In the microstructural observation section there are there are three different zones are found which is base metal, heat affected zone and fusion zone or weld nugget. In the base metal of the low carbon steel side we found large amount of ferrite and low amount pearlite. In the stainless steel side exist twins' structure as unaffected zone and untransformable transition zone. Martensite, grain boundary ferrite, widmanstatan ferrite exist in the heat affected zone of the low carbon steel side with transition zone where partial allotropic recrystallizations take place and refined zone with finer ferrite and pearlite and widmanstaten structure in austenitic matrix and lamellar form extending base metal austenitic steel to fusion zone. In the fusion zone cast structure, some amount of grain boundary phase such as proeutectoid, widmanstaten ferrite and polygonal ferrite present in the weld nugget. Here surface weld is dendritic with excess delta ferrite in austenitic matrix. Here also found coarse columnar grain.

- **Micro hardness test**

Average micro hardness value is higher in the weld nugget than in the heat affected zone and lower at base metal in both base metals. This is proof the production of martensite in the weld nugget. Welding parameter has no different effect on hardness value. It has the main effect on size of fusion zone and heat affected zone.

- **Tensile properties**

Tensile properties show that higher welding current and higher welding cycle makes higher strength of the welded coupon.

- **Failure mode**

Fractured sample show the failure mode of the resistance welded dissimilar metal. Firstly Failure occurs in the base metal of the low carbon steel side which is not close enough to weld nugget. Higher welding current and welding cycle makes higher strength in the welds nugget which is larger than base metal so base metal tearing occurs. Another type of failure mode is pullout failure, where weld nugget gets out from the welded coupon and leaves behind a circular impression of the failure in the low carbon steel side. This is because a reasonable combination of the weld nugget diameter, thickness of the sheet metal and width of the testing samples corresponds with process parameter. Lastly another failure mode is

interfacial failure mode, where coupons are detached from each other at the spot weld joints. It is occurred where lower amount of welding current and lower welding cycle is used. From SEM observation we see that interfacial and pullout failure mode shows ductile fracture because large plastic deformation occurs before final facture.

- **EDX tests**

From EDX test. It is found that chromium and nickel dilution occurs from austenitic stainless steel to fusion zone towards low carbon steel side.

At the end of this research work we are trying to find optimum parameter of this welding process, here we use two different sheet steel, so it is not easy to find actual process parameter for this welding process. By considering different results and failure modes for this welding arrangement proper weld nugget size is 5mm to 6 mm and optimum tensile load is 10 KN and for this combination we need 5 to 7 kA welding current.

5.2 Suggestions for further studies

The effect of welding parameters on the properties of resistance welded dissimilar sheet metal was studied in the present work. Two different sheet metals such as austenitic stainless steel and low carbon steel were used in this experiment. Here various tests were performed to established process optimization. The following is recommended for future studies

- In this experiment we use maximum 9 kA welding current but for process optimization we can use more welding current.
- We use higher welding cycle, next time lower welding cycle will be used for process optimization.
- Welding force may be another process parameter.
- Corrosion study of the welded coupon can be performed to observed the effect of heat input on the corrosion properties of weldments
- Fatigue test may be performed.
- Homogenization of hardness profile of weld nugget formed in resistance spot welding.

References

1. ANSI/AWS/SAE, “Recommended Practices for Evaluating the Resistance Spot Welding Behavior of Automotive Sheet Steel Materials” 1997.
2. RWMA, “Resistance Welding Manual” 4th edition, 2003.
3. Hofman, K., Soter, M. , Orsette, C., Villaire, S. , Prokator, M. “ AC or DC for Resistance Welding Dual Phase 600”, Welding journal, vol:84 iss:1 pp:46 -48, 2005.
4. Tawade, G. and Boudreau, G., "Robust Schedules for Spot Welding Zinc- Coated High Strength Automotive Steels," Great Design in Steel, 2004.
5. Khan, M.I., Kuntz, M.L., Zhou, Y, Chan, K. and N Scotchmer. “Monitoring the Effect of RSW Pulsing on AHSS using FEA (SORPAS) Software” SAE technical paper (2007-01-1370), 2007.
6. Dickinson, D.W., “Welding in the Automotive Industry”. AISI Report SG81-5, August, 1981.
7. Darwish, S. M. H., & Ghanya, A., “Critical assessment of weld bonded technologies.” Journal of Materials Processing Technology, vol: 105, pp.: 221-229, 2000.
8. Bouyousfi, B., Sahraoui, T., Guessasma, S., & Chaouch, K. T., “Effects of process parameters on the physical charecteristics of spot weld joints.” Materials and Design, (Article in press), 2005.
9. Tumuluru M. D, “An Overview of the Ressitance Spot Welding of Coated High-Strength Dual-Phase Steels” Sheet Metal Welding Conference XII, Levonia Michigan May 2006.
10. Marya, Manuel, Wang, Kathy, Hector, L. G. Jr.., & Gayden, X. “Tensile shear forces and fracture modes in single and multiple weld specimens in dual phase steels.” Journal of Manufacturing Science and Engineering, Transactions of ASME, vol: 128(1), pp. 287 – 298, 2006.
11. Donders, S., Brughmans, M., Hermans, L., Liefooghe, C., Van der Auweraer, H., and Desmet, W. “The robustness of dynamic vehicle performance to spot weld failures.” Finite Element in Analysis and Design, vol: 42(8-9): pp. 670–682, 2006.
12. “Key factors influencing mechanical performance of dual phase steel resistance spot welds.” Science and Technology of Welding and Joining vol: 15(2), pp.149–155.

13. Pouranvari, M., Asgari, H. R., Mosavizadeh, S. M., Marashi P. H., and Goodarzi, M. “Effect of weld nugget size on overload failure mode of resistance spot welds.” Science and Technology of Welding and Joining. vol:12 (3), pp 217–225, 2007.
14. VandenBossche, D.J., “Ultimate Strength and Failure Mode of Spot Welds in High Strength Steels.” SAE Technical Paper, 770214, 1977.
15. Nakano, R. K., “Strain rate influence in the spot welding joint failure” M.Sc. Thesis, Escola Politecnica da Universidade de Sao Paulo,2005.
16. Zuniga, S., Sheppard, S. D., “Resistance Spot Weld Failure Loads and Modes in Overload Conditions.” Paper presented at the Fatigue and Fracture Mechanics: 27th volume ASTM STP1296, 1997.
17. Brown, J., Cai, W., Clay, N., Faitel, B., Johnson D., Bilge, U., “Weld Help Program”, Auto Body Consortium Inc., 1999.
18. Mansouri,M., Pouranvari, M., “Correlation between macro/micro structure and mechanical properties of dissimilar resistance spot welds of AISI 304 austenitic stainless steel and AISI 1008 low carbon steel.” MJoM Vol 15 (3), pp 149-157,2009.
19. Pouranvari,M., Marashi P., Goodarzi, M., “Failure mode of dissimilar resistance spot welds between austenitic stainless steel and low carbon steel.” Metal, pp. 13-15, 2008.
20. Nizamettin,K.,“The influence of welding parameters on the joint strength of resistance spot welded titanium steels.” Materials and design, vol 28, pp 420-427, 2007.
21. Gould, J.E “An examination of nugget development during spot welding using both experimental and analytical techniques.” Weld journal, 66, 1-s, 1987.
22. Marashi,P., “Microstructure and failure behavior of dissimilar resistance spot welds between low carbon galvanized and austenitic stainless steels.” Materials science and Engineering A, vol:480 pp175-180, 2008.
23. Hasanbasoglu,A., Kacar,R., “Resistance spot weldability of dissimilar materials (AISI 316L-DIN EN 10130-99 steels)” Materials and design, vol 28, pp 1794-1800, 2007.
24. Rajkumar,R.K., Hamimi,F., Charde,N., “Investigating the dissimilar weld joints of AISI 302 austenitic stainless steel and Low Carbon Steel” International journal of scientific and Research Publication, Vol 2, Issue 11,2012.

25. Alenius, M.,Pohjanne,P.,Somervuori,M.,Hanninen,H., “Exploring, the mechanical properties of spot welded dissimilar joints for stainless and galvanized steels.” welding journal, pp-305-313, 2006.

26. Pouranvari M., Abedi A., Marashi P., Goodarzi M., “Effect of expulsion on peak load and energy absorption of low carbon resistance spot welds.” Sci. Technol. Weld. Joining, Vol.13, pp.39-43, 2008.
27. Chao Y J, “Failure mode of resistance spot welds: interfacial versus pullout.” Sci.Technol. Weld Joining, Vol. 8, pp.133-137, 2003.
28. Datsko,J., Hartwig, L., McClory,M., J Mater Eng Perform, 10, pp.718-722,2001.
29. K.J. Ely, Y. Zhou, Sci. Technol. Weld. Join. 6, pp.63–72,2001.
30. A.L. Schaeffler, Met. Prog. 56 , 680–680B, 1949.
31. M.V. Li, D. Dong, M. Kimchi, SAE Technical Paper 982278, SAE international,Warrendale, PA (1998).
32. Lippold, J.C. , Kotecki, D.J. Welding Metallurgy and Weldability of Stainless steels. John Wiley & sons, 2005.
33. Deng, X. Chen,W., Shi, G., Finite Elem. Anal. Des. 35, pp.17–39, 2000.
34. Radaj,D., Sonsino, C.M., “Fatigue Assessment of Welded Joints by Local Approaches” Abington Publishing, Abington, Cambridge, England, 1998.
35. Bernabai, U., Brotzu, A., Felli, F., and Polidori, A. “Analysis of the problems in spot welding AISI 301 high-strength austenitic stainless steels and galvanized steel plates.” Welding International 11(10): pp.788-s to 794-s, 1997.
36. Akdut, N., Corostola, J. R., Koruk, A. I., Cretteur, L., and Maronna, I. “Joining technologies to realize dissimilar joints for automotive applications.” Automotive and Transportation Technology Congress and Exposition, Barcelona, Spain, 2001.
37. Zuniga S. M., “Predicting overload pull-out failures in resistance spot welded.” Ph.D. thesis, Stanford University,1994.
38. Lippold ,C., Kotecki, D. J., “Welding Metallurgy and Weldability of Stainless Steels.” John Wiley & Sons, 2005.
39. Khan MS, Bhole SD, Chen DL, Biro E, Boudreau G, Deventer JV. “Welding behaviour, microstructure and mechanical properties of dissimilar resistance spot welds between galvannealed HSLA350 and DP600 steels.” Sci Technol Weld Joining, vol.14, pp.616-25,2009.
40. Heuschkel, J.”Some metallurgical aspects of carbon steel spot welding.” Welding

Journal 26(10) , pp.560-s to 582-s, 1947.

41. Zhang, H., Hu, S. J., Senkara, J., and Cheng, S. 1998. “A statistical analysis of expulsion in resistance spot welding.’submitted to ASME Journal of Manufacturing Science and Engineering,1998.
42. Williams, N. T. , Parker, J. D. “Review of resistance spot welding of steel sheets Part 1 Modelling and control of weld nugget formation.” International Materials Reviews, vol.49,pp.45-75,2004.
43. Allanki, Y. R., & Kumar, C. A. “Failure load evaluation of resistance spot weld subjected to tensile and shear load.” SAE Technical Paper, 2005-26-045, 2005.
44. Bouyousfi, B., Sahraoui, T., Guessasma, S., & Chaouch, K. T. “Effect of process parameters on the physical charecteristics of spot welds joints.” Materials and Design, (Article in press),2005.
45. Chao, Y. J. “Ultimate Strength and Failure Mechanism of Resistance Spot Weld Subjected to Tensile, Shear, or Combined Tensile/Shear Loads.” Journal of Engineering Materials and Technology, Vol. 125, pp. 125-132,April 2003.
46. Lee, H., Kim, N., & Lee, T. S. “Overload failure curve and fatigue behaviour of spot-welded specimens.” Engineering Fracture Mechanics, Vol. 72, pp. 1203–1221, 2005.
47. Lin, S.-H., Pan, J., Wu, S., & Tyan, T. “ Failure Loads of Spot Weld Specimens under Impact Opening and Shear Loading Conditions." Experimental Mechanics, pp. 147-157, 2004.
48. Pollard, B. “Spot Welding Characteristics of HSLA Steel for Automotive Applications.’ Welding Journal, Welding Research Supplement, pp. 343s-350s, August,1974.
49. Radaj, D., & Zhang, S. “Geometrically Nonlinear Behaviour Of Spot Welded Joints In Tensile And Compressive Shear Loading.” Engineering Fracture Mechanics, Vol. 51(2), pp. 281-294, 1995.
50. Williams, N. T and Parker J. D., " Review of resistance spot welding of steel sheets: Part 1 -Modelling and control of weld nugget formation", International Materials Review, Vol.49,pp.45-75, 2005.
51. Goodarzi M., Marashi S.P.H., Pouranvari M., “Dependence of overload performance on weld attributes for resistance spot welded galvanized low carbon steel.” J. Mat. Process. Tech, Vol. 209, pp. 4379-4384, 2009.
52. Sun X., Stephens E.V., Khaleel M.A., “Effects of fusion zone size and failure mode on peak load and energy absorption of advanced high strength steel spot welds under

lap shear loading conditions.” Engineering Failure Analysis, Vol. 15, pp.356-367, 2008.

53. Zhang H., Senkara J., “Resistance welding: fundamentals and applications.’ Taylor & Francis CRC press, 2005.
54. Zhou, M. “A unified approach to assessing the mechanical performance of resistance spot welds.” PhD Dissertation, University of Michigan, An Arbor, MI, 2003.
55. Houldcroft, P. T.,'Welding process technology', 3nd edn,Cambridge University Press, 2004.